

Master's thesis

2019

Master's thesis

Ilyas Anindita

**NTNU**  
Norwegian University of  
Science and Technology  
Faculty of Engineering  
Department of Geoscience and Petroleum

Ilyas Anindita

# **Reservoir Prediction and Controlling Factors of the Cenozoic Deepmarine System at the Sørvestsnaget Basin, Southwest Barents Sea**

August 2019





Norwegian University of  
Science and Technology

# **Reservoir Prediction and Controlling Factors of the Cenozoic Deepmarine System at the Sørvestsnaget Basin, Southwest Barents Sea**

Ilyas Anindita

Petroleum Geoscience

Submission date: August 2019

Supervisor: Ståle Emil Johansen

Co-supervisor: Dicky Harishidayat

Norwegian University of Science and Technology  
Department of Geoscience and Petroleum



---

# Abstract

Sørvestsnaget Basin is one of the most underdeveloped basin in Barents Sea, with only one exploration well, 3 sets of 3D seismic covering this basin, and 150+ 2D seismic lines per August 2019. One of the main exploration problem in this area is the quality and quantity of the data itself also the complexity of fault system influenced pre-dominantly by Senja Fault Zone in Pre-Paleogene Epoch.

Therefore using conventional method, such as stochastic modelling, to model and visualise the subsurface condition will be highly inaccurate and risky. This study will focus on simulating sedimentation process and result using Stratigraphic Forward Modelling method through Geological Process Modelling, a plugin in Petrel 2017 © Schlumberger by reconstructing paleo-Topography of Cenozoic era as one of the simulator input.

The simulator input are Paleo-Water Depth/Paleo-Bathymetri/Paleo-Topography which is reconstructed using Clinoform Analysis and Seismic Sequence Stratigraphy, Sea Level Changes especially in Cenozoic Era, Subsidence and Uplift rate in Sørvestsnaget Basin, Source-sinks and boundary conditions, and lastly sediment components and their properties. Tetzlaff et al. (2014)

The result of this study showed plausible model of Sorvestnaget Basin from Miocene (2.3 Ma) to Seabed (0 Ma). Each model is guided with Paleo-topography derived from clinoform analysis and biostratigraphy analysis, tectonic evolution based on changing rate from paleo-topography to present-topography, sea level changes from Miller et al. (2005) and sedimentation rate from well log and literature study.

The result of simulation could be directly used for Facies Model in Petrel 2017, along with several other model such as, Porosity Model, and Unconformities Model, or could be a trend for geo-statistical modelling with guidance of well log analysis.

keywords : Sorvestnaget Basin, Clinoform Analysis, Seismic Sequence Stratigraphy, Stratigraphic Forward Modelling, Geological Process Modelling,

---

# Preface

This thesis was made as a completion of two years master education in Petroleum Geosciences at Norwegian University of Science and Technology (NTNU) in Trondheim, Norway, to complete an Master of Science (MSc) degree in Petroleum Geology. The study was performed under supervision and guidance from Professor Ståle Emil Johansen.

This study is a continuation of my specialisation project performed in Fall 2018 with the title "Tectonostratigraphic Evolution of Cenozoic Era in Sørvestsnaget Basin, Southwest Barents Sea."

---

# Acknowledgement

Firstly and most importantly, I would like to thank God, Allah, Subhanahu Wa Ta'ala and His Prophet, Muhammad, Salallahu'Alaihi Wasalam, for giving me serenity and faith in completing this study.

I would like to send my greatest gratitude and deepest acknowledgement to my supervisor Professor Ståle Emil Johansen for accepting under your supervision, although my under-performance and condition through times you still give me chance with kindness.

To Dicky Harishidayat, Phd. My utmost gratitude for helping me in all technical matter from specialisation course, project until thesis while still tutoring me in any academic problems and also for your advice about living in Norway, also Benjaminn Udo Emmel for his kindness and guidance during my short work in SINTEF.

To my family, my mother Sri Mulyati, my late father Soekimin, my father Eko Amroji, my brother Budyanung Anindita, my sisters Latifah Adha, and Halimah Arum. Thank you for being my family.

To my fellow Indonesian student who studied at the same batch of year 2017 - 2019, Theresia Margareth S, Ragil Destriawan Prasetyo, Maresda Satria, Pomto Jaya, Vincent August Harahap, Julianti Putri Setiawan, Muhammad Iffan Hannanu, I Gusti Gede Agung Angga, Steven Sergij Salim, Maillisa Fitria, and Zwestin Gomgom Welfry Situmorang thank you for your support and friendship, I hope you all succeed in the future both your study and life in Norway or wherever you are.

To my fellow international master student in Petroleum Geoscience at NTNU 2017-2019, Hieu Trong Nguyen, Wasif Rehman Raja, Ilgar Azizov, Ofeliya Ibrahim, Patience Ankah, Zhang Xinyu, Saboor Khan, and Umer Azam, thank you for giving me your utmost support, sharing your experiences and memories.

To entire Indonesian family along with friends of Perhimpunan Pelajar Indonesia-Trondheim. Thank you for supporting me and making me feel at home every time.

To residents of Moholt Alle 16, Harbi Qodri, Mikael Yuan Estuariwinarno, and Ilgar Azizov. Thank you for your support and cooperation during my stay in Moholt Alle 16 - 31.

To Joko Pamungkas M.T., as Chief of Pusat Studi Pengembangan Migas and Panas Bumi University of Pembangunan Nasional "Veteran" Yogyakarta, who has let me use the laboratory facility to finish my thesis in Indonesia, Bambang Triwibowo, M.T., Ardian Novianto M.T., Haviz Hamdalah, M.Sc. My utmost gratitude for the discussion both academically and personally about this Thesis.

---

To (late) Dr. Premononowati and Dr. Carolus Prasetyadi, thank you for the motivation and recommendation about continuing study to master degree.

To my all friends in Indonesia who helped me even way before I come to Norway, Grant and Pugeran's Crew, Aprilana Cahyono, Hery Gunawan, Dea Natalia H, Faizal Agung Riyadi and all Pangea 2009 members of University of Pembangunan Nasional "Veteran" Yogyakarta, Indonesia. You are all the best.

To Indonesia Endowment Fund for Education (LPDP) by Ministry of Finance, Indonesia, for all their financial and training support before and during my study in Trondheim.

Yogyakarta, August 2019

Ilyas Anindita



# Table of Content

<b>Abstract</b>	<b>i</b>
<b>Preface</b>	<b>ii</b>
<b>Acknowledgement</b>	<b>iii</b>
<b>Table of Content</b>	<b>6</b>
<b>List of Tables</b>	<b>7</b>
<b>List of Figures</b>	<b>13</b>
<b>1 Introduction</b>	<b>5</b>
1.1 Exploration Background . . . . .	5
1.2 Problem and Objectives . . . . .	6
<b>2 Literature Review</b>	<b>7</b>
2.1 Regional Structural Geology . . . . .	7
2.1.1 Structural Geology of Sørvestsnaget Basin . . . . .	8
2.2 Regional Stratigraphy . . . . .	9
2.2.1 The Upper Regional Unconformity (URU) . . . . .	9
2.2.2 Stratigraphy of Sørvestsnaget Basin . . . . .	10
2.2.3 Deep Marine Deposit . . . . .	12
<b>3 Data and Methodology</b>	<b>23</b>
3.1 Data . . . . .	23
3.1.1 Data Quality Control . . . . .	23
3.2 Methodology . . . . .	24
3.2.1 Electrofacies Analysis for Sequence Stratigraphy . . . . .	24
3.2.2 Seismic Sequence Stratigraphy . . . . .	24
3.2.3 Seismic Sequence Analysis . . . . .	24
3.2.4 Seismic Facies Analysis . . . . .	25

---

3.2.5	Clinoforms Analysis and Paleo-Bathymetri Reconstructions. . . .	25
3.2.6	Stratigraphic Forward Modelling and Geological Process Modelling ©. . . . .	26
<b>4</b>	<b>Results</b>	<b>47</b>
4.1	Seismic Well-Tie . . . . .	47
4.1.1	Sonic Calibration . . . . .	47
4.1.2	Synthetic Generation . . . . .	47
4.2	Well Log Analysis . . . . .	48
4.2.1	Volume Shale (VSL) . . . . .	48
4.2.2	Net to Gross (NtG) . . . . .	49
4.2.3	Porosity Density ( $\phi\rho$ ) . . . . .	49
4.2.4	Porosity Total ( $\phi_{total}$ ) . . . . .	49
4.2.5	Porosity Effective ( $\phi$ effective) . . . . .	49
4.2.6	Sequence Stratigraphy . . . . .	50
4.2.7	Well Correlation . . . . .	50
4.3	Seismic Interpretation . . . . .	50
4.3.1	Time Maps . . . . .	51
4.3.2	Depth Maps . . . . .	52
4.4	Clinoform Analysis . . . . .	52
4.5	Stratigraphic Forward Modelling . . . . .	54
<b>5</b>	<b>Discussion</b>	<b>89</b>
5.1	Controlling Factors of Deep-Marine System, in Sørvestnaget Basin. . . . .	89
5.1.1	Allogenic Factors . . . . .	89
5.1.2	Autogenic Factors . . . . .	90
5.2	Geological Process Modelling Results for Hydrocarbon Exploration. . . .	91
<b>6</b>	<b>Conclusion</b>	<b>97</b>
	<b>Bibliography</b>	<b>99</b>

# List of Tables

3.1	Wells and Seismic Data Availability . . . . .	23
4.1	Summary of correlation between well marker and seismic wavelet in well 7216/11-1S modified from, Anindita (2018) . . . . .	48
4.2	Horizons and Well Top Marker (7216/11-1S) compared to previous study.	51
4.3	Clinofom Analysis Variables Summary . . . . .	53

---

# List of Figures

2.1	Tectonic Setting in Southwestern Barent Sea. Area of study within red rectangle modified from Faleide et al. (1996) taken from (Ryseth et al., 2003) and Structural Geology Model from (Kristensen et al., 2018). . . .	13
2.2	Main stages evolution of the Western Barents Sea and surrounding area. 1 = stable elements - continental cratons and intrabasinal highs; 2 = sedimentary basins; 3 =active foldbelts; 4 = normal and wrench faults; 5 = deformation front of active foldbelts; 6 = intrusions; 7 = volcanic (Faleide et al., 1984) . . . . .	14
2.3	Stratigraphic relationship of the late Pliocene to Pleistocene succession in the southwestern Barents Sea. Age correlations are given in 4.2. Line B is from Butt et al. (2000). Line C is from Vorren et al. (1991) and western part is from Andreassen et al. (in prep.) taken in Larsen et al. (2003) . . .	15
2.4	The Mesozoic and Cenozoic development of Southwestern Barent Sea, modified from Nøttvedt et al.,1993, with the Geological Time Scale, based on Gradstein et al.,2004. in (Worsley, 2008) . . . . .	16
2.5	Well Correlation from Northwest to Southeast with mean sea level as datum modified from (Ryseth et al., 2003) . . . . .	17
2.6	Stratigraphy, lithology and depositional environments of Late Eocene - Late Miocene strata, well 7216/11-1S. The measured depths (mRKB) refer to the rig's Kelly Bushing, 24 m above mean sea level (Ryseth et al., 2003)	18
2.7	Illustration showing discrepancy in Deep water definition (Shanmugam, 2000) taken in (Akbar, 2018) . . . . .	19
2.8	Conceptual model depicting the mode of propagation or mechanism for mass wasting or slope failure (Dykstra, 2005), and (from Vorren and Laberg, 1997), taken from (Omosanya et al., 2016). . . . .	20

---

2.9	Block diagrams showing the evolution of the shelf and slope in the study area. There is a general westward migration of the shelf-edge from the Miocene times to the present day. The margin has witnessed increasing sea-level conditions since Mid-Pliocene to Pleistocene times. The maximum fall in sea level was during the beginning of the Pliocene. Inferred sediment source or provenance is to the northern part of the study area in Stappen High. from (Omosanya et al., 2016). . . . .	21
3.1	The blue solid line is Sørvestsnaget Basin boundary, while the red dashed-line is the boundary of seismic interpretation. Well DW-A,B,C,D, and E are dummy wells for Time-Depth Conversion since Velocity Model is not available. . . . .	30
3.2	Well Correlation with standard markers from NPD in West Barents Sea, flattened on Nordland GP as datum. The grey boxes indicate interval of missing curve logs. Well names from upper left to bottom right: 73165-1, 7216/-11-1S, . . . . .	31
3.3	Checkshots of All well which used in this study. the highlight points showing some error data, which need correction. Anindita (2018) . . . . .	32
3.4	The comparison between line NPD-TR-82-7157-82-A-RMTVFGC (yellow rectangle = poor condition) and GVH-90-106-FM-TVFGC (green rectangle = good condition), red circle showing seismic noise. . . . .	33
3.5	Workflow for Paleo-bathymetri Reconstructions and Stratigraphic Forward Modelling. . . . .	34
3.6	Basic Log shapes, stacking patterns, and grain size - gamma ray correlations taken from Rider (2002). . . . .	35
3.7	Facies indications from Gamma Ray (or SP) log shapes. These are idealised examples both of log shape and sedimentological facies. taken from Rider (2002). . . . .	36
3.8	Degree of sequence in well log analysis taken from Rider (2002). . . . .	37
3.9	System tract and its depositional environment interpretation. taken from Rider (2002). . . . .	38
3.10	Geological Interpretation of Seismic Facies Parameters. (Mitchum <i>et al</i> 1977)	39
3.11	Seismic stratigraphic reflection terminations within idealised seismic sequence. (Mitchum <i>et al</i> 1977) . . . . .	39
3.12	Seismic stratigraphic reflection configuration within idealised seismic sequence. (Mitchum <i>et al</i> 1977) . . . . .	40
3.13	Seismic stratigraphic external forms within idealised seismic sequence. (Mitchum <i>et al</i> 1977) . . . . .	40
3.14	Seismic stratigraphic external forms within idealised seismic sequence. (Mitchum <i>et al</i> 1977) . . . . .	41

---

---

3.15	Cross-sectional schemes parallel to the depositional dip, showing idealised compound clinoform systems at different scales. (A) Regional cross-section, highlighting three actively growing clinoforms systems: delta, shelf-edge and continental-margin scale clinoforms (Modified after Henriksen et al, (2009)). (B) Cross-section through the nearshore to inner marine shelf area, showing a typical shoreline to delta-scale sub-aqueous clinoform compound system, (modified after Helland-Hansen and Hampson, 2009) in Patruno et al. (2015). . . . .	42
3.16	Clinoform nomenclature and explanation of abbreviations (adapted from Patruno et al. (2015)). Red indicates parameters related to Paleo-Water Depth, green are geometric parameters for which relationships with Paleo-Water Depth are available in SINTEF 2D Clinoform Analysis. . . . .	43
3.17	Equations describing best-fit lines between parameter pairs showing a moderate-to-strong correlation ( $R^2 > 0.5$ ).in Patruno et al. (2015) . . . . .	44
3.18	Geological Process Modelling basic input, Tetzlaff et al. (2014) . . . . .	45
3.19	Steady flow and transport example showing the formation of a river valley and a fan delta under constant sea level. Four sediment types were used: Coarse sand (red), fine sand (green), silt (blue) and clay (black). Schematic block diagram of main deltaic environments is shown on the upper right: 1. Alluvial valley, 2. Delta plain, 3. Active delta, 4. Undersea delta plain., Tetzlaff et al. (2014) . . . . .	45
3.20	Unsteady flow and transport example showing the formation of turbidite fan after 100 flows. Sediment types are the same as those used in Fig. 2. Upper figure shows carved valley and entire fan. Lower figure shows detailed transversal section of fan., Tetzlaff et al. (2014) . . . . .	46
4.1	Seismic Well Tie, Well 7216/11-1S and NH98 3D seismic, with local stratigraphy, and sea level change based on Miller et al. (2005), taken from Anindita (2018). . . . .	57
4.2	Sonic Calibration of Well 7216/11-1S. . . . .	58
4.3	Synthetic Generation of Well 7216/11-1S. The missing values of Sonic log and Density log are from 976 - 1383 MD Meter.modified from Anindita (2018). . . . .	59
4.4	Composite of Petrophysical logs in Well 7216/11-1S. . . . .	60
4.5	Composite of Sequence Stratigraphy in Well 7216/11-1S. . . . .	61
4.6	Well Correlation North to South, Datum on 0 m SSTVD. . . . .	62
4.7	Well Correlation Southwest to Northeast, Datum on 0 m SSTVD. . . . .	63
4.8	Example of Horizon interpretation in Miocene ages, solid red line is base map of interpretation, pink dashed line is coverage area from previous interpretation (most of interval age, but not all of ages has same coverage size), blue dashed line is the location of seismic section in fig. 4.9 . . . . .	64
4.9	Uninterpreted seismic section (upper) and Horizon and Fault interpretation of Inline 2935 from 3D Seismic NH9803 (lower), location can be seen in fig. 4.8 . . . . .	65
4.10	Fault and Horizon interpretation North to South. . . . .	66
4.11	Fault and Horizon interpretation Southwest to Northeast. . . . .	67

---

---

4.12	Geo-seismic interpretation of N-S regional line seismic. . . . .	68
4.13	Geo-seismic interpretation of SW-NE regional line seismic. . . . .	69
4.14	Summary of Seismic Stratigraphy Analysis from Holocene to Miocene. . . . .	70
4.15	Summary of Seismic Stratigraphy Analysis from Miocene to Cretaceous. . . . .	71
4.16	Time Maps of Top Pliocene 2. . . . .	72
4.17	One Way Time (OWT) Maps of Top Pliocene 2, derived from half values of time surface map Pliocene 2. . . . .	73
4.18	Interval Velocity Maps of Top Pliocene 2, derived from checkshots of well-bore data. . . . .	74
4.19	Depth Map of Top Pliocene 2, derived from OWT map multiplied by Interval velocity map. . . . .	75
4.20	Regional Seismic Line with trend from West to East, including interpretation of clinoform of all ages. . . . .	76
4.21	Results of Digitising 2D seismic section, as part of analysis preparation. . . . .	77
4.22	Results of Clinoform analysis calculation with equations based on Patruno et al. (2015) at Top Pliocene 2. . . . .	77
4.23	Cross-plot between Present Clinoform (x) and Paleo Clinoform (y) taken from Present and Paleo Depth from Clinoform analysis in table 4.3. . . . .	78
4.24	Paleobathymetri Map of Top Pliocene 2. derived from regression function of figure 4.23 Note : Map has been extrapolated for simulation in GPM. . . . .	79
4.25	Thickness Map of Top Pliocene 2 to Top Pleistocene 1, overlying to Paleobathymetri Map of Top Pliocene 2. . . . .	80
4.26	Source Position Map of Top Pliocene 2, the value of 1 means location of steady flow, and value 2 means location of unsteady flow. . . . .	81
4.27	Comparison among sea level change, by Miller, Haq and Exxon. As it is shown in the Miller et al. (2005), Sea Level Change only covers from Miocene to Present, but offers more detailed sea level change. . . . .	82
4.28	Diffusion equation from Lejri et al. (2017). . . . .	83
4.29	Subsidence/Uplift Rate Map from 13 Ma to 0 Ma, of Pliocene 2, Positive value means Uplift phase, and Negative value means Subsidence phase. . . . .	84
4.30	Sediment source and water supply chart. . . . .	85
4.31	An Example of Dialog Box Setting in Geological Process Modelling (GPM), in Pliocene 2 to Pleistocene 1. . . . .	86
4.32	Results of GPM Simulation at 0.99 Ma, Sediment package/clinothem of Pliocene 2 to Pleistocene 1. . . . .	87
5.1	An example of Oblique Type of Clinoform in Pleistocene 3 (URU) to Pleistocene 4, viewed from South and exaggerated 10 times. . . . .	91
5.2	An example of Sigmoidal Type of Clinoform in Pleistocene 2 to Pleistocene 2.5, viewed from South and exaggerated 10 times. . . . .	92
5.3	Dialog box setting for sediments type properties, from upper left to bottom right: sand (coarse), sand (fine), silt, and clay. . . . .	93
5.4	An example of Unsteady Flow Type Deposit in Pliocene 2 to Pleistocene 1, viewed from west , section is perpendicular to incision valley, and exaggerated 100 times. . . . .	94

---



---

5.5 An example of Porosity Model in sediment package (clinothem) of Pliocene  
2 to Pleistocene 1, viewed from Southwest and exaggerated 20 times. . . 95

# Introduction

## 1.1 Exploration Background

Hydrocarbon exploration in the Barents Sea commenced in 1979 (5th Norwegian licensing round). Prior to the year 2000, 53 exploration wells had been drilled, proving total hydrocarbon resources of about  $288 \times 10^6 \text{ Sm}^3$  oil equivalents (Knutsen et al. 2000) in (Ryseth et al., 2003).

The Sørvestsnaget Basin is located in the southwestern part of the Norwegian sector Barents Sea. The limited number of wells and 3D seismic data causes high risks in the exploration for hydrocarbon. This basin is one of the most underdeveloped basin in Barents Sea, with only one exploration well, 3 sets of 3D seismic covering this basin, and 100+ 2D seismic lines per August 2019. One of the main exploration issue in this area is the quality of the data itself and complexity of fault system influenced by Senja Fault Zone in Pre-Paleogene Epoch.

Therefore using conventional method, such as stochastic or deterministic modelling, to model and visualise the subsurface condition would be highly inaccurate and risky. On other other side numerical modelling especially Stratigraphic Forward Modelling method is advancing progressively in geoscience branch. This study will try to apply and focus on, reconstructing paleo-topography/paleo-water depth/paleo-bathymetri as main input for simulator, simulating sedimentation process and result through Geological Process Modelling, a plugin in Petrel 2017 © Schlumberger .

---

## 1.2 Problem and Objectives

### 1. **Problem :**

Several exploration wells had been drilled during the last three decades targeting the Cenozoic deep-marine system in the Sørvestsnaget basin resulted as dry hole with little presences of good reservoir quality. Therefore lithofacies and depositional environment need to be addressed as lead to determine geometry of reservoir rock.

### 2. **Objective :**

2a.) Building low risk and better resolution geomodels of Cenozoic Era deposits in Sørvestsnaget basin that can be used directly as reservoir geometry for volume reserves estimation.

2b.) Building tectonostratigraphic evolution of Cenozoic Era deposits, based on up-date data and previous study.

2c.) Identifying possible new lead or prospect as suggestion for further exploration.

### 3. **Methodology :**

Seismic Sequence Stratigraphy, Clinoform Analysis, PaleoWater-depth Reconstructions, and Stratigraphic Forward Modelling.

# Literature Review

## 2.1 Regional Structural Geology

The Western Barents Sea is a part of the continental shelf of north-western Eurasia, located in the North of Norway, bordered by the Norwegian-Greenland Sea, and the Svalbard Archipelago in the West. The Western Barents Margin includes the continental margin from Svalbard in the north to the Norwegian mainland in the South, The distance approximately 1000 km (Kristensen et al. (2018)). The continental margin of the western Barents Sea and Svalbard was developed by transtensional movements between Eurasia and Greenland during the Paleogene period, with final continental separation between 35 and 25 Ma due to a shift in relative movements between the plates. The margin comprises three main structural segments;

1. A southern shear margin segment, the Senja Fracture Zone
2. A central volcanic rift segment, the Vestbakken volcanic province
3. A northern shear and subsequently rift margin along the Hornsund Fault Zone. (Fig.2.1 part A) (Mjelde et al., 2014).

The Barents sea area has undergone several phases of tectonism and sedimentation since the Devonian, eventually leading to crustal break-up and sea floor spreading in the North Atlantic Rift. At least five phases of basin development are widely recognisable throughout the area, according to Nøttvedt et al., 1992 in (Ryseth et al., 2003).

1. Late Devonian - middle Carboniferous rifting (figure 2.2),
2. Late Carboniferous - Permian carbonate platform development (figure 2.2),
3. Triassic - Cretaceous siliciclastic shelf development (figure 2.2)
4. Early Cenozoic crustal break-up (figure 2.2), and

---

## 5. Late Cenozoic passive margin development (figure 2.1 part B.).

In figure 2.2 part **B.**) shows redrawn map after (Faleide et al., 1996) showing the opening angles (DV = divergence vector) and the relationship between the transpression along Western Svalbard, Extension in the ‘pull-apart’ basin in Vestbakken and northern Sørvestsnaget and the transension along the Senja Fracture Zone. Thick black arrows illustrate the orientation of plate motion.

Meanwhile in part **C.**) explains the Model for initial orientation of extensional (E) and compressional (C) axis during trans-tension (redrawn after Sanderson and Marchini, 1984). Full and half arrows on the sides of the model illustrate the components of pure and simple shear intran-tension respectively. F = fold, T = thrusts, N = normal faults. Lastly, the part **D.**) shows observed orientations off old axis relative to expected range off old axis from formation along ISAH max (based on Fossen et al., 2013) and rotation towards parallelism with the opening direction relative to the Senja Fracture Zone. (Kristensen et al., 2018))

### 2.1.1 Structural Geology of Sørvestsnaget Basin

The Sørvestsnaget Basin is delineated to the west by the Senja Fracture Zone and is characterized as a deep Cretaceous and Cenozoic basin (approx. location: 71°–73°N, 15°–18°E) Ryseth et al. (2003) in Kristensen et al. (2018). The pre-Tertiary evolution of the Sørvestsnaget is not well established but Breivik et al. (1998) stated that the thick late Cretaceous (approx. 6 km thickness) interval may be related to a phase of Late Cretaceous rifting climaxing in Cenomanian and Middle Turonian as recorded on the conjugate east coast of Greenland.

The central and northern parts of the Sørvestsnaget basin formed a pull-apart basin in Late Cretaceous–Early Palaeocene and a relatively complete Palaeocene succession was deposited under deep marine conditions Ryseth et al. (2003). The deep marine conditions continued throughout the Eocene with deposition of significant sandy submarine fans during the Middle Eocene.

Middle-late Eocene active salt diapirism in the Sørvestsnaget Basin was coeval to the opening of the Norwegian–Greenland Sea Perez-Garcia et al. (2013). Coeval to the shear along the Senja Fracture Zone and basin formation in the Sørvestsnaget Basin transpression along the Hornsund Fault Zone led to orogenesis along the western part of Svalbard creating the W Spitsbergen Fold Belt. The orogenesis along western Svalbard led to Palaeocene–Eocene basin formation in the Spitsbergen Central Basin. The Svalbard Fold and Thrust Belt orogenesis is characterized by a partitioning of strain between strike slip faults and broad zones of convergent strain during overall transpression. During the earliest Oligocene the relative plate motion changed and shear along the Western Barents Margin was followed by east-west oriented extension seen as a series of NNW-SSE trending normal faults. Uplift and burial of the margin by a thick clastic wedge is characteristic of the late Cenozoic evolution Faleide et al. (1996). Erosion estimates of the Palaeogene sequence range from 1000 to 1500 m in the southwestern Barents Sea Faleide et al. (1996).

---

## 2.2 Regional Stratigraphy

Three main sediment packages/clinothems (GI, GII, and GIII) and seven regionally correlative reflectors (R7-R1) have been identified within the Plio-Pleistocene sedimentary succession along western margin of Svalbard and the Barents Sea Faleide et al. (1996) Table 4.2 summarises the age estimates evaluated to be the most reliable for the identified reflectors and units in the area Fig 2.3 with reference to Cenozoic formations commonly identified on the Norwegian Shelf by the oil industry, the sediment packages/clinothems GI-GIII would correspond to the Naust Formation of the Nordland Group, when used as a succession of Upper Pliocene to Recent, including glacial and interglacial sequences. Larsen et al. (2003)

The following phases of depositional events are related to the glacial history of the Western Barents Sea – Svalbard Margin:

1. Glacially influenced deposition became dominant on the continental margin at about 2.3 Ma. This event is represented by the unconformity R7, which is also the base of the western margin trough mouth fans Faleide et al. (1996). R7 marks an increase in general sedimentation rate along the entire margin. Large parts of the Barents Sea may have been emergent at this time, and fluvial systems may therefore have been an important.(Larsen et al. (2003))
2. The first glacial advance reaching the shelf break west of Svalbard happened at R6 time ( 1.6 Ma; based on results from ODP Site 986) Butt et al. (2000). At the Bear Island Trough Margin the first ice streams reached the shelf break at R5 time ( 1.4-1.5 Ma), probably draining out the Bear Island Trough from an ice sheet situated over Svalbard and northern Barents Sea (suggested from 3D seismic of Sørvestsnaget), model of Fig.2.3; Middle Phase.sediment transport mechanism.(Larsen et al. (2003))
3. The first grounded ice draining from the Scandinavian mainland to the Bear Island Trough Margin seems, based the Sørvestsnaget 3D seismic, to have taken place at R1 time ( 0.5 Ma).(Larsen et al. (2003))

### 2.2.1 The Upper Regional Unconformity (URU)

The boundary between the pre-glacial bedrock and the relatively thin cover of glacial deposits on the continental shelf is termed the Upper Regional Unconformity (URU, Solheim and Kristoffersen 1984). Although direct correlation between URU and the seismic stratigraphy defined at the margin is not straightforward, the available seismic data indicate that URU corresponds to progressively older slope reflectors from south to north along the outermost continental shelf (Faleide et al. (1996); Solheim et al. 1998). In the Bear Island Fan, URU corresponds to R1 Faleide et al. (1996), whereas it corresponds to R3 in the Storfjorden Fan (Hjelstuen et al. 1996), and most likely to R5 in the Isfjorden Fan (Solheim et al. 1996).

Although URU most likely represents the erosional base for several continental shelf glaciations, the correlation between URU and R5, R3, and R1, respectively, indicate that the last major erosion down to the level of URU at the outer shelf, occurred at a time

---

corresponding to R5 adjacent to Svalbard, and subsequently later off the central Barents Sea Faleide et al. (1996). URU represents a change from an early erosional glacial regime, to a later aggradational regime. (Larsen et al. (2003))

## **2.2.2 Stratigraphy of Sørvestsnaget Basin**

There is only one well that drilled in Sørvestsnaget Basin (per August 2019 by Norwegian Petroleum Directorate), which is 7216/11-1S. This well penetrated from Cretaceous to Pleistocene Epoch, stratigraphically included into Sotsbakken Group and Nordland Group (Torsk formation), as can be seen in figure 2.3. Due to limitation and position of well data, stratigraphic analysis and biostratigraphy is conducted only in Well 7216/11-1S. This well drilled with Total Depth of 4125 mMSL (3079 mTVD), resulting two cores at 2964 - 2972.4 mMSL and 4206 - 4214 mMSL. In figure 2.4 The sedimentological description and well log interpretation is taken from (Ryseth et al., 2003), (Marheni et al., 2015), (Omosanya et al., 2016), and (Knies et al., 2009).

### **Cretaceous-Paleocene**

Significant subsidence persisted through the Late Cretaceous along the western margin and thick Late Cretaceous strata are present for instance in the Tromsø and Sørvestsnaget basins, where thicknesses exceeding 2 km can be inferred from seismic data. However, these strata are generally truncated to the east, below Cenozoic and Quaternary unconformities (Henriksen et al., 2011). In this study Cretaceous age is dominated by mudrock, sandstone, shaly sandstone, volcanic rock, and carbonate rock with varicoloured, grey, greenish to blackish mudrocks dominate throughout, associated with limestone / dolomite stringers and traces of very fine to fine-grained sandstone. (Anindita (2018))

### **Paleocene-Eocene-Oligocene**

In well 7216/11-1S this interval age deposits are dominated by greyish mudrocks, with traces of very fine to fine-grained sandstone. Furthermore, stringers of limestone and dolomite occur throughout, and the section is also characterized by abundant siderite. The completely fine-grained nature of the Paleocene Lower Eocene succession is indicative of deposition in a generally low-energy marine environment. Middle Eocene (Lutetian - Bartonian) strata rest with a possibly faulted stratigraphic break on Lower Eocene deposits. This interval dominated by agglutinated foraminifera and pyritised diatoms, but lacking calcareous micro fossils. Grey to dark grey mudrocks with limestone/dolomite stringers and scattered traces of very fine- to fine-grained sandstone dominate in throughout with the notable exception of a significant sandstone unit (2888 - 3102) mMSL. The assemblage of agglutinated foraminifera in the Middle Eocene and the Paleocene - Lower Eocene successions described above, are almost identical, and reflect rather similar, deep marine (bathyal) conditions throughout Paleocene - Middle Eocene time. Lastly in Late Eocene, The lithology comprises varicoloured grey, green, and brown to blackish mudrocks associated with minor limestone. The fine-grained nature of the Upper Eocene interval would generally testify to deposition by settling of suspended fines in a low-energy

---

environment, However, the near disappearance of agglutinated foraminifera most likely records significant marine shallowing during the latest Eocene.(Ryseth et al., 2003).

### **Oligocene-Miocene**

This interval consist of Lower Oligocene which dominated by generally grey/dark grey mudrocks and The Upper Oligocene comprises grey to brown mudrocks associated with a significant limestone (cemented) bed, while Middle - Upper Miocene succession consist silty mudrocks and scattered fine-grained sand-stones,associated with dolomite-cemented stringers.The Oligocene - Miocene succession was probably deposited in a shallow marine environment. On-lap of these strata towards the western marginal high is a clear indication that the high formed a topographic element or at least a submarine high during deposition The marginal high,therefore,was re-activated at the Eocene - Oligocene boundary. (Ryseth et al., 2003).

### **Pliocene- Pleistocene**

The lithology is dominated by grey clays and claystones with minor beds of fine to very coarse sand. the Pliocene interval is characterized by westward dipping clinofolds. Deep incisions occur within the clinofolds, apparently truncating deposits of Eocene - Paleocene age in the vicinity of the marginal high (Ryseth et al., 2003). Based on the seismic data The Plio-Pleistocene boundary has been defined from the seismic data and is placed at 382 mbsf (743 m MSL). The Plio-Pleistocene boundary in the well 7216/11-1S is at a depth of about 1861–1961 m MSL (Knies et al., 2009). (Fig2.5)



---

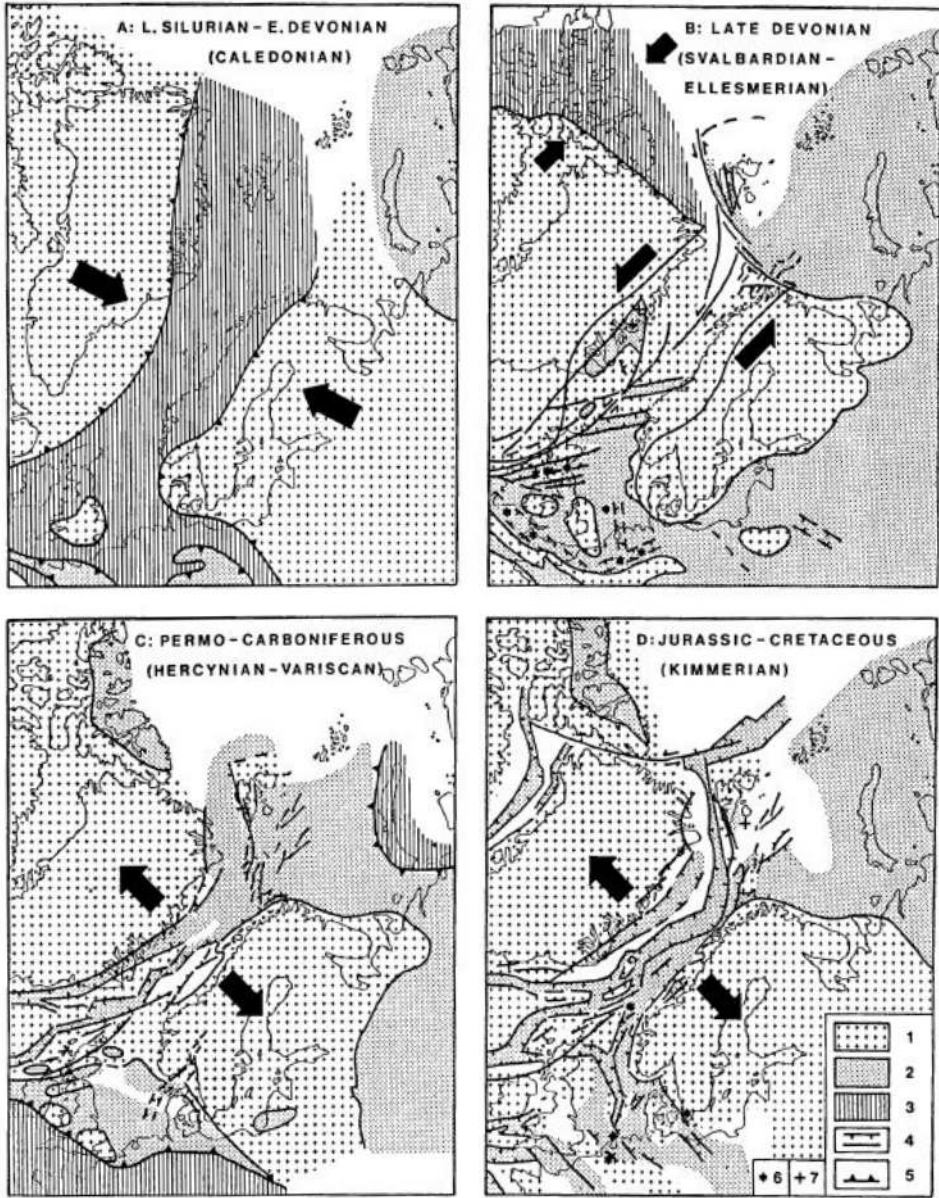
### 2.2.3 Deep Marine Deposit

The term deep marine deposit has been used in oil and gas industry, by both geologist and engineer in different understanding. While engineer sees it based on present water depth level between 500 - 2000 meter (Fig.2.7), geologist conceives it based on its paleo depositional environment. Definition by (Slatt, 2006) which refers to sediment deposit in marine environment, under influence of gravity driven processes, at the depth below storm wave based area, is used in this study, taken in Akbar (2018).

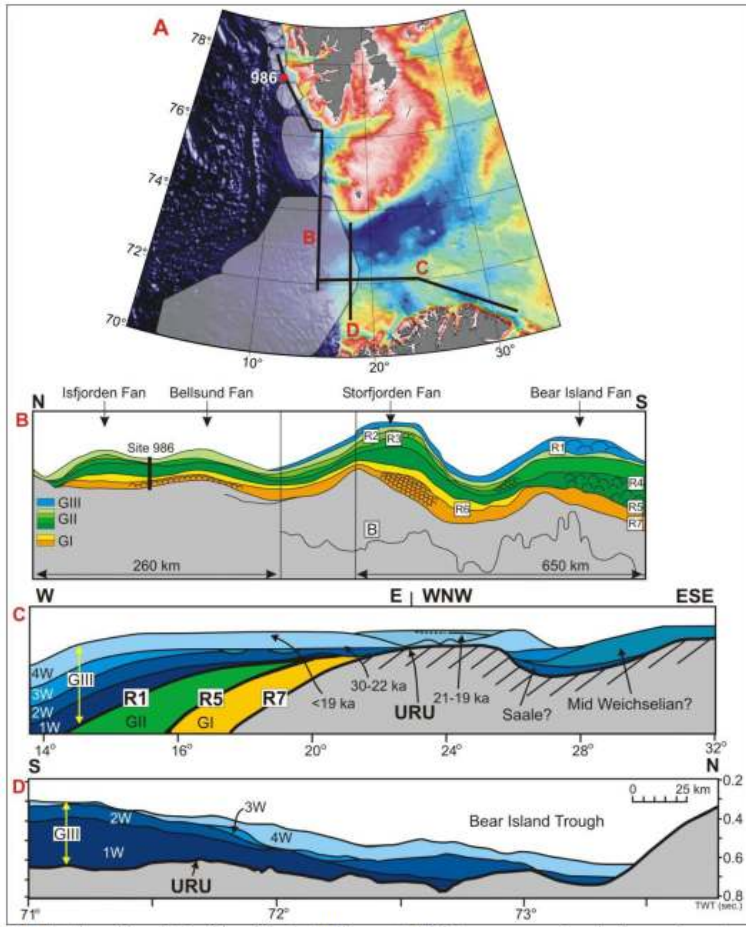
Due to the different glacial events, the thick Cenozoic sedimentary successions in the Sørvestsnaget Basin have been, for several decades regarded as glaciogenic wedges. They are often linked to Neogene glaciation that affected the entire Barents Sea. Faleide et al. (1984); Ryseth et al. (2003). explained in Fig. 2.8 (a) The removal of sediment from the head-wall region causes a decrease in the lithostatic stress in the orientations shown by the tension arrows ( $\sigma_T$ ), while deposition of the MTD at the toe region causes an increase in the vertical stress ( $\sigma_X$ ). (b) Progressive failure occurs where a series of failures sequentially cut further down-dip. Mass-transport essentially involves down-slope movement of sediments. (c) Retrogressive failure involves a series of failures that sequentially knick further headward, eventually stopping at the final head-wall. (d) Whole-body failure involves an initial movement throughout all of the failing mass at the same time, after which the mass may become internally deformed. In the boxes are the listed examples of MTDs failing through each of the methods. (e) Schematic model showing the main sedimentary processes on the shelf break and upper slope during the presence of the ice sheet at the shelf break (from Vorren and Laberg, 1997), taken in Omosanya et al. (2016).

Since Sørvestsnaget Basin was located in continental margin from its forming until today, therefore the sediment deposit of this basin most likely will be deep marine deposit, which formed as mass-transport deposits (MTDs), incised valley (V-shaped canyon), submarine channel, and submarine fan deposit. Omosanya et al. (2016). (Fig.2.9)

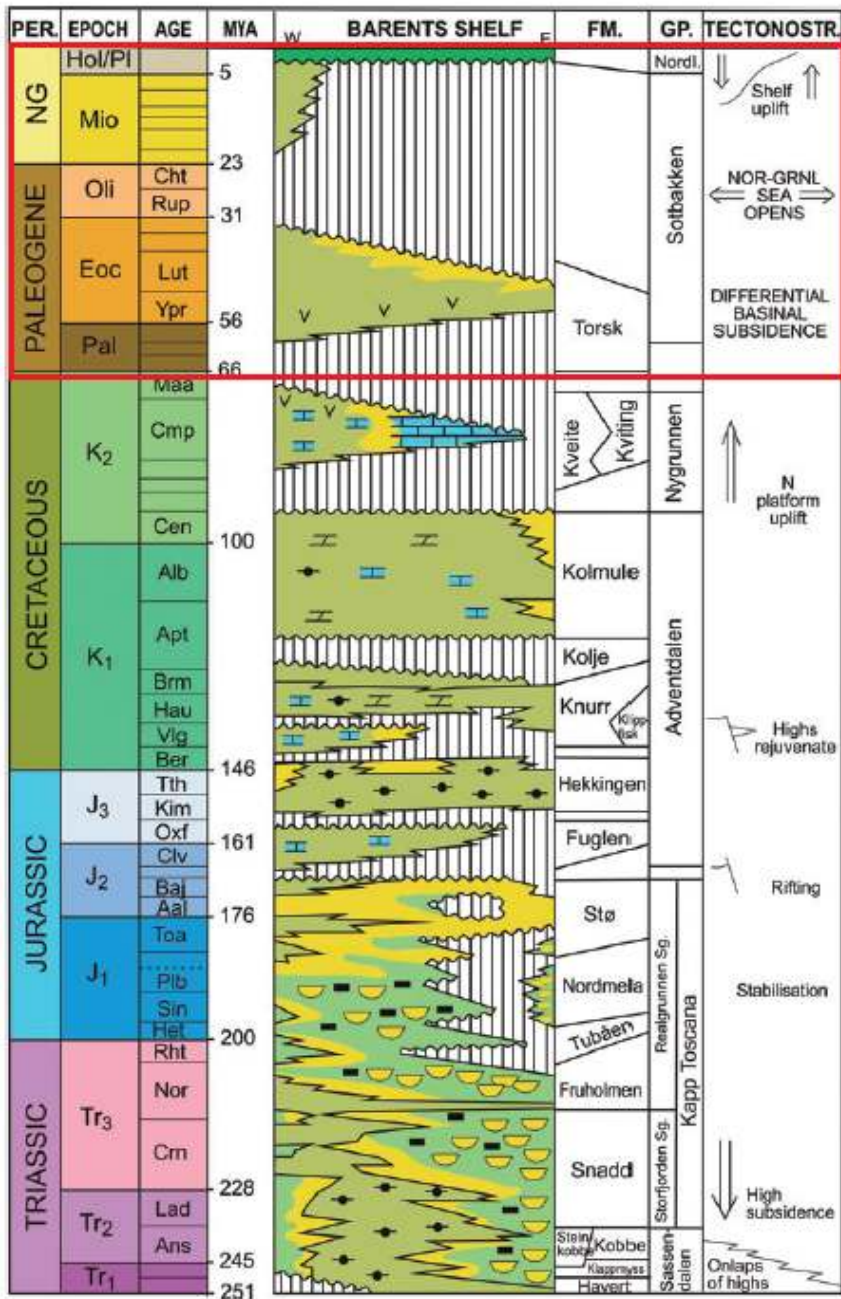




**Figure 2.2:** Main stages evolution of the Western Barents Sea and surrounding area. 1 = stable elements - continental cratons and intrabasinal highs; 2 = sedimentary basins; 3 = active foldbelts; 4 = normal and wrench faults; 5 = deformation front of active foldbelts; 6 = intrusions; 7 = volcanic (Faleide et al., 1984)



**Figure 2.3:** Stratigraphic relationship of the late Pliocene to Pleistocene succession in the south-western Barents Sea. Age correlations are given in 4.2. Line B is from Butt et al. (2000). Line C is from Vorren et al. (1991) and western part is from Andreassen et al. (in prep.) taken in Larsen et al. (2003)



**Figure 2.4:** The Mesozoic and Cenozoic development of Southwestern Barent Sea, modified from Nøttvedt et al.,1993, with the Geological Time Scale, based on Gradstein et al.,2004. in (Worsley, 2008)



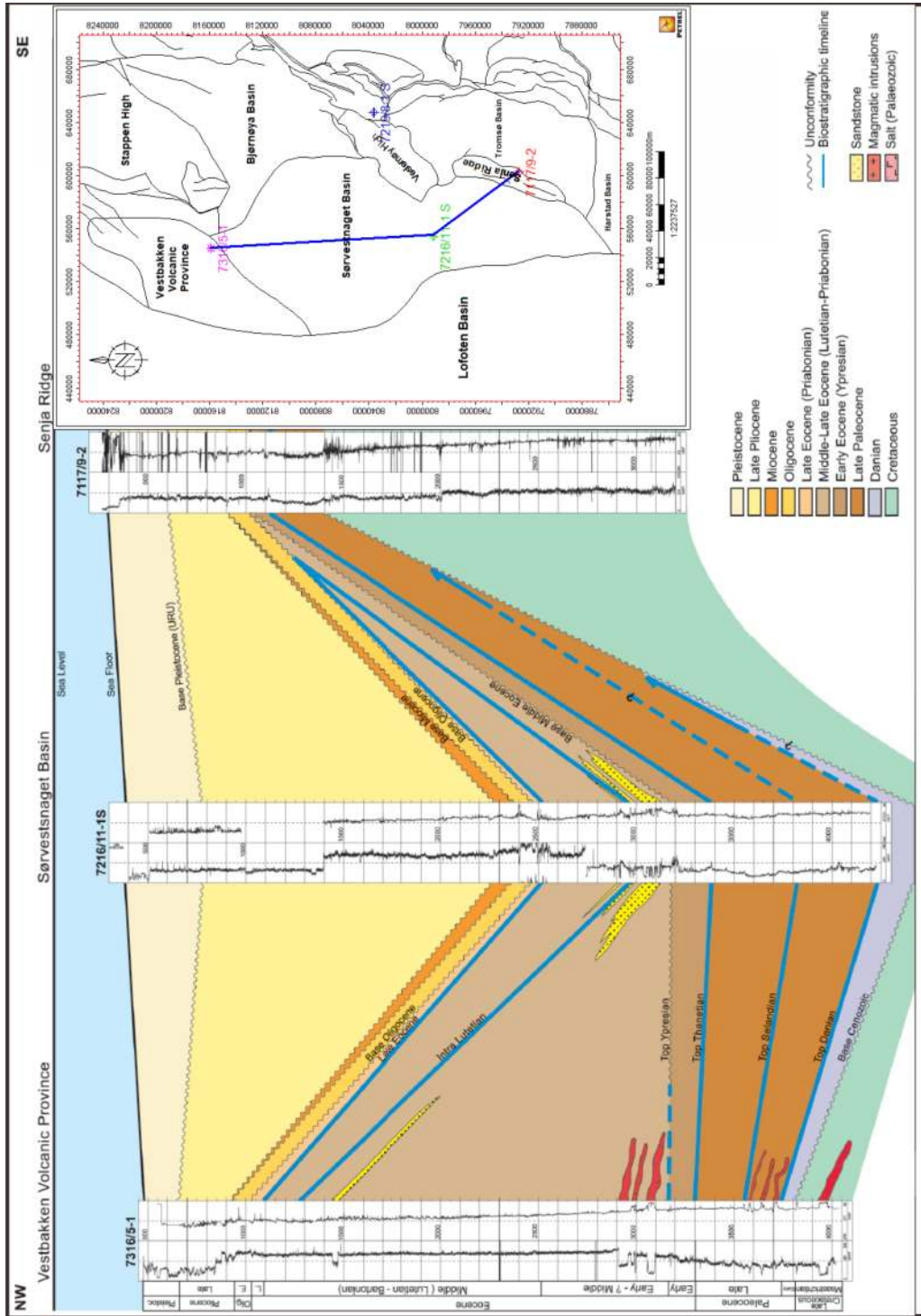
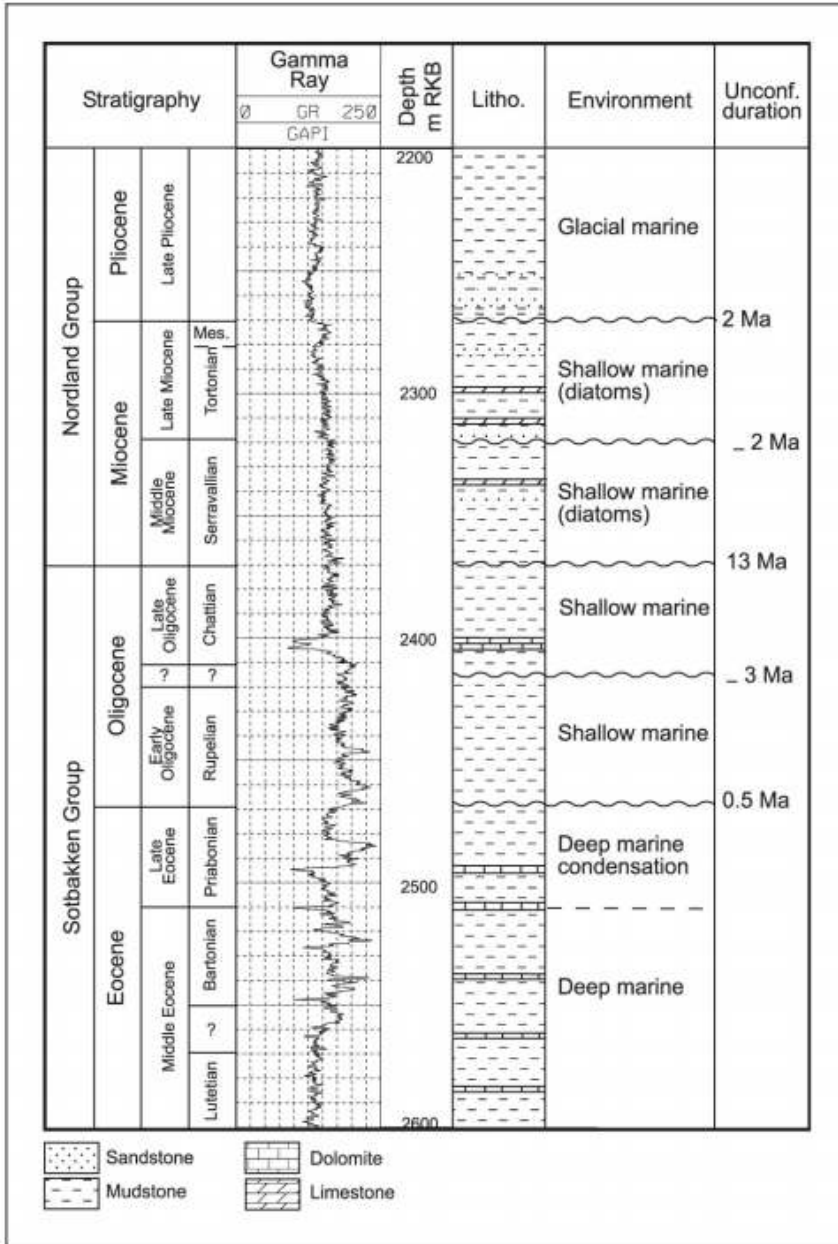
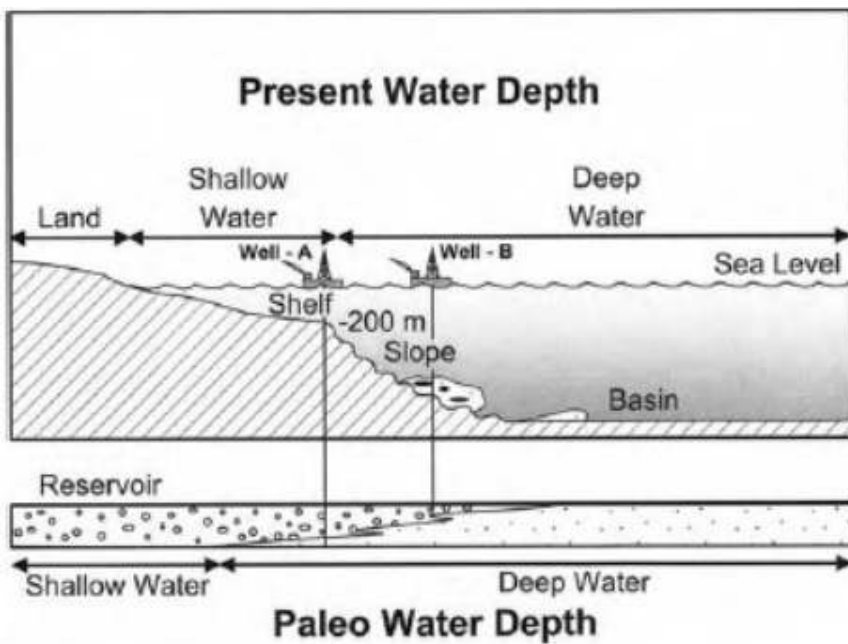


Figure 2.5: Well Correlation from Northwest to Southeast with mean sea level as datum modified from (Ryseth et al., 2003)

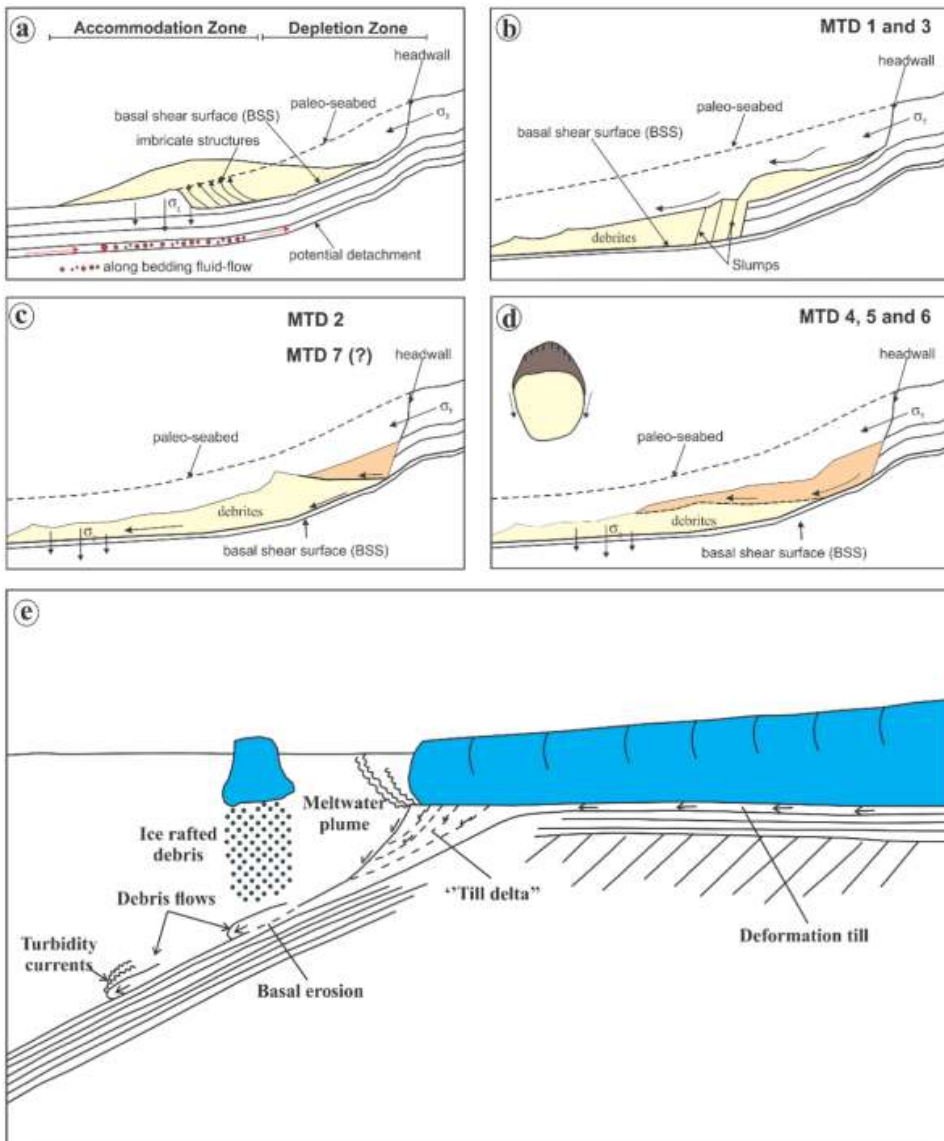


**Figure 2.6:** Stratigraphy, lithology and depositional environments of Late Eocene - Late Miocene strata, well 7216/11-1S. The measured depths (mRKB) refer to the rig's Kelly Bushing, 24 m above mean sea level (Ryseth et al., 2003)

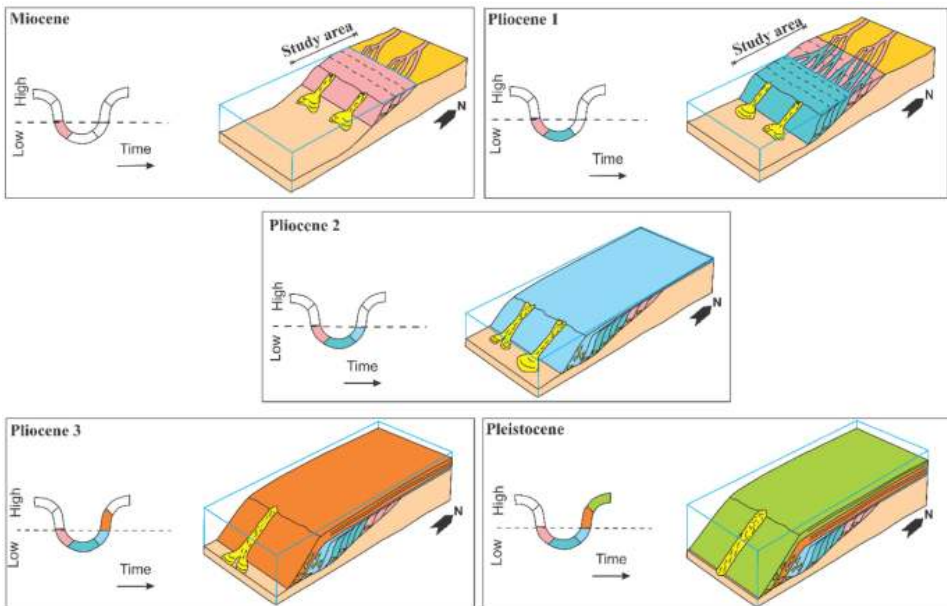


**Figure 2.7:** Illustration showing discrepancy in Deep water definition (Shanmugam, 2000) taken in (Akbar, 2018)





**Figure 2.8:** Conceptual model depicting the mode of propagation or mechanism for mass wasting or slope failure (Dykstra, 2005), and (from Vorren and Laberg, 1997), taken from (Omosanya et al., 2016).



**Figure 2.9:** Block diagrams showing the evolution of the shelf and slope in the study area. There is a general westward migration of the shelf-edge from the Miocene times to the present day. The margin has witnessed increasing sea-level conditions since Mid-Pliocene to Pleistocene times. The maximum fall in sea level was during the beginning of the Pliocene. Inferred sediment source or provenance is to the northern part of the study area in Stappen High. from (Omosanya et al., 2016).



# Data and Methodology

## 3.1 Data

This study used 2 sets of seismic 3D and 147 lines 2D, 6 wells data (only well 7216/11-1S located in Sørvestsnaget Basin), the base map of wells and seismic location is showed in 3.1. Wells and Seismic Data summary can be seen in table 3.1. The missing curve log mostly occurred in Neutron, Density, and Sonic logs, this could be challenge to calculate porosity for paleo-depth reconstruction. The example can be seen in figure 3.2.

**Table 3.1:** Wells and Seismic Data Availability

Well Name	Composite Log	Well Test	Biostratigraphy	Checkshot	Missing Log
7117/9-1	Yes	Dry	Yes	Yes	255-1200 MD
7117/9-2	Yes	Dry	Yes	Yes	1922 - 1980 MD
7216/11-1S	Yes	Dry	Yes	Yes	976 - 1383 MD
7218/11-1	Yes	Dry	No	Yes	453-1138 MD
7219/8-1S	Yes	Dry	Yes	Yes	400 - 2041 MD
73165-1	Yes	Gas	Yes	Yes	2914 - 2957 MD
Survey	Type	Lines	Survey	Type	Lines
NPD-BJV1- 86 NPDBJV2-86	2D	19	NH9703R99-PHASE2	2D	22
NPD-HB-86	2D	7	NPD-BJRE-84-NPD-FL-84	2D	20
NPD-BV-87	2D	3	NH9803-3D	3D	I: 1941 X: 6501
NPD-BJV2-86	2D	16	EL-0001-3D	3D	I: 1761 X: 3588
NPD-TR-82	2D	31	GVH-90	2D	42

### 3.1.1 Data Quality Control

Quality control is conducted in wells and seismic data in order to used as preparation of well seismic tie and petrophysical analysis (Volume Shale, Net to Gross, and Porosity). However, due to limited time and resource, the quality checking here only covering well log conditioning, seismic quality checking and checkshots data correction. Log conditioning will cover identification of spiked curves, discontinued logs curves, and normalisation of logs in all wells. Seismic quality checking equalises the ranges of energy and seismic

---

reflection colours of all surveys that used. While checkshot data correction is elimination of points of interval velocity that discrepant with other points in one well, as well as sonic calibration, and seismic well tie. These steps has conducted in previous study, Anindita (2018). figure 3.3.

## **3.2 Methodology**

This study conducted using 5 methods, there are :

1. Electrofacies Analysis for Sequence Stratigraphy.
2. Seismic Sequence Analysis and Seismic Facies Analysis.
3. Clinoform Analysis and Paleo-bathymetri Reconstructions.
4. Stratigraphic Forward Modelling.

The workflow of this study is explained in figure 3.5

### **3.2.1 Electrofacies Analysis for Sequence Stratigraphy**

Sequence stratigraphy is conducted in well logs curves mainly from Gamma Ray log, but sometimes involves several other logs, such as resistivity logs, and porosity logs. This interpretation includes volume shale, and net to gross calculation as cut-off to lithology interpretation based on Rider (2002).

This analysis will include analysis on logs shapes/patterns (Bell, Cylindrical, Funnel) and the stacking pattern of sedimentation packages (coarsening or fining upward) from lithology interpretation (Fig.3.6, also this analysis will focus on degree of sequence stratigraphy (parasequence, parasequence set, and sequence) and its sequence boundaries (SB, MFS, and TSE) (Fig.3.7). Lastly the interpretation will define system tract (Highstand, Lowstand, Transgressive, and Falling-stage), (Fig 3.8 of each ages as confirmation to seismic sequence stratigraphy for determining depositional environment.(Fig.3.9)

### **3.2.2 Seismic Sequence Stratigraphy**

Seismic Sequence Stratigraphy based on article of American Association of Petroleum Geologist Memoir No. 66, by (Mitchum Jr et al., 1977). He classified seismic characteristic into three different major parameters that we can see in figure 3.5. All these parameters can be inferred as geological information to interpret seismic data both 2D and 3D as in figure 3.13.(taken from Anindita (2018)),

### **3.2.3 Seismic Sequence Analysis**

As part of Seismic Sequence Stratigraphy seismic sequence analysis is focus on subdividing the seismic section into packages of concordant reflections separated by surfaces of discontinuity, and interpreting them as depositional sequences. This surfaces of discontinuity are called as reflection termination, in figure 3.10 one can see the characteristic of each termination and how they depicted in seismic section, taken from Anindita (2018).

---

### 3.2.4 Seismic Facies Analysis

seismic facies analysis is analysing the configuration, continuity, amplitude, frequency, and interval velocity of seismic reflection patterns within seismic sequence. Seismic reflector patterns are interpreted in terms of environmental setting and interpretation of lithology, (from Anindita (2018)). The example and observed characteristics of seismic reflection that can be inferred to seismic configuration and seismic external forms, can be seen in figure 3.12 and 3.13.

### 3.2.5 Clinoforms Analysis and Paleo-Bathymetri Reconstructions.

Clinoforms are basinward-dipping, chronostratigraphic stratal surfaces that constitute the dominant architectural component of most deltaic-to-continental-slope successions. Two clinoforms bound a sediment packages called Clinothem. They usually comprise a central seaward-dipping portion (fore set) and two gently dipping parts, respectively up-dip (top set) and down-dip (bottom set) of the foreset, even though the complete visualisation of a 'full' clinoform in seismic data is heavily reliant on seismic resolution and the acoustic impedance contrast across it. Clinoform cross-sectional profiles vary from planar to sigmoidal to concave-upward (or 'oblique'). In response to environmental forcing, basin physiography and average sediment grain-size. The cross-sectional geometry of clinoforms has therefore been used to characterise ancient environmental conditions, taken from Patruno et al. (2015). A Clinoform is divided into several parts based on elevation and slope of clinoform surface in certain point, see in figure 3.15. This clinoform parts is quantitatively defined in figure 3.16.

In implication for sequence stratigraphic models there are positive correlations exist between water depths of topset-to-foreset rollover points and various geometric and stratigraphic parameters (total relief, foreset height, topset height, bottomset height, duration, progradation resistance ratio). That means it is possible to quantitatively infer paleo-bathymetries of clinoform-bearing sedimentary successions once one or more of these parameters have been constrained. This has potentially important implications, as paleo-bathymetry is a crucial constraint for established sequence stratigraphic and quantitative stratigraphic techniques. This new technique to infer the palaeo-water depth at the rollover point, together with the geometric method proposed by for estimating the palaeo-bathymetry at any point on a clinoform surface away from the rollover, has the potential to complement palaeontologically-constrained palaeobathymetry estimates or to replace them completely in Patruno et al. (2015).(Fig.3.17 and Fig. ??)

In this study, Clinoform Analysis is conducted using SINTEF 2D Clinoform Analysis Software. This software is based on Patruno et al. (2015), and able to define the clinoform nomenclature along with its values based on seismic 2D section, then calculate it the correlation between clinoform parameters automatically, then the result converted into depth domain and reconstruct it into paleo-bathymetri 2D clinoform. Next step is populating the result of the 2D paleobathymetri clinoform to 3D map of each ages to make paleo-bathymetri as main input for simulator (GPM).

---

### 3.2.6 Stratigraphic Forward Modelling and Geological Process Modelling ©.

Stratigraphic Forward Modelling (SFM) is a technique that aims to model the processes of erosion, transport and deposition of clastic sediments, as well as carbonate growth and redistribution on the basis of quantitative deterministic physical principles Tetzlaff et al. (2014).

The technology adopted here is an experimental simulator called Geological Process Modeler (GPM) a plugin in Petrel 2017 ©Schlumberger which is implemented as a plugin within a major geologic modeling package. It is based on numerical sedimentary modeling principles that have been originally developed in the 1980's (Tetzlaff and Harbaugh 1989) Lejri et al. (2017).

During numeric modeling of sedimentation, the modeler is faced with assigning values to several parameters that are difficult to estimate (sediment input, sediment diffusion and transport coefficients, for various environments and sediment types). Even after a result has been achieved that approximately matches observations, the model is usually run several times varying the unknown parameters within ranges of uncertainty. The ranges of uncertainty are selected so that the differences between results and data do not exceed a predetermined value. The set of results is used for statistical inference of model results, providing information such as uncertainty in reservoir geometry and petrophysical parameters, as well as geostatistical information for detailed reservoir modeling (Doliguez et al. 1999); in Tetzlaff et al. (2014).

#### Basic input and boundary conditions

In GPM the user can choose which processes to model, but some input is common to all models (Fig. 3.18) Tetzlaff et al. (2014). This input consists of:

1. **Sediment component and their properties :**

GPM works with a small number of pure sediment components and their mixtures in all proportions. Typically, four components suffice, as for example, “gravel”, “sand”, “silt” and “clay”, or “reef carbonate”, “silt”, “clay 1” and “clay 2. The user also need to define the value of this component including grain density, grain size, compaction coefficient, initial depositional porosity, and permeability, and in case of carbonates, growth rate dependency on light and wave action. Tetzlaff et al. (2014).

2. **Pre-existing basin configuration :**

this is typically a surface represents a basin floor or basement this can be obtained with many methods, seismic reconstruction or palinspatic analysis, but in this study, the paleo-bathymetri acquired based on clinofom analysis.

3. **Sources, sink, boundary conditions :**

This element defines trend of sedimentation and type of flow that will occurred This information obtained from regional geology and sedimentological concept, specifically in deep-marine deposit in Southwestern Barent Sea. this study used reference from Omosanya et al. (2016) Marheni et al. (2015) Faleide et al. (1996).

---

#### 4. **Sea level curve :**

this element defined the sea level change of area that will influence the behaviour of sedimentation process. There are already two sea level curves by default in GPM, from Haq et al, and Exxon. However in this study, sea level change curves is taken and used from Miller et al. (2005), which considerably much more detail, especially in Miocene to Pleistocene epoch.

#### 5. **Modelling Time interval :**

This element defines the duration of sedimentation that will be simulates. the duration is typically defined by the age of specific paleo-basement/paleo-bathymetri which is one of element in these basic inputs.

### **Diffusion**

Perhaps the simplest way to model sediment transport processes is diffusion. Diffusion simply assumes that sediment will move down slope at a rate proportional to the slope and to sediment characteristics (fine sediment will move farther than coarse sediment). Diffusion is often used in conjunction with other sediment transport modelling methods in order to model processes that occur at a sub-cell scale. For example, fluvial action would only move sediment within the river's flow, and would not affect any sediment above water. Therefore river banks would become vertical. In reality, this might not happen because there are slumps, soil creep, and biological activity that cause the banks to slope. Tetzlaff et al. (2014)

These processes typically occur at a scale smaller than one cell in the model, and can be jointly modelled by diffusion. Diffusion does not occur equally everywhere. It is often a function of elevation or depth below sea level. Therefore, the software accepts a vertical diffusion curve. If wave action is not modelled separately (as described later in this paper), it may be approximated by using a diffusion curve with high values at sea level, decreasing exponentially with depth. Diffusion may also be used to model the erosion of high mountains by glacial action in first approximation (without expecting details of glacial land-forms). Tetzlaff et al. (2014).

The diffusion curve has a strong impact on erosion, sequence thickness and delta front slope; e.g. using an inappropriate diffusion curve can lead to a lack of sediments in the distal region of the model. Lejri et al. (2017). The diffusion equation that used in this study is explained below Lejri et al. (2017):

$$\frac{dZ}{dT} = K \nabla^2 * Z \quad (3.1)$$

Where :

Z = Topographic/basement elevation

K = Diffusion coefficient

T = Time

$\nabla^2 * Z$  = Laplacian of Z



---

## Free surface flow and sediment transport.

Free surface water flow (by rivers, floods, turbidity currents, long shore currents) is the most ubiquitous mechanism of sediment transport. It is notoriously difficult to model with engineering precision. In a geologic setting this difficulty increases because the flow may be unsteady and the topographic surface and source intensity are constantly changing through geologic time. Tetzlaff et al. (2014)

The GPM model provides two ways of simulating flow:

1. Steady flow is used when flow velocity and depth do not change rapidly through time, e.g. like in a river at normal stage. 3.19
2. Unsteady flow is used when flow velocity and depth change rapidly as in a turbidity current or a river flood. 3.20

All flow in nature eventually changes and is thus unsteady. There is no clear division between the two processes, and some flow models might be simulated by either method. In general, when the flow does not change appreciably over the course of a few hours, it can be considered steady for the purpose of GPM. Tetzlaff et al. (2014) Numerically, steady flow is modeled using a finite-difference scheme within a rectangular grid. Unsteady flow is modeled with a “particle-in-cell” method, which uses a large number of particles (or fluid elements), each of which representing a finite volume of fluid, while a grid keeps track of the local depth and average flow velocity. (Grigoryev et al. 2002)

There are two more geological process setting that available in GPM, there are :

1. Wave action
2. Carbonate growth

However in this study, those two element will not applied due to its absent in geological condition of Sørvestsnaget Basin, as Deep-water/Deep-Marine Environment.

## Tectonics

In the present version of GPM, tectonics can be represented in the form of vertical movement of the basement which raises or lowers the overlying sediments. It is possible to model vertical faults, subsidence or uplift, the vertical component of folds, tilting, and the surface effect of diapirs. Tectonic movement is specified in the form of a surface in which each node contains the local uplift rate in units of meters per 1,000 years. Negative uplift corresponds to subsidence. In order to model faults, the user generates a surface that contains a sharp boundary of uplift rates. One side of the boundary will move at a different rate than the other side, thereby modelling a vertical fault. It is also possible to model tectonics at rates that vary – or even reverse – through time. This is achieved by specifying a curve that contains multiplier values (positive, zero, or negative) that vary as a function of time. The multiplier value of the curve for a given time is applied to the tectonic rate surface, to yield an uplift value for a given place and time. Thus it is possible to model tectonic movement that varies through both space and time. Tetzlaff et al. (2014).

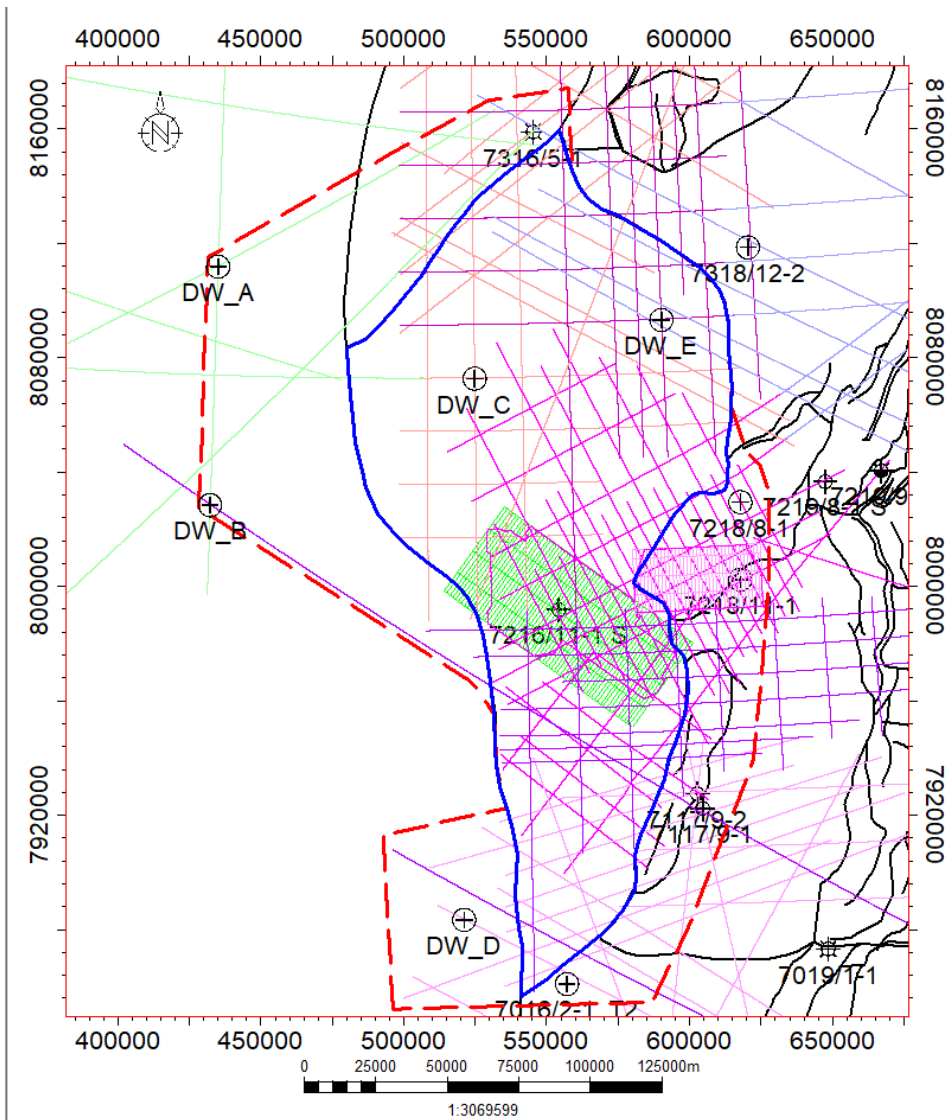
---

## **Compaction**

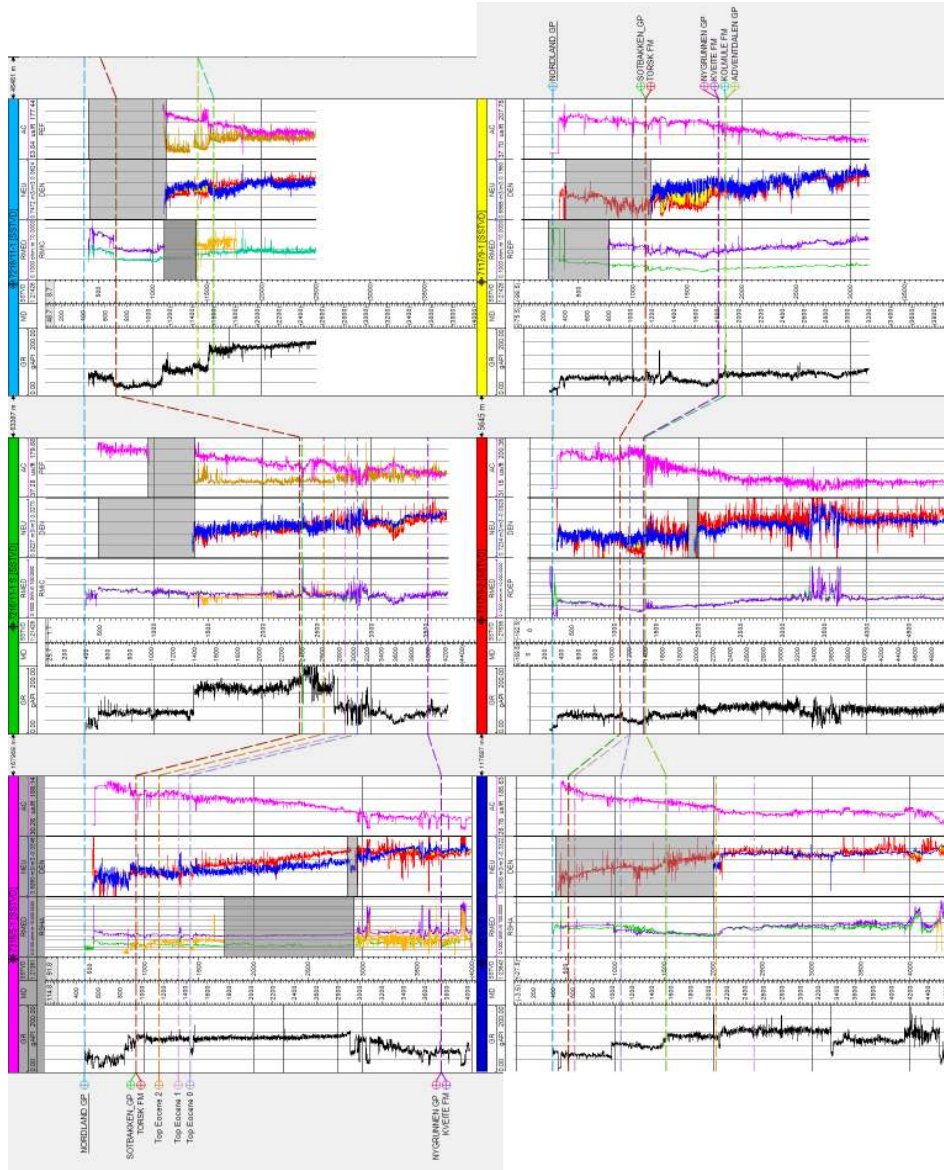
Presently, GPM contains an algorithm for sediment compaction based on simple load. It models the elastic compaction of sediment due to the load above it. Despite its simplicity, it is adequate to model the increase in accommodation space due to compaction and the ensuing changes in sedimentation patterns, as well as the changes in geometry and thickness due to differential compaction of contrasting lithologies such as sand and shale. A model of compaction that takes into account pore pressure and fluid flow in full three dimensions within the sediment accumulation is in preparation. This algorithm is similar to the ones used in basin modeling programs. This will result in more realistic compaction calculations, and will enable the use of GPM as a tool to predict overpressure, independently from other methods (such as seismic velocities) and possibly with more precision than basin modeling programs due to the higher stratigraphic resolution of GPM. Tetzlaff et al. (2014).

## **Limitation**

GPM only models sedimentation, but not post-depositional processes other than compaction. Full understanding of diagenetic processes (i.e., compaction, cementation, grain replacement and dissolution), would require running a separate package to model in detail. However, GPM does provide the setting for the geological evolution for every volume of sediment (depth of deposition, primary lithology, overburden, and compaction), thus adding greater certainty and detail about deposition and burial history, so that some diagenetic effects could be better understood when evaluating reservoir quality risk. Tetzlaff et al. (2014)



**Figure 3.1:** The blue solid line is Sørvestsnaget Basin boundary, while the red dashed-line is the boundary of seismic interpretation. Well DW-A,B,C,D, and E are dummy wells for Time-Depth Conversion since Velocity Model is not available.



**Figure 3.2:** Well Correlation with standard markers from NPD in West Barents Sea, flattened on Nordland GP as datum. The grey boxes indicate interval of missing curve logs. Well names from upper left to bottom right: 73165-1, 7216/-11-1S,

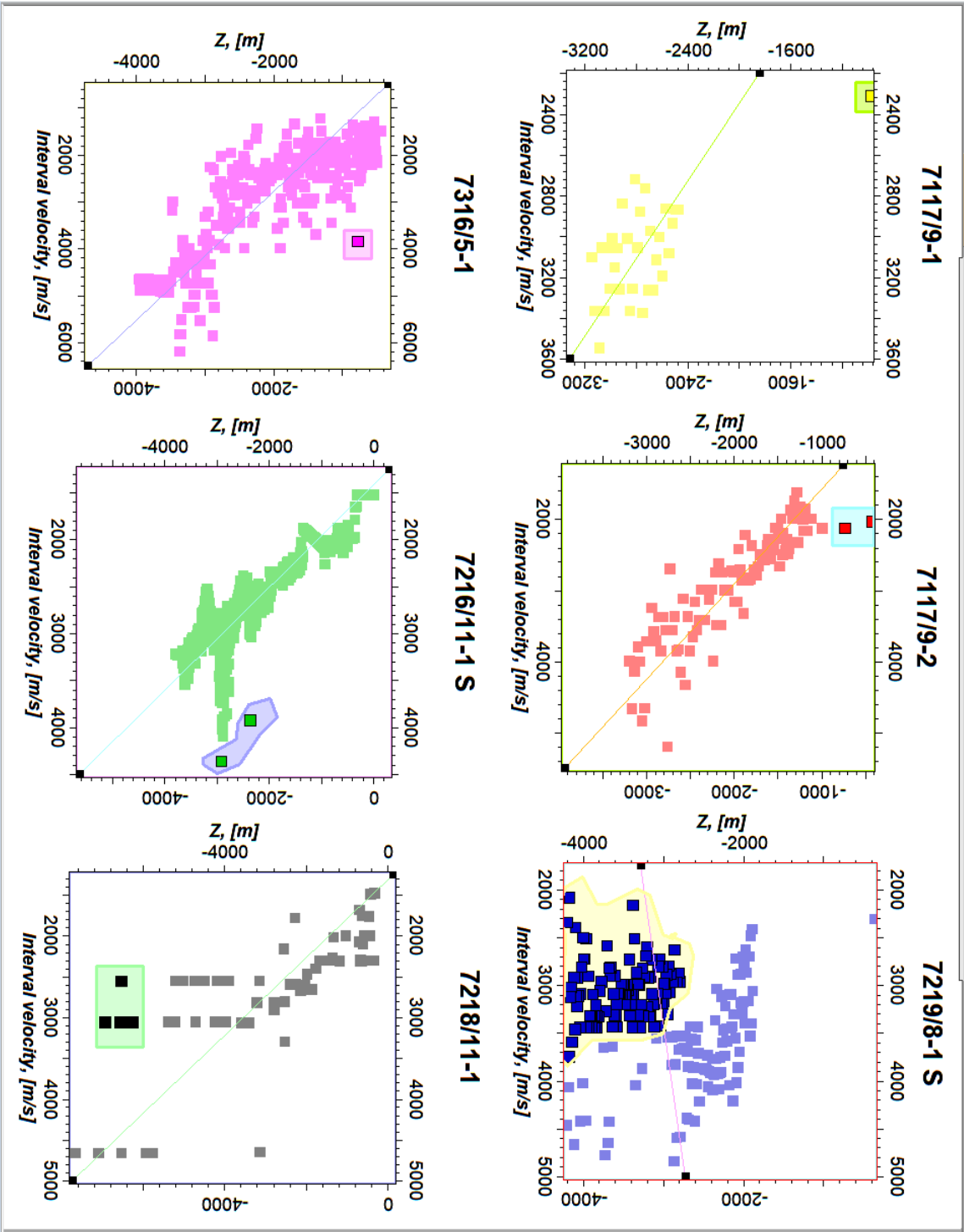
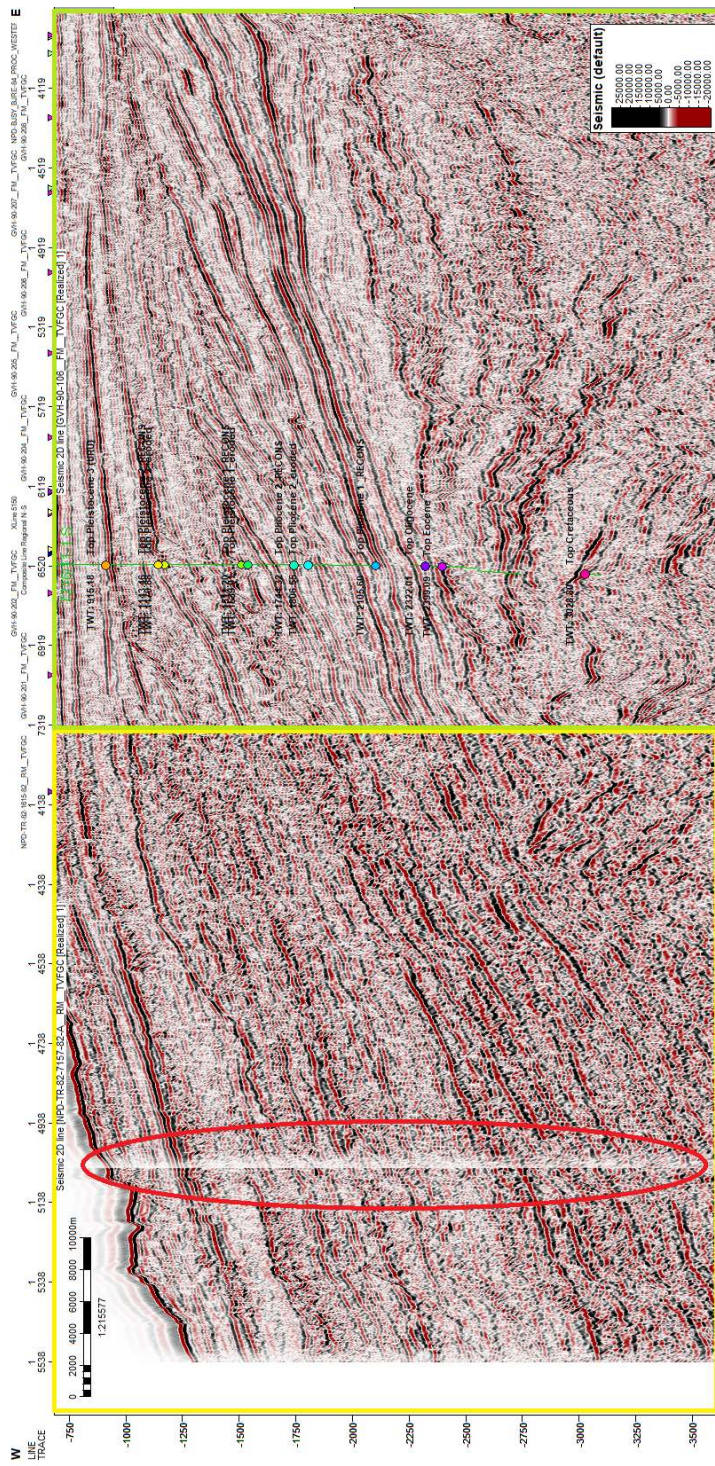


Figure 3.3: Checkshots of All well which used in this study. the highlight points showing some error data, which need correction. Anindita (2018)





**Figure 3.4:** The comparison between line NPD-TR-82-7157-82-A-RMTVFGC (yellow rectangle = poor condition) and GVH-90-106-FM-TVFGC (green rectangle = good condition), red circle showing seismic noise.

# Workflow

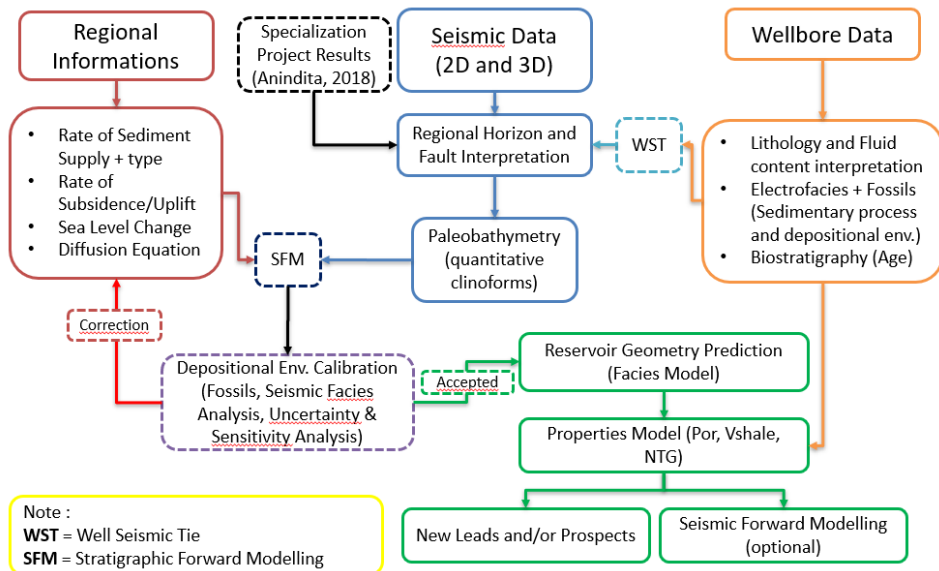
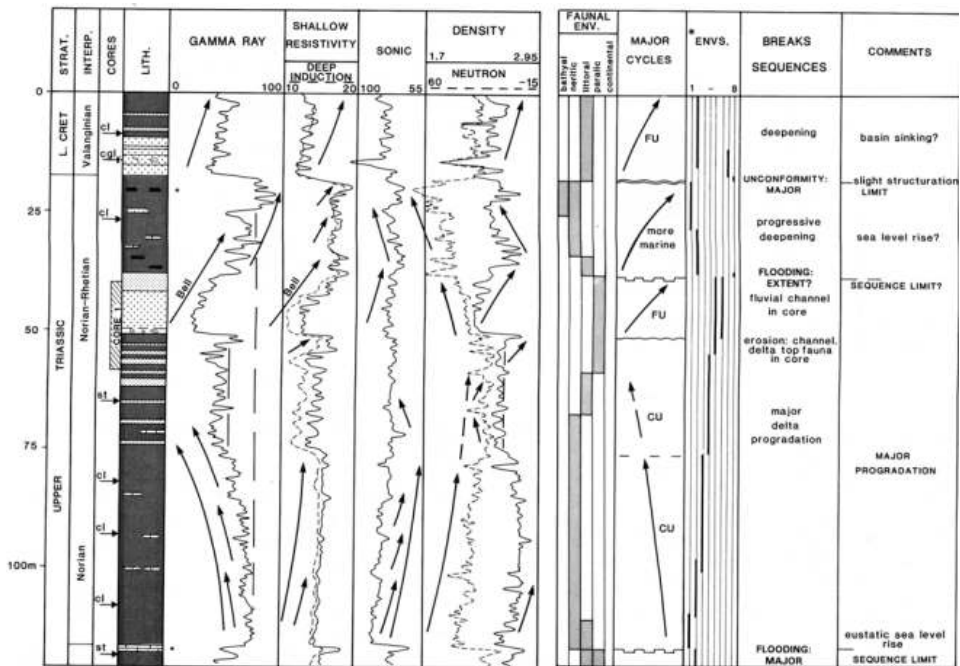
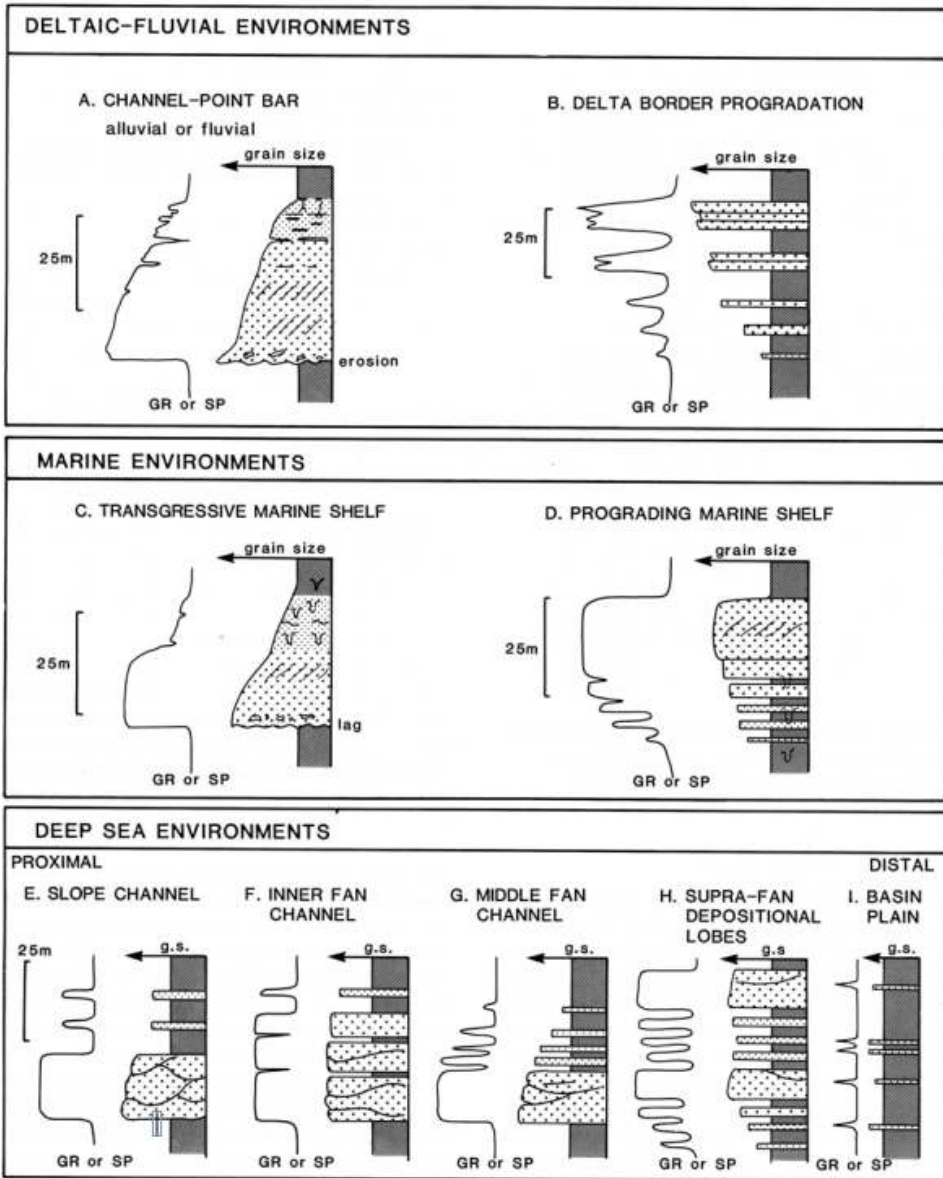


Figure 3.5: Workflow for Paleobathymetry Reconstructions and Stratigraphic Forward Modelling.



**Figure 3.6:** Basic Log shapes, stacking patterns, and grain size - gamma ray correlations taken from Rider (2002).





**Figure 3.7:** Facies indications from Gamma Ray (or SP) log shapes. These are idealised examples both of log shape and sedimentological facies. taken from Rider (2002).

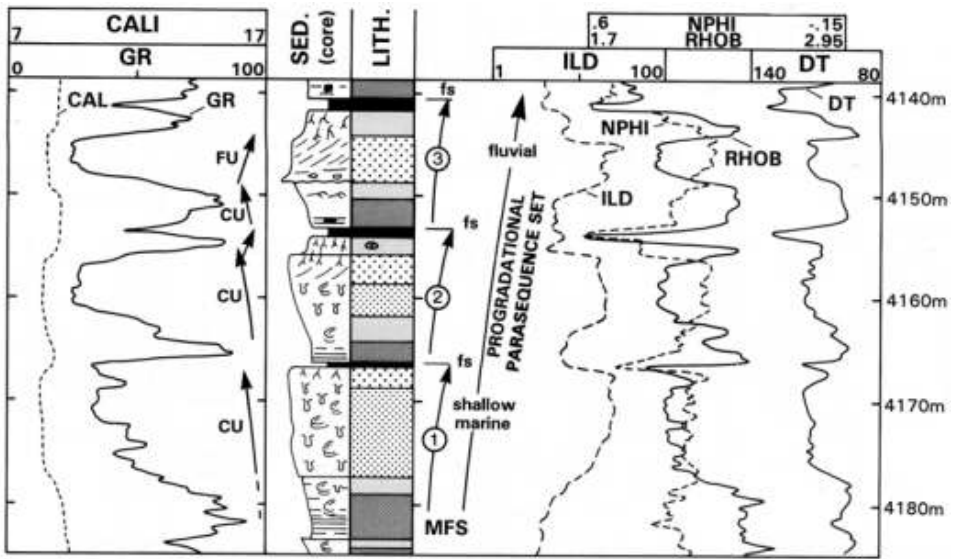
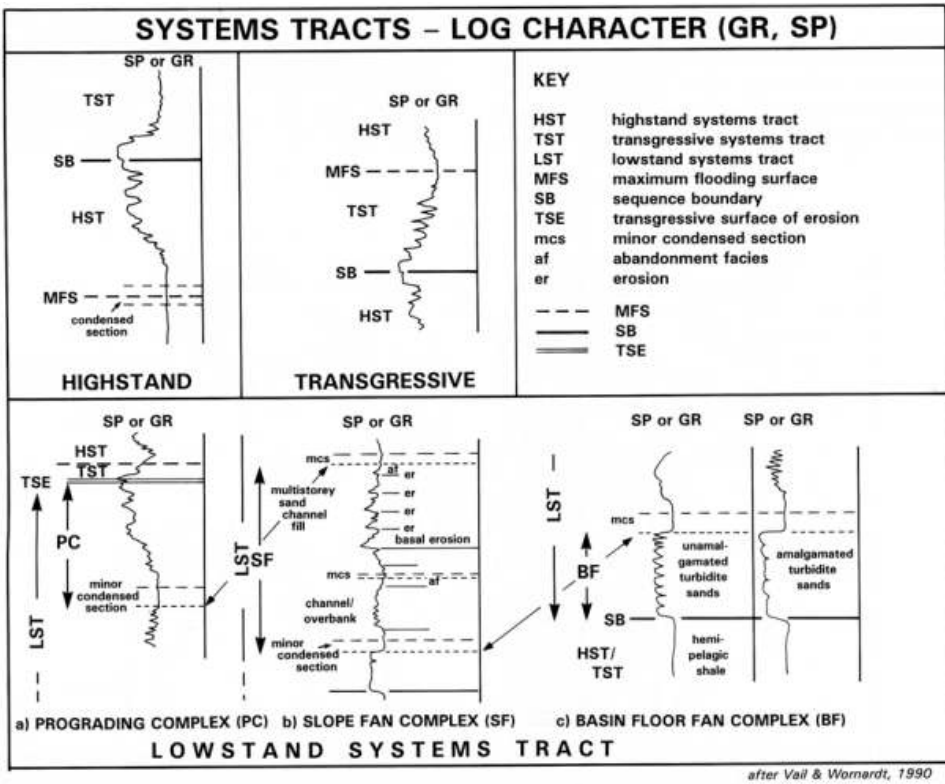


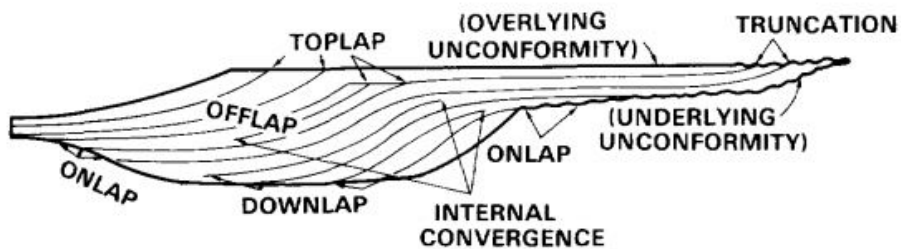
Figure 3.8: Degree of sequence in well log analysis taken from Rider (2002).



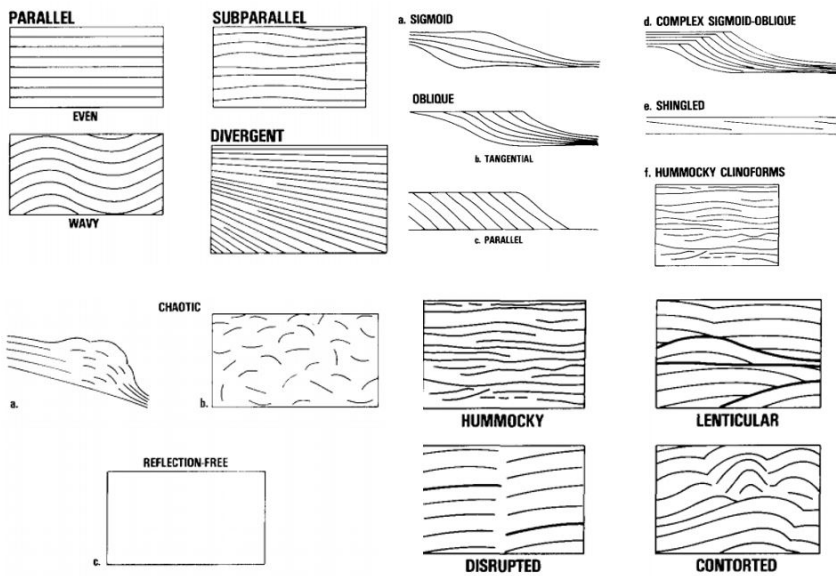
**Figure 3.9:** System tract and its depositional environment interpretation. taken from Rider (2002).

<u>REFLECTION TERMINATIONS (AT SEQUENCE BOUNDARIES)</u>	<u>REFLECTION CONFIGURATIONS (WITHIN SEQUENCES)</u>	<u>EXTERNAL FORMS (OF SEQUENCES AND SEISMIC FACIES UNITS)</u>
<u>LAPOUT</u>	<u>PRINCIPAL STRATAL CONFIGURATION</u>	<u>SHEET</u>
<u>BASELAP</u>	<u>PARALLEL</u>	<u>SHEET DRAPE</u>
<u>ONLAP</u>	<u>SUBPARALLEL</u>	<u>WEDGE</u>
<u>DOWNLAP</u>	<u>DIVERGENT</u>	<u>BANK</u>
<u>TOPLAP</u>	<u>PROGRADING CLINIFORMS</u>	<u>LENS</u>
<u>TRUNCATION</u>	<u>SIGMOID</u>	<u>MOUND</u>
<u>EROSIONAL</u>	<u>OBLIQUE</u>	<u>FILL</u>
<u>STRUCTURAL</u>	<u>COMPLEX SIGMOID-OBLIQUE</u>	
<u>CONCORDANCE</u>	<u>SHINGLED</u>	
(NO TERMINATION)	<u>HUMMOCKY CLINIFORM</u>	
	<u>CHAOTIC</u>	
	<u>REFLECTION-FREE</u>	
	<u>MODIFYING TERMS</u>	
	<u>EVEN</u> <u>HUMMOCKY</u>	
	<u>WAVY</u> <u>LENTICULAR</u>	
	<u>REGULAR</u> <u>DISRUPTED</u>	
	<u>IRREGULAR</u> <u>CONTORTED</u>	
	<u>UNIFORM</u>	
	<u>VARIABLE</u>	

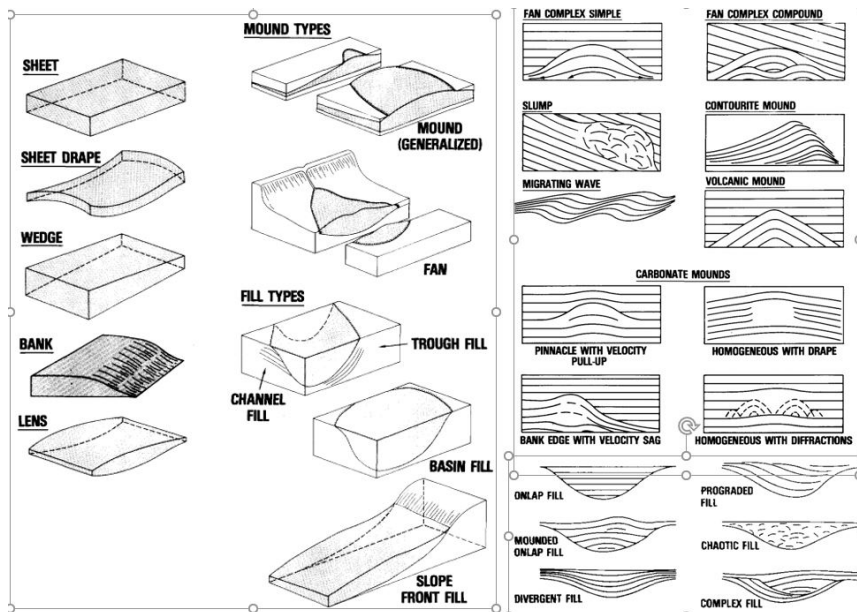
**Figure 3.10:** Geological Interpretation of Seismic Facies Parameters.(Mitchum *et al* 1977)



**Figure 3.11:** Seismic stratigraphic reflection terminations within idealised seismic sequence. (Mitchum *et al* 1977)



**Figure 3.12:** Seismic stratigraphic reflection configuration within idealised seismic sequence. (Mitchum *et al* 1977)

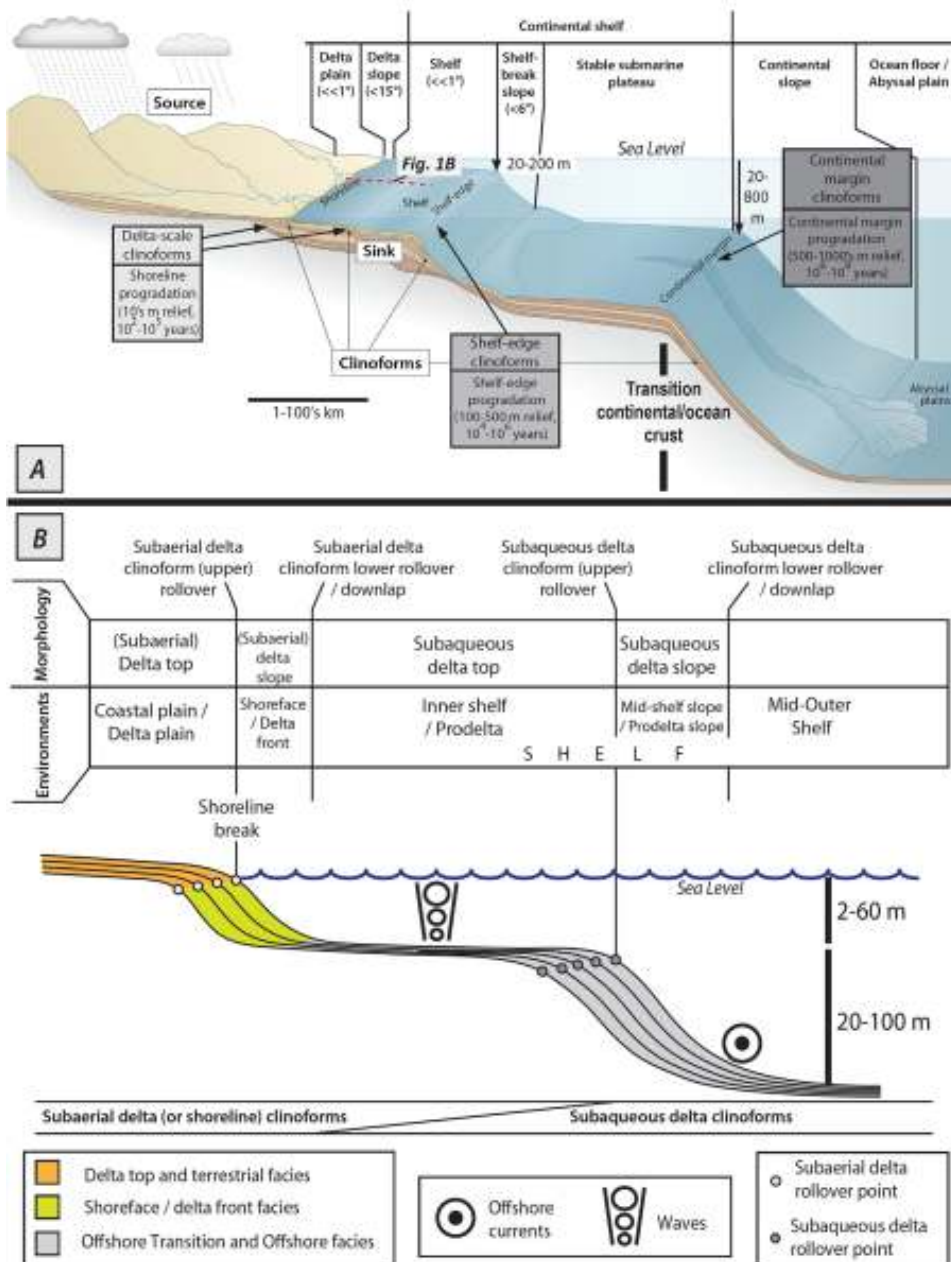


**Figure 3.13:** Seismic stratigraphic external forms within idealised seismic sequence. (Mitchum *et al* 1977)

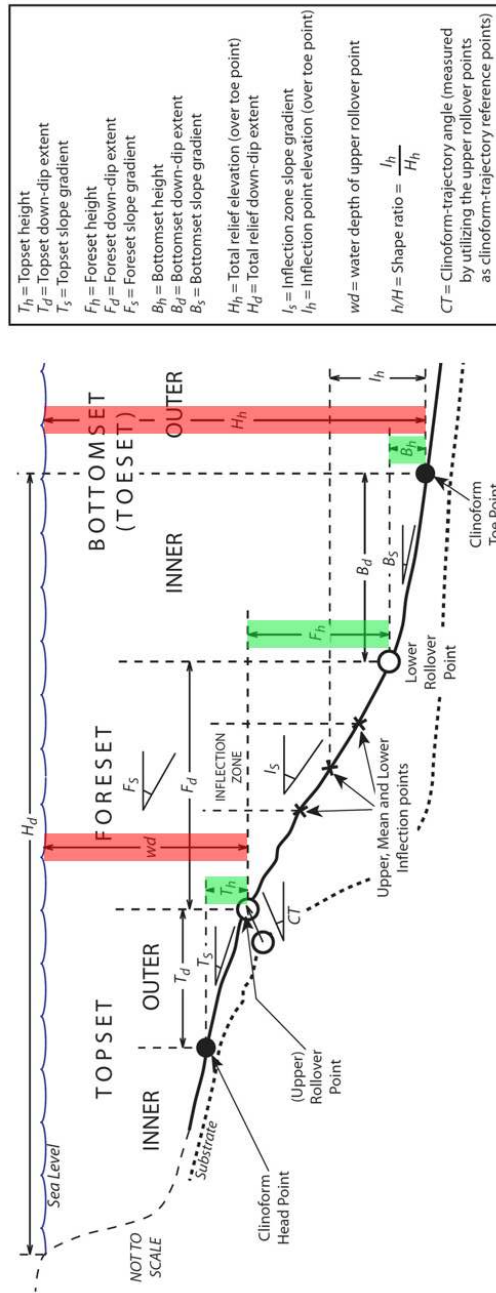
---

<u>SEISMIC FACIES PARAMETERS</u>	<u>GEOLOGIC INTERPRETATION</u>
REFLECTION CONFIGURATION	<ul style="list-style-type: none"> <li>• BEDDING PATTERNS</li> <li>• DEPOSITIONAL PROCESSES</li> <li>• EROSION AND PALEOTOPOGRAPHY</li> <li>• FLUID CONTACTS</li> </ul>
REFLECTION CONTINUITY	<ul style="list-style-type: none"> <li>• BEDDING CONTINUITY</li> <li>• DEPOSITIONAL PROCESSES</li> </ul>
REFLECTION AMPLITUDE	<ul style="list-style-type: none"> <li>• VELOCITY-DENSITY CONTRAST</li> <li>• BED SPACING</li> <li>• FLUID CONTENT</li> </ul>
REFLECTION FREQUENCY	<ul style="list-style-type: none"> <li>• BED THICKNESS</li> <li>• FLUID CONTENT</li> </ul>
INTERVAL VELOCITY	<ul style="list-style-type: none"> <li>• ESTIMATION OF LITHOLOGY</li> <li>• ESTIMATION OF POROSITY</li> <li>• FLUID CONTENT</li> </ul>
EXTERNAL FORM & AREAL ASSOCIATION OF SEISMIC FACIES UNITS	<ul style="list-style-type: none"> <li>• GROSS DEPOSITIONAL ENVIRONMENT</li> <li>• SEDIMENT SOURCE</li> <li>• GEOLOGIC SETTING</li> </ul>

**Figure 3.14:** Seismic stratigraphic external forms within idealised seismic sequence. (Mitchum *et al* 1977)



**Figure 3.15:** Cross-sectional schemes parallel to the depositional dip, showing idealised compound clinoform systems at different scales. (A) Regional cross-section, highlighting three actively growing clinoforms systems: delta, shelf-edge and continental-margin scale clinoforms (Modified after Henriksen et al. (2009)). (B) Cross-section through the nearshore to inner marine shelf area, showing a typical shoreline to delta-scale sub-aqueous clinoform compound system, (modified after Helland-Hansen and Hampson, 2009) in Patruno et al. (2015).

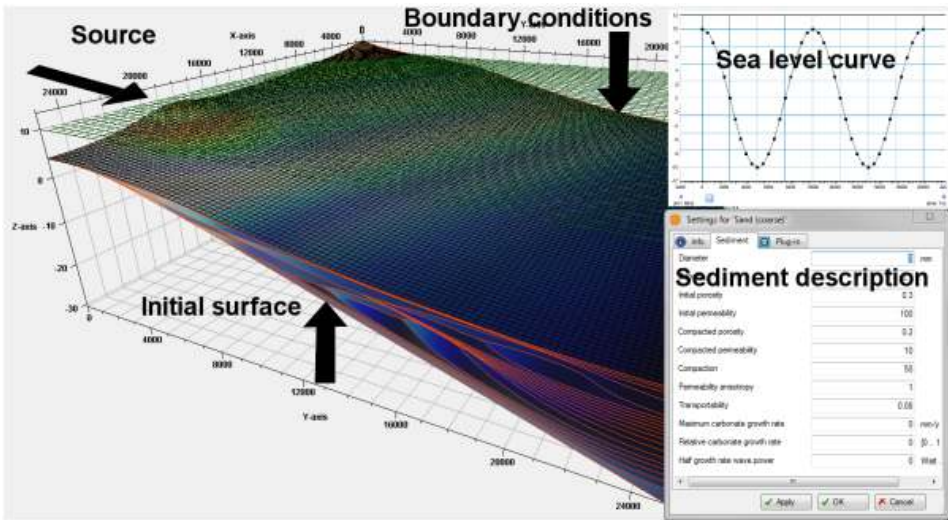


**Figure 3.16:** Clinoform nomenclature and explanation of abbreviations (adapted from Patruño et al. (2015)). Red indicates parameters related to Paleo-Water Depth, green are geometric parameters for which relationships with Paleo-Water Depth are available in SINTEF 2D Clinoform Analysis.

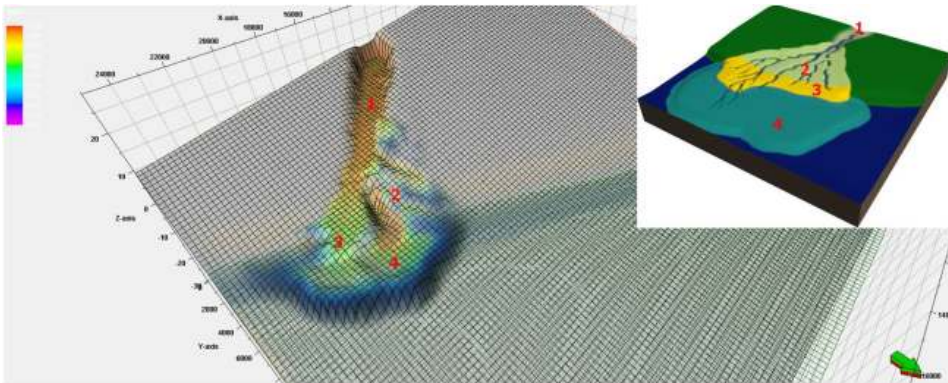


Correlations		All clinoforms		Sand-prone subaqueous delta clinoforms	
No.	Type	Regression equation	No.	Type	Regression equation
1	Positive polynomial	$Fh = [4 \cdot 10^{-5}(Hh)^2 + 0.271(Hh) - 4.331] (R^2 = 0.98)$	-	Positive weak correlation ( $R^2 \leq 0.40$ )	
2	Positive polynomial	$Bh = [-10^{-5}(Hh)^2 + 0.161(Hh) - 2.101] (R^2 = 0.80)$	-	Positive, weak correlation ( $R^2 \leq 0.30$ )	
3	Positive polynomial	$Th = [-2 \cdot 10^{-5}(Hh)^2 + 0.11(Hh) + 0.471] (R^2 = 0.7551)$	-	No correlations at all ( $R^2 \leq 0.12$ )	
7	Positive power	$Fh = [0.4859(Hh)^{0.8881}] (R^2 = 0.8834)$	36	Positive power	$Fd = [1.2386(Hd)^{0.8588}] (R^2 = 0.62)$
8	Positive polynomial	$Bd = [8 \cdot 10^{-5}(Hd)^2 + 1.721(Hd) + 2.7524] (R^2 = 0.91)$	-	Positive, weak correlation ( $R^2 \leq 0.50$ )	
9	Positive power	$Fh = [0.271(Hh)^{0.94}] (R^2 = 0.94)$	38	Positive power	$Td = [0.43(Hd)^{0.891}] (R^2 = 0.63)$
10	Positive power	$Fs = [0.24(Ss)^{0.94}] (R^2 = 0.98)$	42	Positive power	$Fs = [0.77(Ss)^{0.9691}] (R^2 = 0.97)$
11	Positive power	$Fs = [0.27(Ss)^{0.88}] (R^2 = 0.84)$	43	Positive power	$Bs = [0.45(Ss)^{0.73}] (R^2 = 0.695)$
12	Positive power	$Ts = [0.265(Ts)^{0.881}] (R^2 = 0.84)$	45	Positive power	$Ts = [0.43(Ss)^{0.609}] (R^2 = 0.72)$
13	Positive power	$Bh = [0.19(Fh)^{0.688}] (R^2 = 0.75)$	-	No correlations at all ( $R^2 \leq 0.1$ )	
14	Positive polynomial	$Th = [-3 \cdot 10^{-5}(Hh)^2 + 0.135(Hh) + 2.231] (R^2 = 0.68)$	46	Negative power	$Fs = [794.68(Fs)^{-0.921}] (R^2 = 0.89)$
-	Negative, weak correlation ( $R^2 \leq 0.38$ ) (relationship breaks down at $Fd > 2000$ m)		47	Positive polynomial	$Bd = [0.0002(Fd)^2 + 0.04(Fd) + 77.481] (R^2 = 0.84)$
17	Positive power	$Bd = [0.21(Fd)^{0.841}] (R^2 = 0.83)$	49	Positive polynomial	$Td = [-2 \cdot 10^{-5}(Fd)^2 + 0.58(Fd) - 2.17] (R^2 = 0.745)$
18	Positive power	$Td = [0.9062(Fd)^{0.881}] (R^2 = 0.82)$	50	Positive power	$Bd = [0.5559(Fs)^{0.711}] (R^2 = 0.70)$
19	Positive power	$Bs = [0.594(Fs)^{0.881}] (R^2 = 0.825)$	54	Positive power	$Ts = [0.528(Fs)^{0.681}] (R^2 = 0.72)$
20	Positive power	$Bd = [0.2327(Fs)^{0.921}] (R^2 = 0.85)$	-	Positive, weak correlation ( $R^2 \leq 0.33$ )	
21	Positive polynomial	$Th = [0.0546(Bh)^2 + 74.57(Bh) + 1354.41] (R^2 = 0.62)$	-	No correlations at all ( $R^2 \leq 0.1$ )	
22	Positive polynomial	$Th = [-5 \cdot 15 \cdot 10^{-4}(Bh)^2 + 6.217(Bh) + 2.6899] (R^2 = 0.78)$	55	Negative power	$Bs = [440.265(Bs)^{-0.6651}] (R^2 = 0.61)$
24	Negative, weak correlation ( $R^2 \leq 0.33$ ) (relationship breaks down at $Fd > 2000$ m)		56	Positive polynomial	$Td = [0.0001(Bd)^2 + 0.40(Bd) + 78.35] (R^2 = 0.76)$
25	Positive power	$Td = [12.714(Bd)^{0.861}] (R^2 = 0.7458)$	57	Positive power	$Ts = [1.1535(Bs)^{0.951}] (R^2 = 0.53)$
27	Negative power	$Ts = [0.8653(Bs)^{-0.94}] (R^2 = 0.805)$	58	Negative power	$Ts = [125.949(Td)^{-0.541}] (R^2 = 0.63)$
28	Negative power	$Sv = [95.827(Age)^{-0.6691}] (R^2 = 0.57)$	60	Negative power	$Sv = [2.1202(Age)^{-0.741}] (R^2 = 0.63)$
29	Negative power	$P = [1.9(Age)^{-0.881}] (R^2 = 0.73)$	61	Negative power	$P = [9930.6(Age)^{-0.761}] (R^2 = 0.73)$
32	Maximum point at $Sv \approx 200$ m/Myr, $R \approx 0.6$	$F = [0.067(Sv)^{0.681}] (R^2 = 0.72)$	62	Positive polynomial	$F = [10^{-4}(Sv)^2 - 0.0051(Sv) + 9.68] (R^2 = 0.83)$
33	Maximum point at $Sv \approx 200$ m/Myr, $R \approx 0.6$	$F = [8.95 \cdot 10^{-4}(R)^{0.71}] (R^2 = 0.87)$	63	Positive power	$F = [3 \cdot 10^{-5}(Sv)^{0.741}] (R^2 = 0.74)$
-	Positive power		64	Positive power	$F = [0.0013(R)^{0.681}] (R^2 = 0.71)$
All clinoforms					
No.	Type	Regression equation	No.	Type	Regression equation
4	Positive linear <sup>a</sup>	$Age = [0.03(Hh) - 1.363] (R^2 = 0.57)$	-	No correlation at all ( $R^2 \leq 0.10$ )	
5	Positive polynomial	$P = [5 \cdot 10^{-4}(Hh)^2 - 4 \cdot 10^{-2}(Hh) + 0.011] (R^2 = 0.60)$	-	Positive, weak correlation ( $R^2 \leq 0.17$ )	
6	Positive linear	$Wd = [0.48(Hh) + 16.331] (R^2 = 0.83)$	35	Negative power	$Is = [935.31(Hd)^{-0.754}] (R^2 = 0.60)$
10	Negative, weak correlation ( $R^2 \leq 0.34$ ) (relationship breaks down at $Hd > 5000$ m)		37	Negative power	$Fs = [876.14(Hd)^{-0.784}] (R^2 = 0.63)$
11	Negative, weak correlation ( $R^2 \leq 0.3751$ ) (relationship breaks down at $Hd > 5000$ m)		39	Negative logarithmic <sup>a</sup>	$h/H = [-0.09 \ln(Hd) + 0.97] (R^2 = 0.50)$
-	No correlation at all ( $R^2 \leq 0.1$ )		40	Positive power	$Sv = [0.00021(Hd)^{0.834}] (R^2 = 0.73)$
-	Positive <sup>b</sup> , weak correlation ( $R^2 \leq 0.38$ ) (relationship breaks down at $l^* < l_s < 10^3$ )		44	Negative power	$Td = [120.111(S)^{-0.655}] (R^2 = 0.72)$
15	Negative, weak correlation ( $R^2 \leq 0.34$ ) (relationship breaks down at $l^* < l_s < 20^3$ )		41	Negative power	$Fd = [1460.5(S)^{-0.961}] (R^2 = 0.84)$
16	Positive polynomial	$P = [7 \cdot 10^{-4}(Hh)^2 - 4 \cdot 10^{-2}(Hh) + 0.0056] (R^2 = 0.60)$	-	No correlation at all ( $R^2 \leq 0.1$ )	
17	Positive polynomial	$Wd = [-1.08 \cdot 10^{-4}(Hh)^2 + 0.819(Hh) + 13.101] (R^2 = 0.81)$	-	No correlation at all ( $R^2 \leq 0.1$ )	
18	Negative, weak correlation ( $R^2 \leq 0.38$ ) (relationship breaks down at $Fd > 2000$ m)		48	Negative exponential	$Bs = [3.50e^{-0.0041Hh}] (R^2 = 0.70)$
19	Negative, weak correlation ( $R^2 \leq 0.33$ ) (relationship breaks down at $Fd > 2000$ m)		50	Negative power	$Ts = [54.52(Fd)^{-0.644}] (R^2 = 0.68)$
-	Negative, weak correlation ( $R^2 \leq 0.28$ )		51	Negative power	$Bd = [3377.49(Fs)^{-0.71}] (R^2 = 0.57)$
-	Negative, weak correlation ( $R^2 \leq 0.28$ )		53	Negative power	$Td = [539.34(Fs)^{-0.941}] (R^2 = 0.74)$
23	Positive polynomial	$Wd = [-0.0111(Bh)^2 + 7.36(Bh) - 19.111] (R^2 = 0.75)$	-	No correlation at all ( $R^2 \leq 0.1$ )	
26	Positive polynomial	$Wd = [-0.0094(Hh)^2 + 8.23(Hh) - 1.521] (R^2 = 0.70)$	59	Positive power	$Sv = [0.096(Fd)^{1.693}] (R^2 = 0.65)$
29	Positive polynomial	$Wd = [3 \cdot 10^{-5}(Age)^2 - 0.0009(Age) + 0.00951] (R^2 = 0.88)$	-	Minimum point at $Age \approx 0.01$ Myr, $R \approx 5 \cdot 10^{-4}$	
30	Positive polynomial	$Wd = [-0.073(Age)^2 + 19.49(Age) + 48.14] (R^2 = 0.72)$	-	Positive, weak correlation ( $R^2 \leq 0.11$ )	
31	Positive power <sup>a</sup>	$P = [521.81(Age)^{0.561}] (R^2 = 0.68)$	-	Positive, weak correlation ( $R^2 \leq 0.26$ )	
34	Positive polynomial	$Wd = [-4.785(R)^2 + 605.03(R) + 30.231] (R^2 = 0.77)$	-	Positive, weak correlation ( $R^2 \leq 0.19$ )	

Figure 3.17: Equations describing best-fit lines between parameter pairs showing a moderate-to-strong correlation ( $R^2 > 0.5$ ) in Patruno et al. (2015)

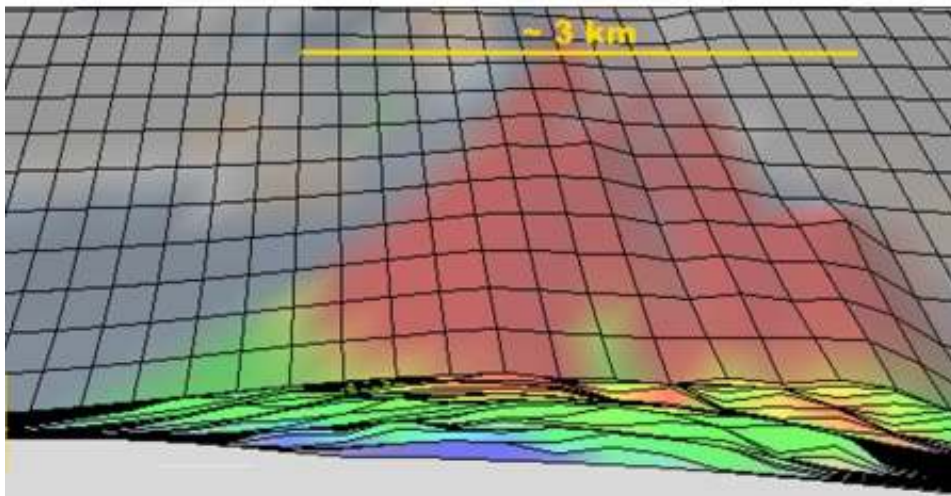
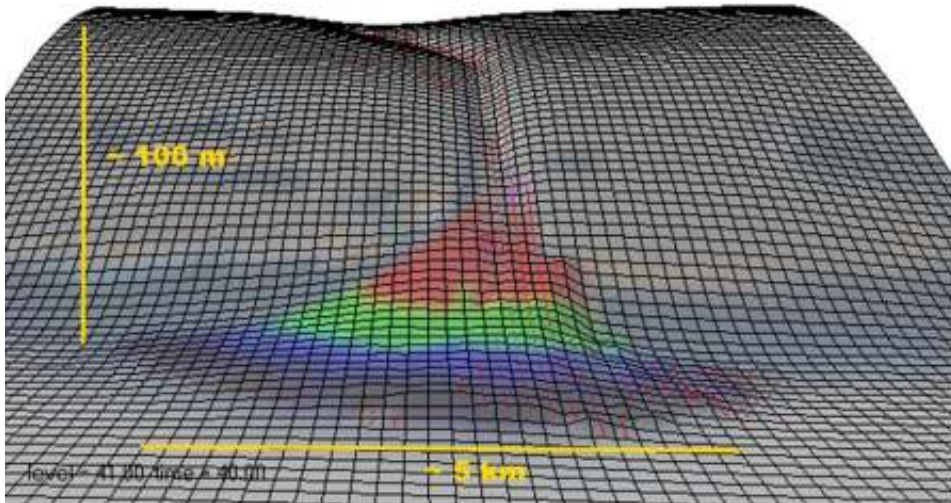


**Figure 3.18:** Geological Process Modelling basic input, Tetzlaff et al. (2014)



**Figure 3.19:** Steady flow and transport example showing the formation of a river valley and a fan delta under constant sea level. Four sediment types were used: Coarse sand (red), fine sand (green), silt (blue) and clay (black). Schematic block diagram of main deltaic environments is shown on the upper right: 1. Alluvial valley, 2. Delta plain, 3. Active delta, 4. Undersea delta plain., Tetzlaff et al. (2014)





**Figure 3.20:** Unsteady flow and transport example showing the formation of turbidite fan after 100 flows. Sediment types are the same as those used in Fig. 2. Upper figure shows carved valley and entire fan. Lower figure shows detailed transversal section of fan., Tetzlaff et al. (2014)

# Results

## 4.1 Seismic Well-Tie

Seismic well tie is a process of correlating well data information, which most of it based on elevation domain (meter or  $m$ ), into seismic data in same domain, usually in time (millisecond or  $ms$ ). In summary, the table below showing correlation between well marker and seismic wavelet in table 4.1 and Fig.4.1, (taken from Anindita (2018).)

### 4.1.1 Sonic Calibration

Sonic log is calibrated in order to accurately hangs the sonic log in time and corrects the log velocities to time-depth data (typically checkshots data). The calibrated sonic log can generate time-depth relationship (Schlumberger, 2017). It is used as the preferred time-depth relationship for the well of study. Some problem occurred when conducted this stage because of missing value in Sonic log, see in figure 4.2, (taken from Anindita (2018)).

### 4.1.2 Synthetic Generation

Synthetic seismograms are the bridges between geological information (well data in depth) and geophysical information (seismic in time). In this procedure the reflectivity coefficient and acoustic impedance, but most important is to check the correlation between well top marker and seismic wavelet, whether it correlates into peak or trough, as guidance in horizon interpretation. In this study due to missing value in Sonic and Density log also the deviation of well there are some unmatched synthetic generation with the wavelet of the seismic, see in figure 4.3, taken from Anindita (2018)).

**Table 4.1:** Summary of correlation between well marker and seismic wavelet in well 7216/11-1S modified from, Anindita (2018)

Well Marker	Horizon Colour	Wavelet	Wavelet Colour
Seabed	Brown	Peak	Black
Pleistocene 4	Orange	Peak	Black
Pleistocene 3 (URU)	Light Green	Through	Red
Pleistocene 2.5	Blue Green	Through	Red
Pleistocene 2	Blue	Through	Red
Pleistocene 1	Purple	Through	Red
Pliocene 2	Dark Pink	Peak	Black
Pliocene 1	Red	Peak	Black
Miocene	Yellow	Peak	Black
Oligocene	Green	Peak	Black
Eocene 3	Light Blue	Peak	Black
Eocene 2	Yellow	Peak	Black
Eocene 1	Green	Peak	Black
Eocene 0	Light Blue	Peak	Black
Paleocene	Dark Blue	Peak	Black
Cretaceous	Light Pink	Peak	Black

## 4.2 Well Log Analysis

This study uses 6 wells to define petrophysical values such as volume shale, net to gross, and porosity. These values will be used as input to Clinofom Analysis and Stratigraphic Forward Modelling. (Fig.4.4)

### 4.2.1 Volume Shale (VSL)

This values derived from Gamma ray log and using Linier-Volume Shale equation, the result will be used as fraction of shale in zone interest and lithology interpretation combined with core data, mudlog, and previous study. Cut-off values for lithology interpretation, except interval with volcanic and limestone rock, is ranged from 0.5 to 0.75 as sand, however due to lack of data core for sand and shale fraction, this calculation can not be validated, except from elevation 2989 - 2999 mD-RKB, Rider (2002)

$$VSL = \frac{GR \log - GR \log \text{ minimum}}{GR \log \text{ maximum} - GR \log \text{ minimum}} \quad (4.1)$$

Note :

1. GR Log = Gamma ray log values from zone/interval of interest.

- 
2. GR Log maximum = Gamma Ray maximum values from zone/interval of interest (shale baseline).
  3. GR Log minimum = Gamma Ray minimum values from zone/interval of interest (sand baseline).

#### 4.2.2 Net to Gross (NtG)

Net to Gross is a fraction of total clean sand compared to total volume of rock, it is simply an opposite of volume shale, therefore this values can be derived from volume shale, with following equation, Rider (2002):

$$NTG = 1 - VSL \quad (4.2)$$

#### 4.2.3 Porosity Density ( $\phi\rho$ )

This values derived from Density log (*rho*) to calculate porosity for every interval with different density coefficient. The equation is explained below. Rider (2002)

$$\phi\rho = \frac{\rho_{matrix} - \rho_{log}}{\rho_{matrix} - \rho_{fluid}} \quad (4.3)$$

Note :

1.  $\rho$  Log = Density log values from zone/interval of interest.
2.  $\rho$  matrix = Density of matrix from zone/interval of interest (  $\rho$  matrix : sand = 2.65 ; carbonate = 2.71 ; shale = 2.725 ; volcanic = 2.75.).
3.  $\rho$  fluid = Density of fluid values from zone/interval of interest (Fluid coefficient: fresh water = 1, saline water = 1.1, oil base mud= 0.8).

#### 4.2.4 Porosity Total ( $\phi_{total}$ )

To derive total porosity the apparent neutron porosity ( $\phi_N$ ) must be corrected in advance, by adding 0.04 to the neutron porosity log values to correct the log from apparent limestone porosity to apparent sandstone porosity. Using the apparent neutron porosity, the total porosity from the average neutron and density porosity ( $\phi_{total}$ ) is calculated. Ravestein (2013)

$$\phi_{total} = \frac{\phi\rho + \phi(N)}{2} \quad (4.4)$$

#### 4.2.5 Porosity Effective ( $\phi_{effective}$ )

The effective porosity ( $\phi_{eff.}$ ) is the average neutron and density porosity ( $\phi_{total}$ ) minus the pore space fraction that is occupied by shale or clay (Volume Shale) or can be replaced by Net to Gross values  $NtG = 1 - VSL$ . Ravestein (2013)

$$\phi_{effective} = (1 - VSL) * \phi_{total} \quad (4.5)$$

---

#### **4.2.6 Sequence Stratigraphy**

Sequence stratigraphy analysis in well data is using electrofacies analysis of well logs as method to define stacking pattern in every well and interpreted the depositional environment. This can help seismic stratigraphy analysis to define elevation of well marker to seismic horizons. Determining Sequence stratigraphy can not be done only using electrofacies method alone, but has to be combined and corrected with other well data, such as petrography and biostratigraphy of core samples. The result of sequence stratigraphy analysis is corrected based on previous study (Ryseth et al. (2003), Knies et al. (2009) and Marheni et al. (2015)).(fig.4.5).

#### **4.2.7 Well Correlation**

After all logs has been obtained, then distribution and continuation every interval of age can be seen in wells correlation from North to South (Fig.4.6) and from Southwest to Northeast (Fig.4.7). From this it can be seen that most of Oligocene to Pleistocene age deposit are pinched out in the north, east, and south, this confirms that well 7216/11-1S is at the depocenter of Sørvestsnaget Basin since Oligocene until now. While Cretaceous, Paleocene, and Eocene has trend thickening in the North and thinning to the South, this can be inferred that depocenter in that time was in the north.

### **4.3 Seismic Interpretation**

Before conducting seismic interpretation, it is important to compare previous study horizons, so as not to cause any confusion in future study. Therefore a comparison and compilation of different previous study is summarise in table 4.2.

Horizons interpretation conducted in all lines that coverage Sørvestsnaget Basin and adjacent areas, including some parts of Veslemøy High, Senja Ridge, Vestbaken Volcanic Province, Bjørnøya Basin, and Lofoten Basin. As for Fault Interpretation since the interval ages are relatively not deformed, except in interval of Top Cretaceous, Paleocene, and Eocene 0 - 2, then only in regional line and key line for Clinoform Analysis that fault interpretation is conducted.

The interpretations may exceed boundary of basin, due to Clinoform Analysis, which needs full scale of clinoform from top set to bottom set. However due to distribution and discontinuation of several ages in Sørvestsnaget Basin, such as Eocene 0 - 3 and Oligocene epoch, then these ages will only interpreted to their continuation. This study also using previous study result of Marheni et al. (2015) as input for time and depth map.

**Table 4.2:** Horizons and Well Top Marker (7216/11-1S) compared to previous study.

Horizons Name (This Study)	Horizon Name (Vorren et al, 1990; Faleide et al, 1996),	Sediment Package (Larsen et al , 2003)	Glaciation phase (Faleide et al 1996)	Age ( Butt et al, 2000; Ryseth et al, 2003; Knies, 2009)
Seabed	4W	H	GIII	0
Top Pleistocene 4	3W	G		<130 ka
	2W	F		<200 ka
	1W	E		<330 ka
Top Pleistocene 3	R1		(URU)	<0.2 - 0.44 ma
		D	GII	
Top Pleistocene 2.5	R2			0.5 ma
Top Pleistocene 2	R3	C		0.78 ma
Top Pleistocene 1	R4			0.99 ma
Top Pliocene 2	R5			1.3 - 1.5 ma
		B	GI	
Top Pliocene 1	R6			1.6 - 1.7 ma
		A		
Top Miocene	R7			2.3 - 2.7 ma
Top Oligocene				10 ma
Top Eocene 3				30.5 ma
Top Eocene 2				37.8 ma
Top Eocene 1	?	?	?	41.2 ma
Top Eocene 0				47.8 ma
Top Paleocene				56 ma
Top Cretaceous				66 ma

### 4.3.1 Time Maps

Horizon interpretation conducted in almost every available seismic data, including 2 sets 3D seismic and 147 lines for 13 horizons, except Eocene 0 - 2 due to its condition which highly structured and eroded of these interval ages. Several lines were not interpret since its poor quality or because it were already interpreted by previous study (Marheni et al. (2015)), which used in this study. The example of horizon and fault interpretation can be seen in figure 4.8 and figure 4.9.

After seismic interpretation of key seismic lines, which cross-sectioned with key well 7216/11-1S, then next step is interpretation of other seismic lines which cross-sectioned with other wells, started with regional lines connecting every well through seismic lines. These regional seismic lines and its interpretation can be seen in figure 4.10 (North to South), figure 4.11 (Southwest to Northeast), also its geo-seismic interpretation in figure 4.12 (North to South), and in figure 4.13 (Southwest to Northeast) taken from Anindita (2018).

The Seismic Sequence Stratigraphy analysis in this study is taken from Anindita (2018) which conducted with guidance from (Omosanya et al., 2016) and summarised into these figures. (Fig.4.14 and Fig. 4.15)

After all seismic lines has been interpreted, then it can generate a time maps, corrected with guidance of well marker in well which has tied in seismic. The example time maps of Pliocene 2 can be seen in figure 4.16.



---

### 4.3.2 Depth Maps

After all surface ages is mapped in time domain, then it has to be converted to depth domain, so it can be interpreted in clinofom analysis and stratigraphic forward modelling. However, without any velocity model through Sørvestsnaget Basin, it can be challenge to convert it accurately. In this study, time to depth conversion used several dummy well to control interpolation values of velocity maps (Fig. 4.18) every surface that generated with help of One Way Time maps (Fig. 4.17). This technique used well data as source of interval velocity in checkshot and extrapolated throughout area. Example depth map of Pliocene 2 can be seen in Fig.4.17.

## 4.4 Clinofom Analysis

This analysis is conducted using SINTEF 2D Clinofom Analysis to reconstruct paleo-clinofom based on Patruno et al. (2015). The summary of Clinofom analysis for each ages can be found in Table 4.2. Due to narrow distribution and highly structured as well as eroded condition of Eocene and Oligocene deposit, therefore Clinofom Analysis will be conducted only from Miocene to Pleistocene 4. The steps to analyse clinofom with this SINTEF 2D Clinofom Analysis software are :

1. Firstly, prepares seismic line which has interpretation of full scale clinofom that will be digitise. to be noted that this seismic line is in time domain, therefore it is necessary to have at least one well as conversion to depth domain. in this study case, it is using interval velocity from well 7216/11-1S and 7316/5-1, as the closest well to the seismic lines location.(Fig. 4.20)
2. Secondly, it is simply digitising all horizons or clinofom of every age. note : this software can not have zero thickness, which means all convergence of horizons need to be put some gap or thickness between two horizons.(Fig.4.21)
3. Lastly, every layer has interpretation by 2 layers, for example, if surface of Pliocene 2 will be analysed then it needs lower layer which is Pliocene 1, as reference to trajectory of rollover point. Next, the nomenclatures that needed to defined are, head point, upper rollover point, lower rollover point, and toe point. In this step, determining nomenclature location is indeed subjective based on interpreter on clinofom parts knowledge, to decide where to pick points of nomenclature, therefore in this software it provides three (3) points each nomenclature to pick, which will be averaged into 1 mean values, as uncertainty or margin error.(Fig.4.22),
4. All of these steps will generate values of clinofom nomenclature from paleo-clinofom (Head point, Upper Rollover Point, Lower Rollover Point, and Toe Point), which can be used for deriving Paleobathymetri Map each age.

After all values of Clinoform nomenclature are obtained, then it should be compared with present clinoform to generate cross-plot and correlation. These correlation will be used directly for generating paleobathymetri map. See figure(4.23) for cross-plot correlation and figure 4.24 for Paleobathymetri map of Pliocene 2.

**Table 4.3:** Clinoform Analysis Variables Summary

Horizons	Clinoform Nomenclatures	Gap to Sea Level (m)	
		Present	Paleo
Miocene	Th (Head to Upper Rollover Points)	112	223.4
	Fh ( Upper Rollover to Lower Rollover Point)	3708	3133.1
	Bh ( Lower Rollover to Toe Point)	300	1804.3
	Top Height (Wd - Th ) or (SL to Head point)	780	134.5
	Wd (SL to UROP)	892	357.9
	Mid Height (Fh + Wd ) or (SL to LROP)	4600	3491
	Hh (SL to Toe Point)	4900	2049
Pliocene 1	Th (Head to Upper Rollover Points)	224	919.5
	Fh ( Upper Rollover to Lower Rollover Point)	3121	2939.6
	Bh ( Lower Rollover to Toe Point)	375	940.8
	Top Height (Wd - Th ) or (SL to Head point)	880	89.7
	Wd (SL to UROP)	1104	1009.2
	Mid Height (Fh + Wd ) or (SL to LROP)	4225	3948.8
	Hh (SL to Toe Point)	4600	3712.4
Pliocene 2	Th (Head to Upper Rollover Points)	117.38	533.7
	Fh ( Upper Rollover to Lower Rollover Point)	3158.33	2550.5
	Bh ( Lower Rollover to Toe Point)	186.4	875.3
	Top Height (Wd - Th ) or (SL to Head point)	963.39	626.1
	Wd (SL to UROP)	1080.77	1159.8
	Mid Height (Fh + Wd ) or (SL to LROP)	4239.1	3710.3
	Hh (SL to Toe Point)	4425.5	3452.0
Pleistocene 1	Th (Head to Upper Rollover Points)	277.6	539.3
	Fh ( Upper Rollover to Lower Rollover Point)	3057.69	2298.6
	Bh ( Lower Rollover to Toe Point)	87.63	1084.1
	Top Height (Wd - Th ) or (SL to Head point)	958.36	538.2
	Wd (SL to UROP)	1235.96	1077.5
	Mid Height (Fh + Wd ) or (SL to LROP)	4293.65	3376.1
	Hh (SL to Toe Point)	4381.28	2957.8
Pleistocene 2	Th (Head to Upper Rollover Points)	222.52	768.2
	Fh ( Upper Rollover to Lower Rollover Point)	2493.49	2268.3
	Bh ( Lower Rollover to Toe Point)	912.46	285.5
	Top Height (Wd - Th ) or (SL to Head point)	918.46	258
	Wd (SL to UROP)	1140.98	1026.2
	Mid Height (Fh + Wd ) or (SL to LROP)	3634.47	3294.5
	Hh (SL to Toe Point)	4546.93	2235.4
	Th (Head to Upper Rollover Points)	154.98	175.9
	Fh ( Upper Rollover to Lower Rollover Point)	2080.11	1994.8

**Table 4.3 continued from previous page**

Horizons	Clinoform Variables	Gap to Sea Level (m)	
		Present	Paleo
Pleistocene 2.5	Bh ( Lower Rollover to Toe Point)	920.79	638.4
	Top Height (Wd - Th ) or (SL to Head point)	1037.32	925.4
	Wd (SL to UROP)	1192.3	1101.3
	Mid Height (Fh + Wd ) or (SL to LROP)	3272.41	3096.1
	Hh (SL to Toe Point)	4193.2	3732.9
Pleistocene 3	Th (Head to Upper Rollover Points)	410.11	1592.5
	Fh ( Upper Rollover to Lower Rollover Point)	2029.09	1043.6
	Bh ( Lower Rollover to Toe Point)	604.3	284.1
	Top Height (Wd - Th ) or (SL to Head point)	556.5	-686.1
	Wd (SL to UROP)	966.61	906.4
	Mid Height (Fh + Wd ) or (SL to LROP)	2995.7	1950
	Hh (SL to Toe Point)	3600	2080.3
Pleistocene 4	Th (Head to Upper Rollover Points)	241.49	89.5
	Fh ( Upper Rollover to Lower Rollover Point)	2083.37	706.5
	Bh ( Lower Rollover to Toe Point)	653.6	1638.8
	Top Height (Wd - Th ) or (SL to Head point)	544.64	439.7
	Wd (SL to UROP)	786.13	529.2
	Mid Height (Fh + Wd ) or (SL to LROP)	2869.5	1235.7
	Hh (SL to Toe Point)	3523.1	992.4

## 4.5 Stratigraphic Forward Modelling

This study using Geological Process Modelling (GPM) software as simulator for Stratigraphic Forward Modelling (SFM) method to visualise and model the Sørvestsnaget Basin. as plugin of Petrel Software, the advantage of this software is that the results of simulation, can be used directly as grid model in facies modelling, even in petrophysical modelling which is porosity model.

Before simulation started, there are components that have to be prepared in advance. Some of it are obtained from analysis, such as paleobathymetri maps, well log analysis for sand/shale fraction from VSL/NtG, tectonic event map, and sediment source map, and from previous study, such as Sea Level Change curve (Miller et al. (2005)), Time interval taken from biostratigraphy and several previous studies, (Knies et al. (2009), Ryseth et al. (2003), and Butt et al. (2000).),

The following maps and values, are the main input and setting in Geological Process Modelling.

### 1. Topography

This field need to be filled with Paleobathymetri map which derived in this study for each ages. This map need to be fully reconstructed from any deformation, such as fold, fault, and salt diapirs. Example of simulation will used paleobathymetri map of Pliocene 2 time.(fig.4.24)

---

## 2. Source Position Map

This field basically provides simulation with trend of paleo-current sedimentation, including type of flow that will be simulated, both steady flow or unsteady flow at certain duration time. In this study source map was derived from using thickness between two surfaces that will be simulated, (for example, if the user want to simulate Pliocene 2 as topography then thickness between Pliocene 2 and Pleistocene 1, which as upper surface, is necessary.) and with help of seismic stratigraphy analysis and previous study, which has done in advance Anindita (2018) Omosanya et al. (2016). The thickness map can be seen in fig.4.25) and source position map in fig. 4.26.

## 3. Sea level

This field defines the sea level change of area that will influence the behaviour of sedimentation process. There are already two sea level curves by default in GPM, from Haq et al, and Exxon. However in this study, sea level change curves is taken and used from Miller et al. (2005), which considerably much more detail, especially in Miocene to Pleistocene epoch. The stratigraphic chart comparison of Sea Level Changes can be seen in figure (4.27)

## 4. Method time increment

This field manages the increment of every equation, geological process and variables that will be measured in time domain, which in year (a). The less value of this field the more accurate its calculation of simulation, however it will spend more time to calculate one cycle of sedimentation simulation. This study used one (1) year increment.

## 5. Time

This field manages the time duration of sedimentation simulation from topography map to certain time. Since this study divided the layer into 8 from Miocene to Pleistocene 4, therefore the simulation will used each time of every surface as 'start' and 'end' year. In this example simulation Pliocene 2 used 1.3 million years (ma) as 'start' year and Pleistocene 1, 0.99 million years (ma) as 'end' year.

## 6. Sediment Types

This field will generate standard sediment physical properties for four sediment, which are sand (coarse), sand (fine), silt, and shale. The physical properties are diameter, density, initial porosity, initial permeability, compacted porosity, compacted permeability, compaction, permeability anisotropy, transportability, erodibility coefficient. This field mostly used standard values which automatically generated in GPM for simulation, but in some field, such as density, compacted porosity, and compacted permeability can be obtained from core analysis.

## 7. Base Topography

This field manages the relationship between topography which is paleobathymetry map as basement, and sediment types that has been defined in advance. The relationship here means whether the sediment will erode the basement (topography) or not. Also this field manages the fraction of sediment package/clinothem that will be

---

simulated, this data can be inferred from Volume Shale or Net to Gross in specific interval, which in this study taken from well 7216/11-1S.

#### 8. **Sediment Diffusion**

In this field the user will provide a diffusion function as basic of numerical modelling in sedimentation simulation. The GPM provides a default diffusion function that can be modified as it fit to the geological concept. The user also can change the magnitude of diffusion equation through diffusion coefficient. In this study, a modified diffusion equation is taken from Lejri et al. (2017), which has study using GPM to model a field that has similarity with Sørvestsnaget Basin.(fig.4.28)

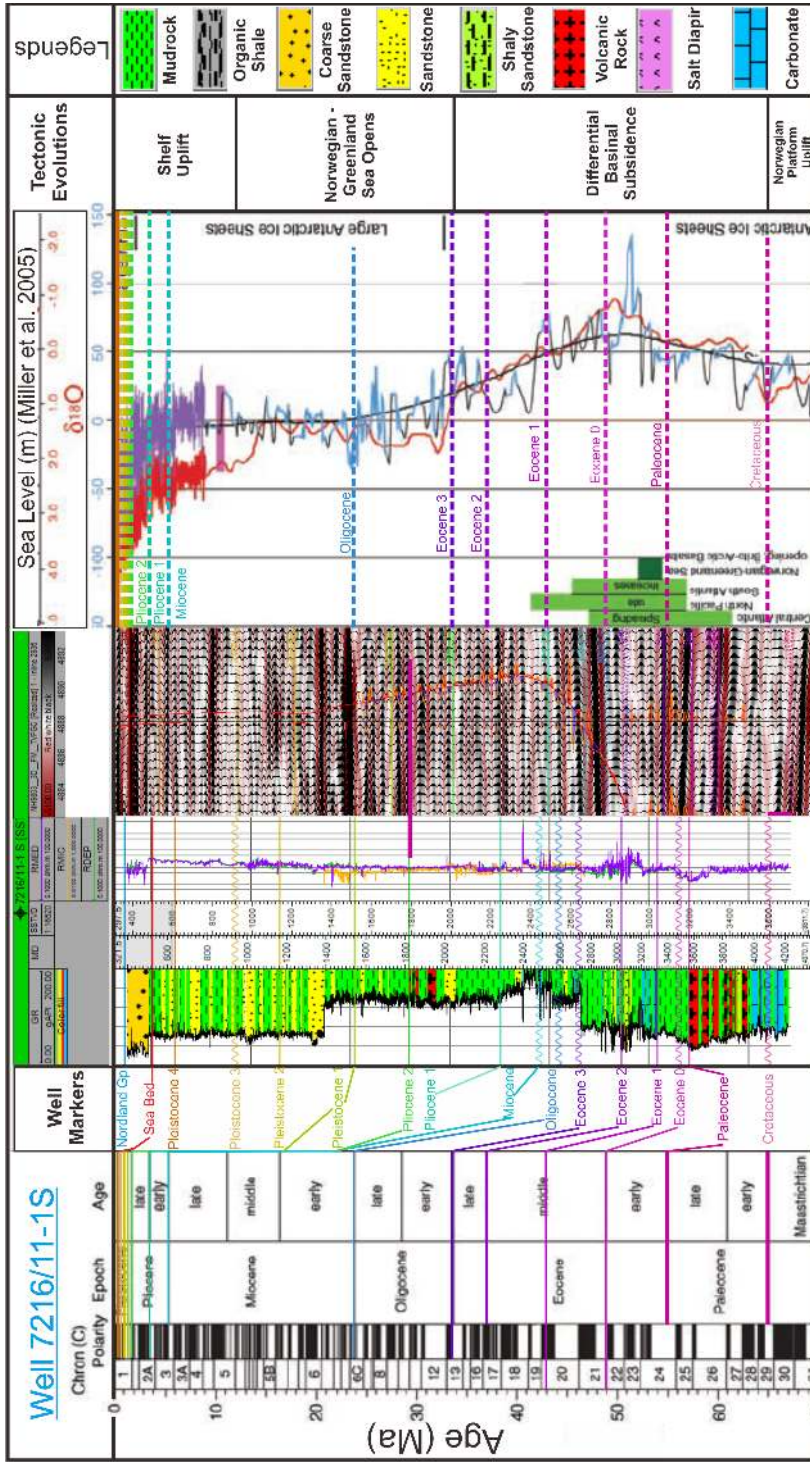
#### 9. **Compaction**

This field provides simple load method as restoration to the present condition, based on vertical load of sediment that has been deposited. This field can be useful if the tectonic event is unknown. In this study, this option is used as complementary of tectonic restoration.

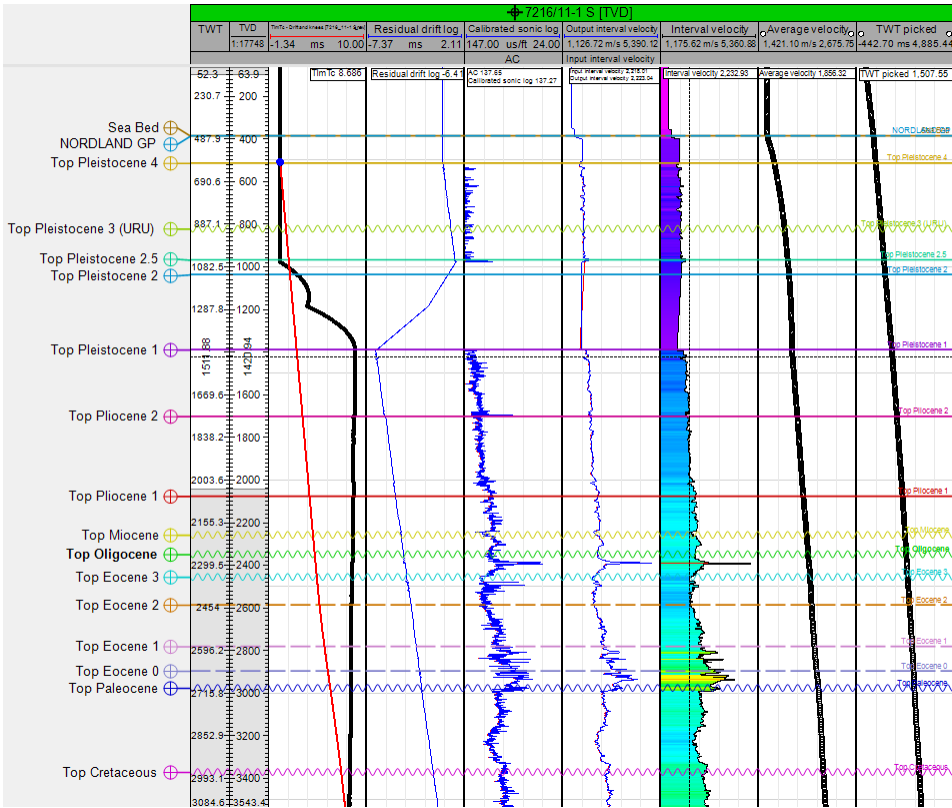
#### 10. **Tectonic**

This field manages the rate of tectonic event, both subsidence and uplift, which linked to stratigraphic Chart in Petrel input. This will influence the movement of topography which in this case is Pliocene 2 as basement for sedimentation above it. The subsidence/uplift rate need to be derived in advance as input for this field. This map derived from thickness (in millimetre, due to unit of subsidence and uplift map is in millimetre/year) between Paleo surface and Present surface and divided by duration of time of each ages. for example Pliocene 2, (1.3 ma - 0 ma). The map can be seen in figure 4.29.

11. **Steady and Unsteady Flow.** This fields has similar input which is sediment source that has been defined in advance. This sediment source is consist of sediment supply velocity (sand and shale), and water velocity. In this study, these values are inferred from Volume Shale and Net to Gross in well 7216/11-1S (Fig. 4.30). In steady flow field, after sediment source is defined and coded (1), the flow iterations and time increment need to be filled, which in this study used default values, 100 number and 1 s, respectively. Meanwhile Unsteady flow, coded with (2), has more input such as, turbidity event interval that need to be set at the time user interpreted turbidity current occurred = set as 100.000 a , fluid element depth = set as 1 m, duration time which duration this flow occurred = set as 2 h, display time = set as 2 h, and delta time interval = 0.5. An example of dialog box setting in GPM can be seen in figure 4.31 and example of results of GPM simulation result from Top Pliocene 2 to Top Pleistocene 1.(Fig.4.32)

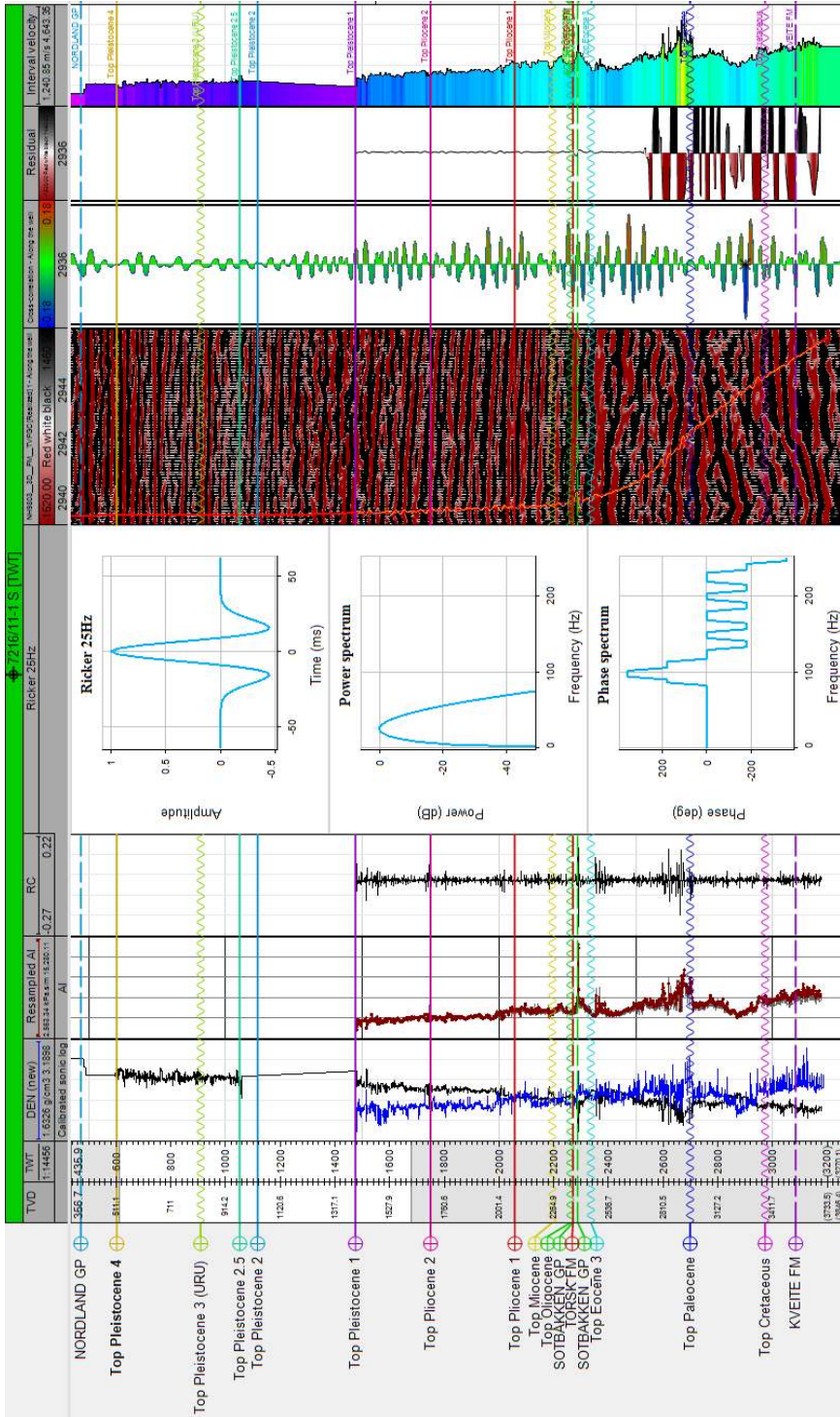


**Figure 4.1:** Seismic Well Tie, Well 7216/11-1S and NH98 3D seismic, with local stratigraphy, and sea level change based on Miller et al. (2005), taken from Anindita (2018).



**Figure 4.2: Sonic Calibration of Well 7216/11-1S.**





**Figure 4.3:** Synthetic Generation of Well 7216/11-1S. The missing values of Sonic log and Density log are from 976 - 1383 MD Meter.modified from Anindita (2018).



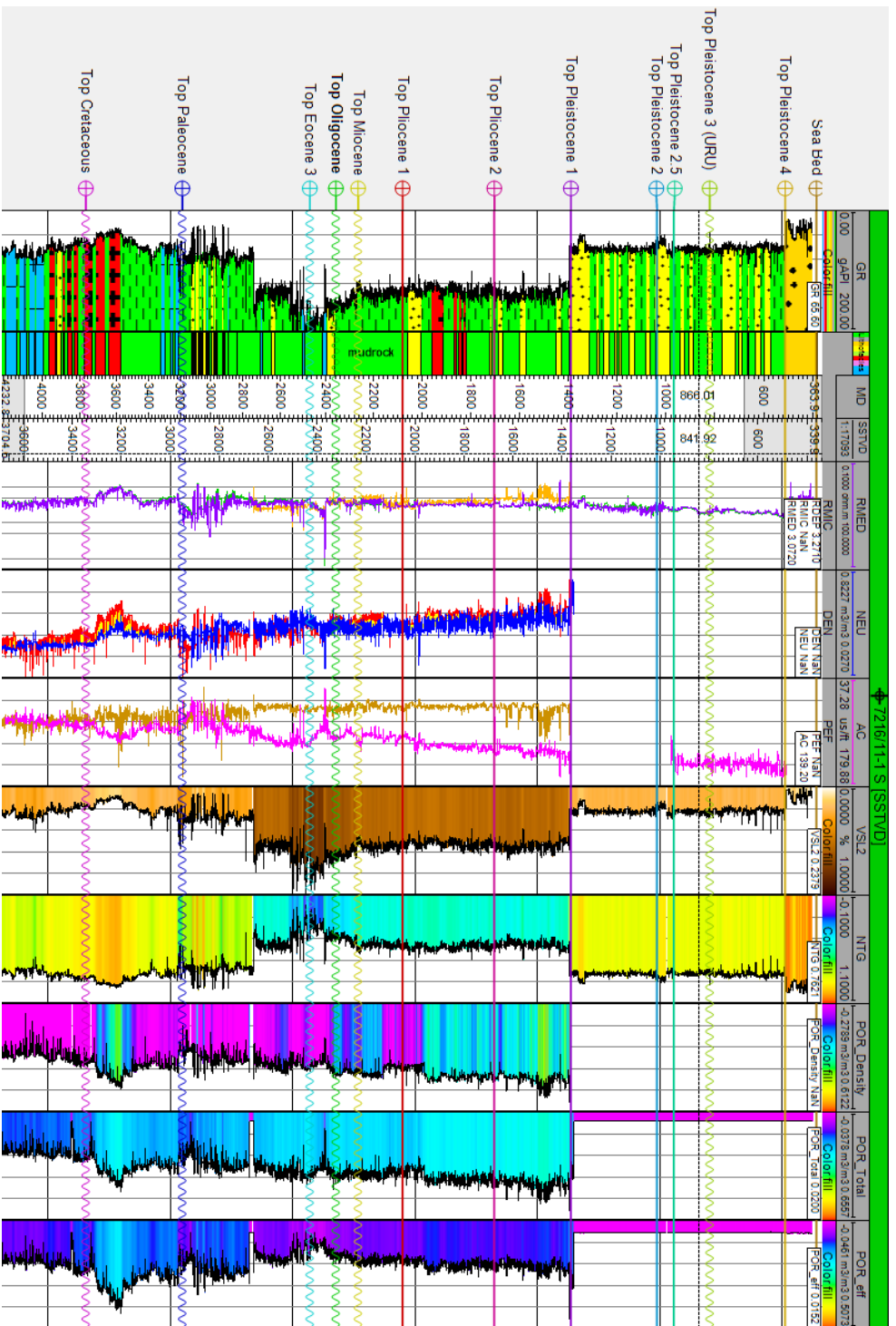


Figure 4.4: Composite of Petrophysical logs in Well 7216/11-1S.

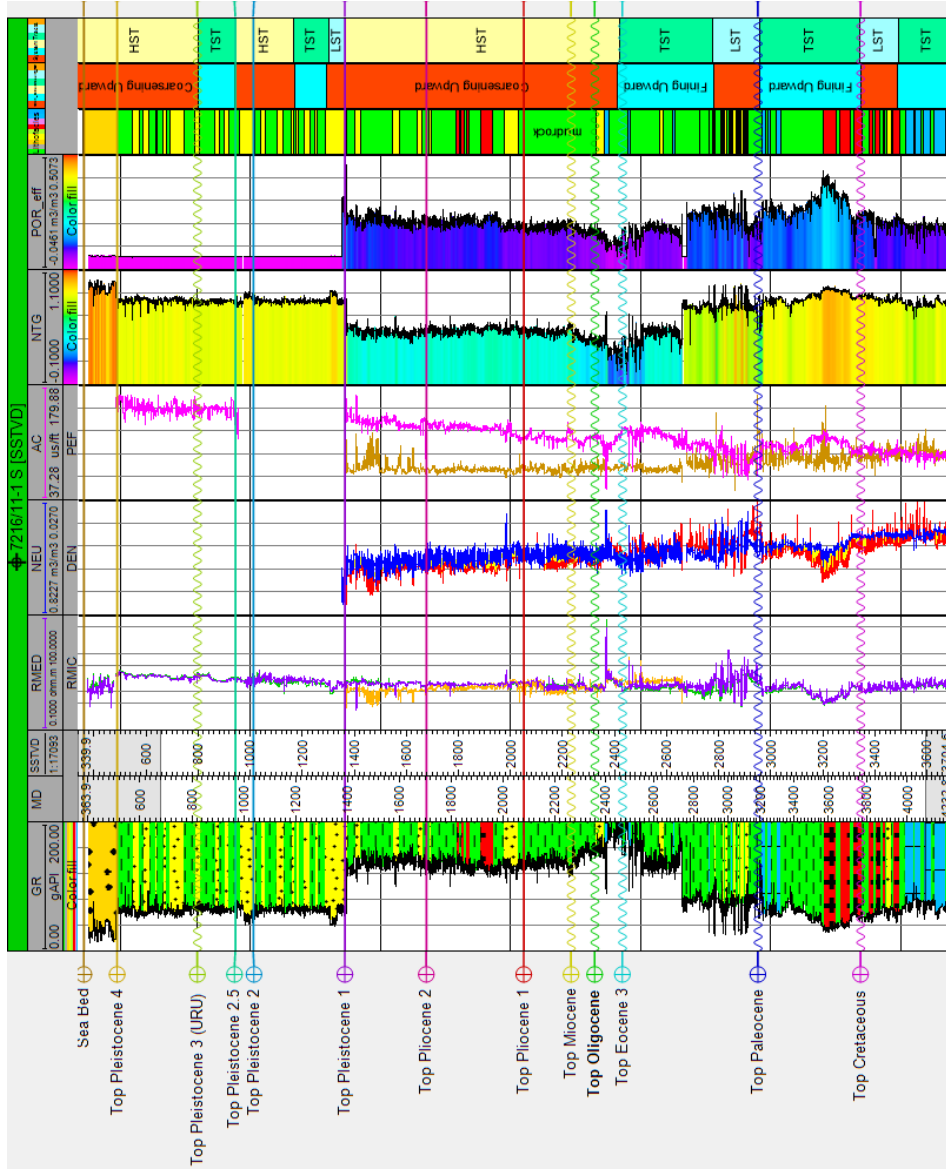


Figure 4.5: Composite of Sequence Stratigraphy in Well 7216/11-1S.



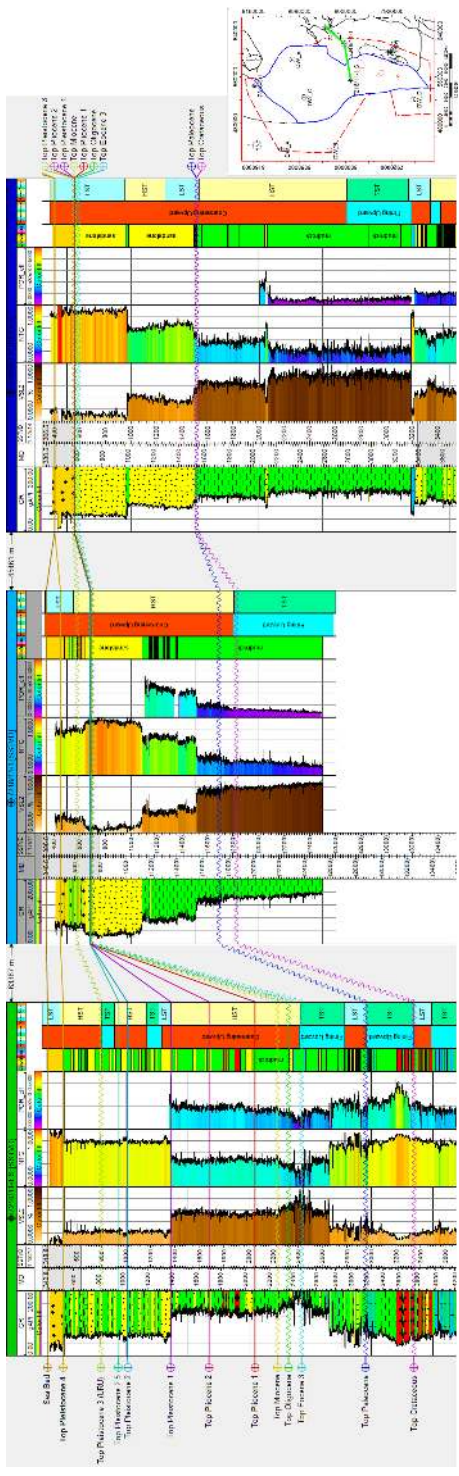
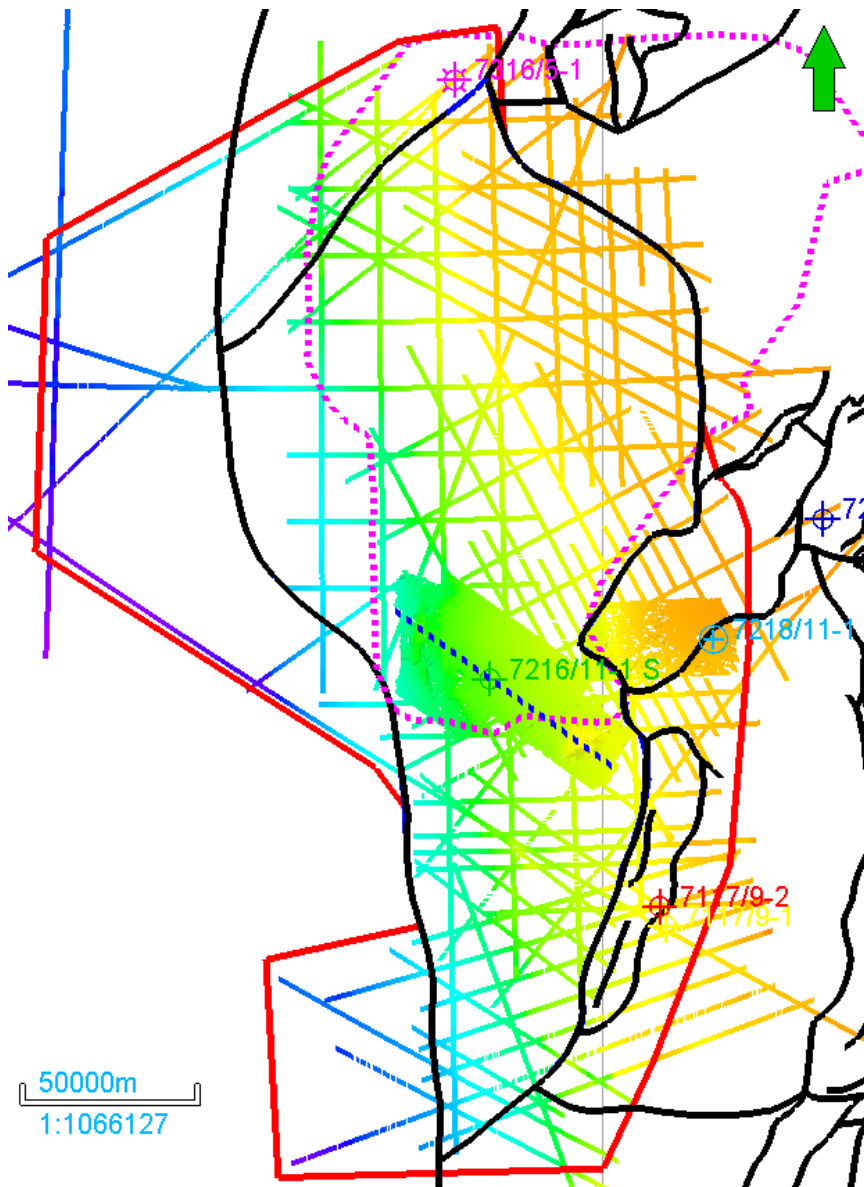
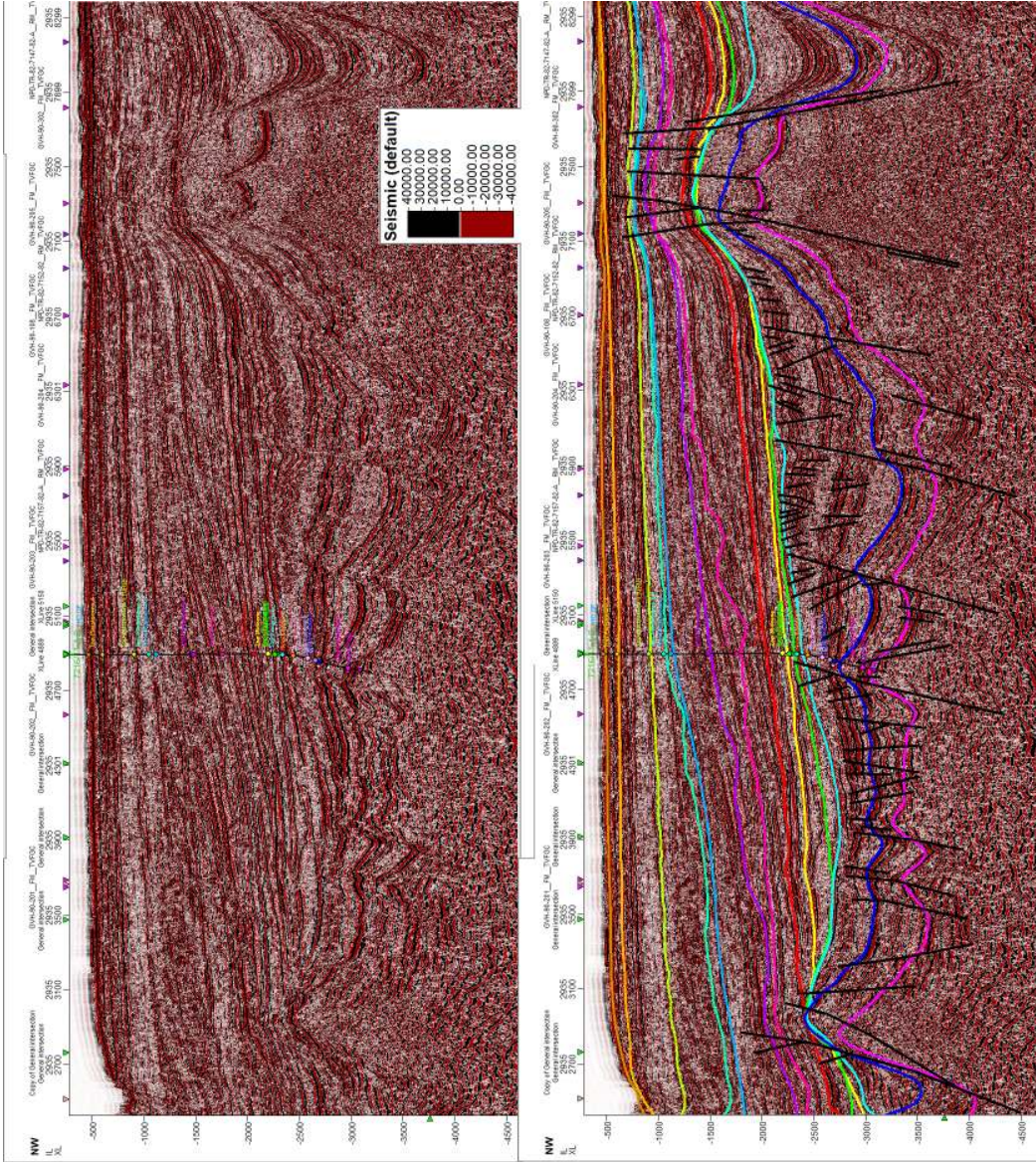


Figure 4.7: Well Correlation Southwest to Northeast, Datum on 0 m SSTVD.



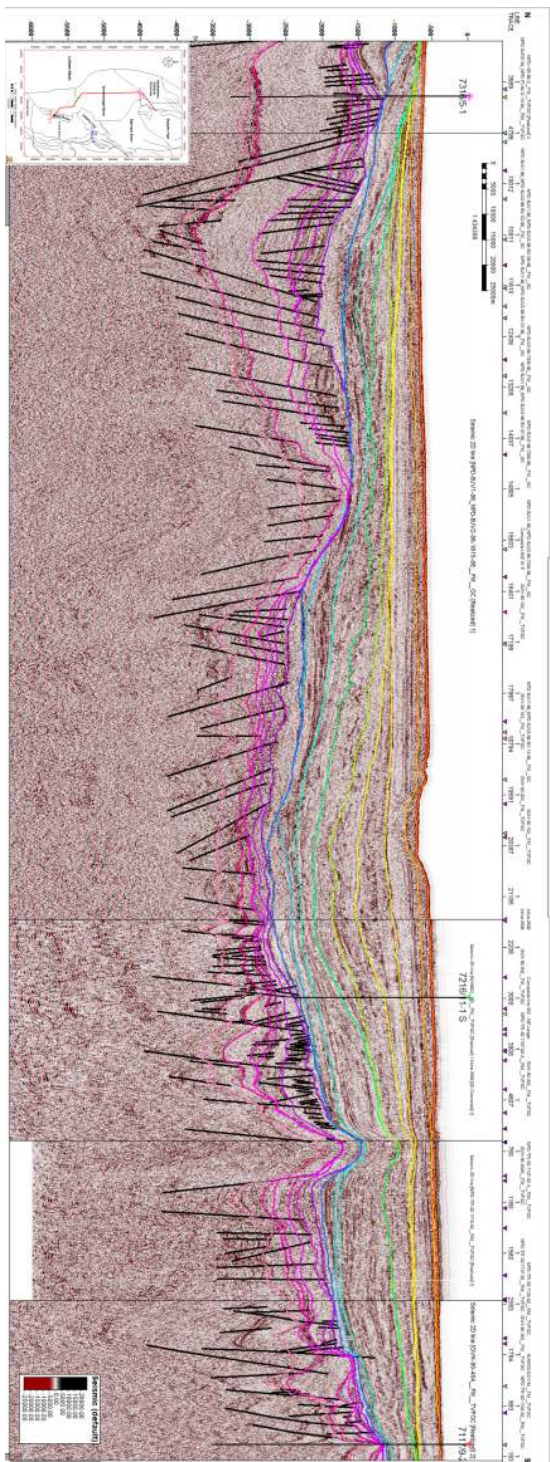
**Figure 4.8:** Example of Horizon interpretation in Miocene ages, solid red line is base map of interpretation, pink dashed line is coverage area from previous interpretation (most of interval age, but not all of ages has same coverage size), blue dashed line is the location of seismic section in fig. 4.9





**Figure 4.9:** Uninterpreted seismic section (upper) and Horizon and Fault interpretation of Inline 2935 from 3D Seismic NH9803 (lower), location can be seen in fig. 4.8





**Figure 4.10:** Fault and Horizon interpretation North to South.

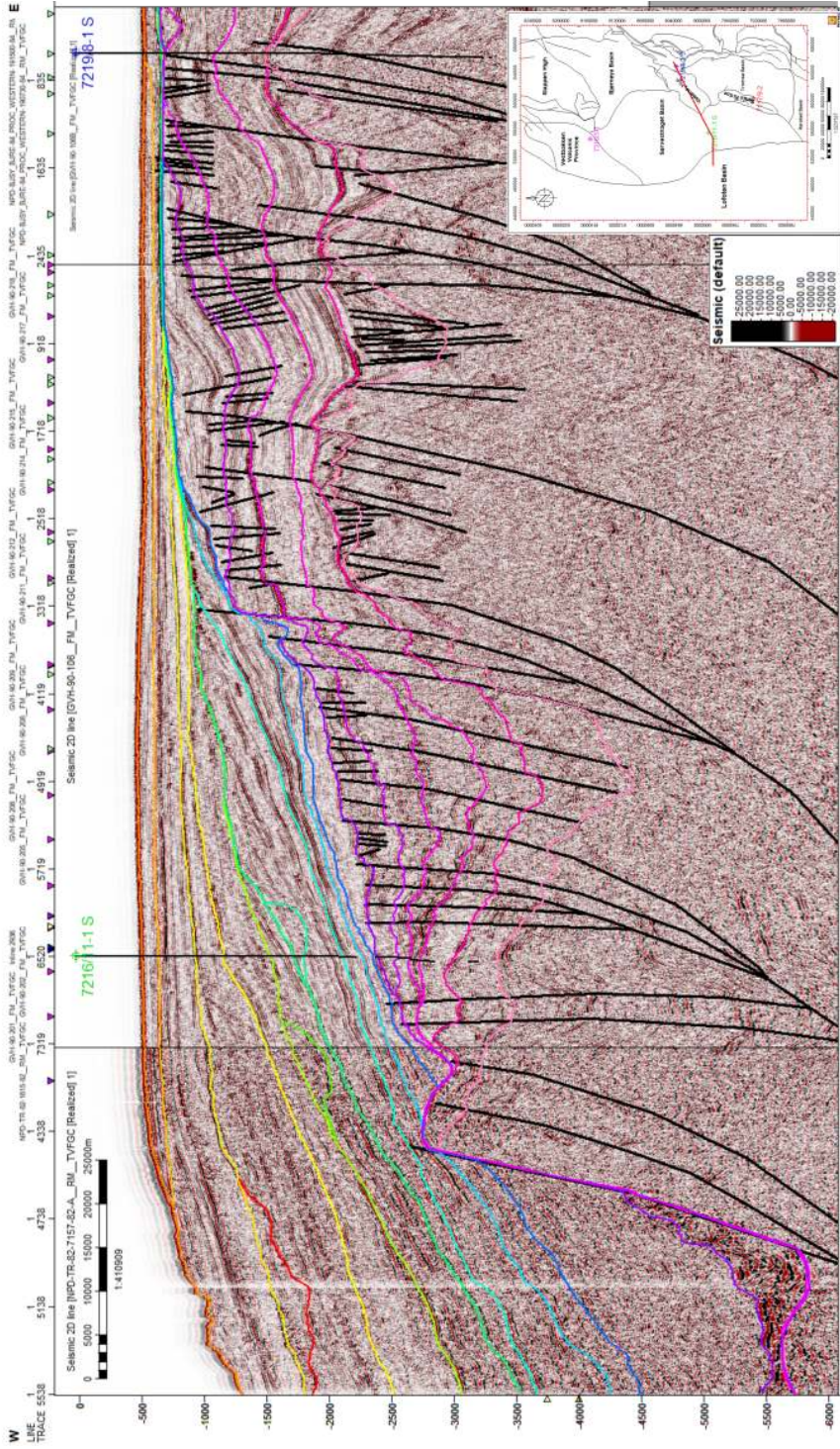
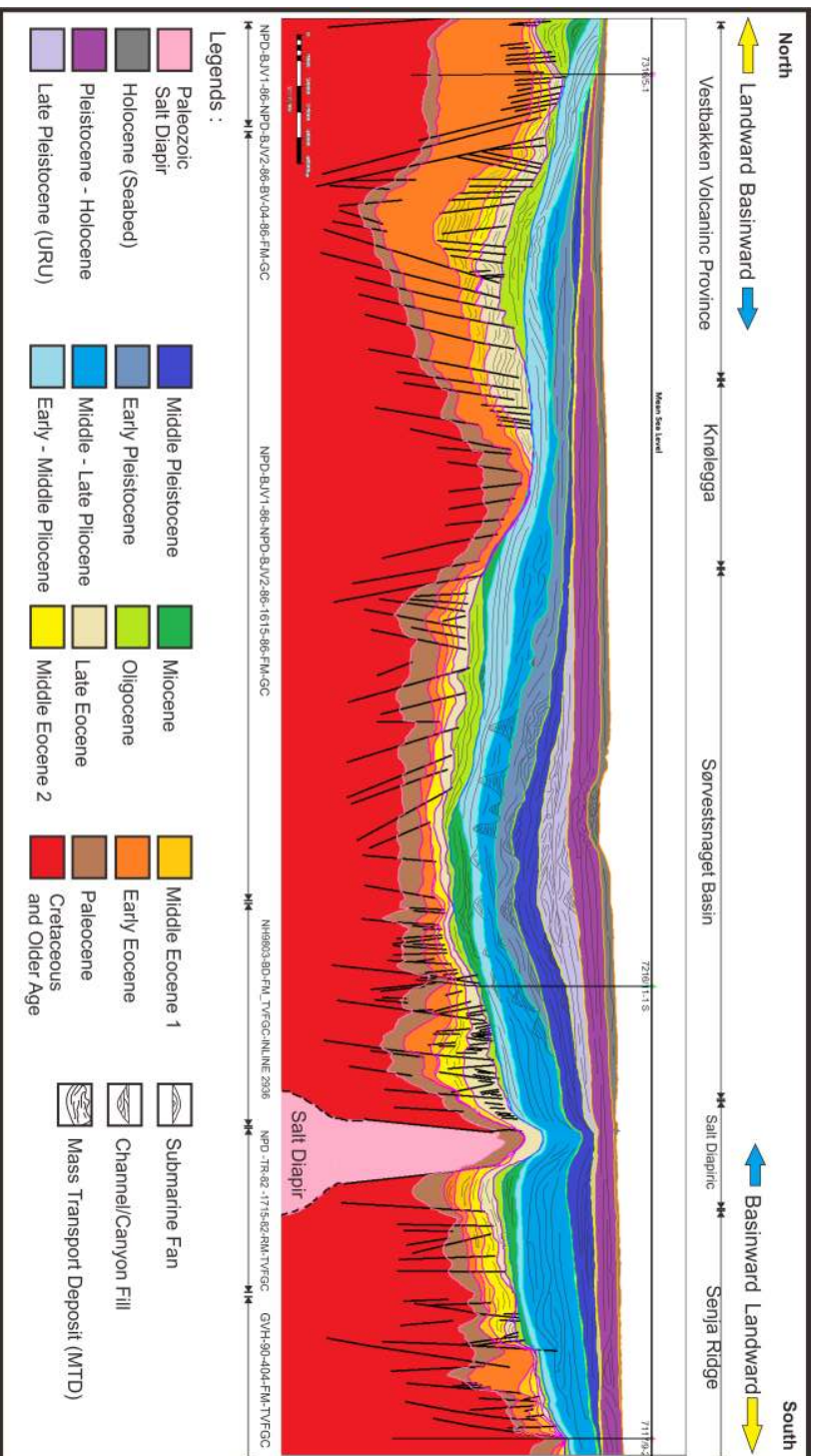


Figure 4.11: Fault and Horizon interpretation Southwest to Northeast.





**Figure 4.12:** Geo-seismic interpretation of N-S regional line seismic.

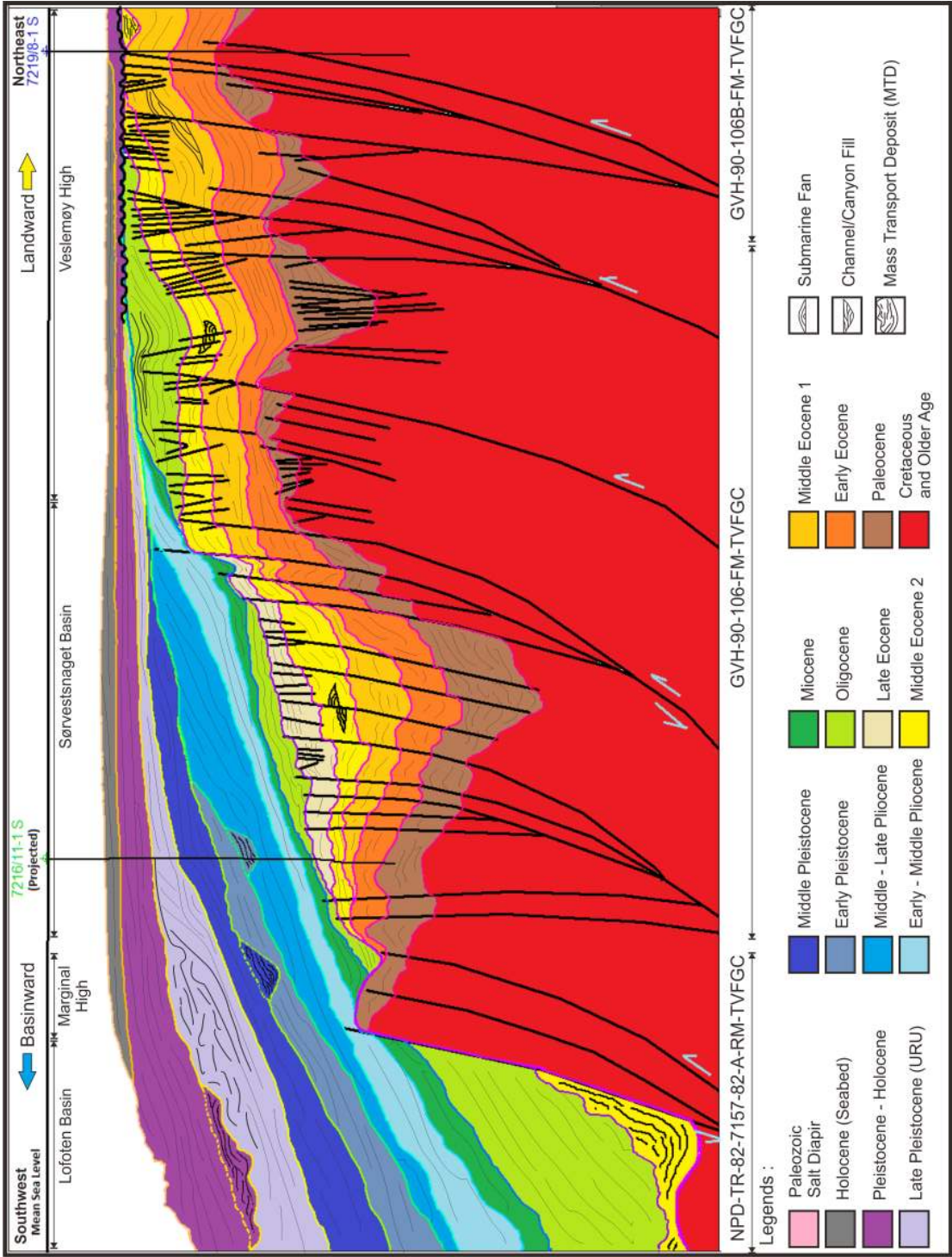


Figure 4.13: Geo-seismic interpretation of SW-NE regional line seismic.

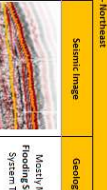


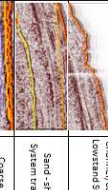

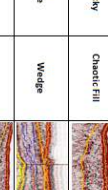

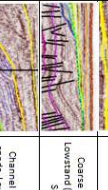
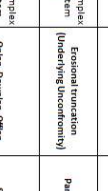


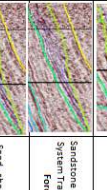



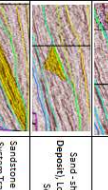
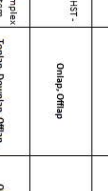


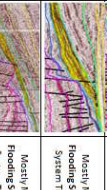



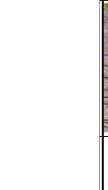



Unit	Interval of Ages	Sub Unit	Line Seismic North - East				Line Seismic Southwest - Northeast				
			Reflection Termination	Reflection Configuration	External Forms	Seismic Image	Geological Interpretation	Reflection Termination	Reflection Configuration	External Forms	Seismic Image
1 Pliocene 4 (Prelim) - Seabed (Recent)	1.1 a	Toplap, Downlap	Parallel, Sub-Parallel, Shingled,	Sheet, Sheet Draped		Miocene, Maximum Flooding Surface, Transgressive System Tract, Sea Level Rise	Toplap, Downlap	Parallel, Sub-Parallel, Shingled,	Sheet - Bank		Miocene, Maximum Flooding Surface, Transgressive System Tract, Sea Level Rise
		1.1 b	Onlap, Downlap, Erosional Truncation	Chaotic, Hummocky	Chaotic Fill		Sand - shale (Mass Transport Deposition), Lowstand System Tract, Sea Level Fall	Erosional truncation	Wavy Parallel	Canyon V-shaped	Channel (Cone) Eroded Surface Lowstand System Tract, Sea Level Fall
2 Pliocene 3 (Late) (Unit) - Pliocene 4 (Prelim - Holoc)	2.a	Toplap, Onlap, Downlap	Sigmoid-Oblique	Wedge		Sand - shale rock - highstand system tract; sea level rise still	Toplap, Onlap, Downlap	Sigmoid-Oblique	Wedge		Sand - shale rock - highstand system tract; sea level rise still
	2. b	Onlap, Downlap	Chaotic, Hummocky	Chaotic Fill		Sand - shale (Mass Transport Deposition), Lowstand System Tract, Sea Level Fall	Onlap, Downlap, Erosional Truncation	Parallel, Sub-Parallel	Channel Fill		Coarse to fine Sandstone, Lowstand System Tract, Sea Level Fall
3 Pliocene 2 (Middle) - Pliocene 3 (Late) (Unit)	3.a	Toplap, Onlap, Downlap, Erosional Truncation, Onlap	Chaotic, Hummocky Clinoforms	Wedge Mound		Sand - Shale, Channel Fan Complex - Slump, Lowstand (Fan) System Tract, Sea Level Fall	Erosional truncation (Underlying Unconformity)	Parallel, Sub Parallel	Sheet Draped - Wedge		Coarse to fine Sandstone, Lowstand (Village) System Tract, Sea Level Fall
	3.b	Toplap, Onlap, Downlap, Erosional Truncation, Onlap	Chaotic, Hummocky Clinoforms	Wedge - Mound		Sand - Shale, Channel Fan Complex - Slump, Lowstand (Fan) System Tract, Sea Level Fall	Onlap, Downlap, Onlap	Sigmoid-Oblique	Channel Fill - Mound		Channel / Overbank channel sands, Lowstand System Tract, Sea Level Fall
4 Pliocene 1 (Early) - Pliocene 2 (Middle)	4.a	Toplap, Onlap, Downlap, Erosional Truncation, Onlap	Chaotic, Hummocky Clinoforms	Wedge - Mound		Sand - Shale, Channel Fan Complex - Slump, Lowstand (Fan) System Tract, Sea Level Fall	Toplap, Downlap, Erosional Truncation	Sub-parallel, Oblique	Wedge		Sandstone dominated, Lowstand System Tract, sea level rise fall, Force Regression.
	4.b	Toplap, Downlap, Erosional Truncation	Sub-Parallel, Oblique	Wedge		Sandstone dominated, Lowstand System Tract, sea level rise fall, Force Regression.	Toplap, Downlap, Onlap	Chaotic, Hummocky	Mound - Slump		Sand - shale (Slump), Lowstand System Tract, Sea Level Fall
5 Pliocene 1 (Middle - Late) - Pliocene 2 (Middle - Late)	5.a	Toplap, Downlap, Erosional Truncation	Sub-Parallel, Oblique	Wedge		Sand - shale (Mass Transport Deposition), Lowstand System Tract, Sea Level Fall	Toplap, Downlap, Onlap	Chaotic, Hummocky	Mound - Slump		Sand - shale (Slump), Lowstand System Tract, Sea Level Fall
	5.b	Toplap, Onlap, Downlap, Erosional Truncation, Onlap	Chaotic, Hummocky	Mound - Slump		Sand - shale (Mass Transport Deposition), Lowstand System Tract, Sea Level Fall	Toplap, Downlap, Onlap	Chaotic, Hummocky	Mound - Slump		Sand - shale (Slump), Lowstand System Tract, Sea Level Fall
6 Pliocene 1 (Early - Middle) - Pliocene 2 (Middle - Late)	6.a	Toplap, Onlap, Downlap	Complex Sigmoid - oblique	Wedge		Sand - shale, Fan - Complex, HT - ISY, sea level changes continuously.	Onlap, Onlap	Chaotic	Channel Fill		Sand - shale (Mass Transport Deposition), Lowstand System Tract, Sea Level Fall
	6.b.	Onlap, Toplap, Downlap,	Conformal, Hummocky	Wedge Mound		Sand - Shale, Channel Fan Complex - Slump, Lowstand (Fan) System Tract, Sea Level Fall	Toplap, Downlap, Onlap	Oblique emergent	Wedge		Sandstone dominated, Lowstand System Tract, sea level rise fall, Force Regression
7 Miocene - Early - Middle	7.a	Onlap, Erosional Truncation	Parallel fan	Canyon - Onlap Fill		Coarse to fine Sandstone, Lowstand System Tract, Sea Level Fall	Onlap, Downlap	Subparallel	Sheet Draped		Mostly Miocene, Maximum Flooding Surface, Transgressive System Tract, Sea Level Rise,
	7.b	Onlap, Downlap	Sigmoid	Wedge		Miocene, Maximum Flooding Surface, Transgressive System Tract, Sea Level Rise, Back-Stepping	Onlap, Downlap	Subparallel	Sheet Draped		Mostly Miocene, Maximum Flooding Surface, Transgressive System Tract, Sea Level Rise, Back-Stepping

Figure 4.14: Summary of Seismic Stratigraphy Analysis from Holocene to Miocene.



Unit	Interval of Ages	Sub Unit	Line Seismic North - East			Line Seismic Southwest - Northeast			Geological Interpretation	
			Reflection Termination	Reflection Configuration	External Forms	Seismic Image	Reflection Termination	Reflection Configuration		External Forms
8	Oligocene - Miocene	8.a	Toplap, Onlap, Downlap, Erosional Truncation, Offlap	Chaotic, Hummocky	Mounded - Slump	Sand - shale, Channel Fan Complex, Lowstand (fan) System Tracts, Sea Level Fall	Onlap, Downlap	Subparallel	Sheet Drap	Misaligned, Maximum Flooding Surface, Transgressive System tract, Sea Level Rise, "back Stepped"
9	Eocene 3 (Late) - Oligocene	9.a	Toplap - Onlap to Downlap,	sigmoid - oblique	Wedge - Mounded	Sand - shale rock, Highstand System tract, Sea level Rise still	Toplap - Onlap to Downlap,	Sigmoid - Oblique	Wedge - Mounded	Sand - shale rock, Highstand System tract, Sea level Rise still
10	Eocene 2 (Middle 2) - Eocene 3 (Late)	10.a	Toplap - Onlap to Downlap,	sigmoid - oblique	Wedge - Mounded	Sand - shale rock, Highstand System tract, Sea level Rise still	Onlap, Downlap, Erosional Truncation	Parallel, Sub-Parallel	Channel Fill	Coarse to fine, Sandstone, Lowstand System Tract, Sea Level Fall
		10.b	Toplap - Onlap to Downlap,	sigmoid - oblique	Wedge - Mounded	Sand - shale rock, Highstand System tract, Sea level Rise still	Onlap, Downlap, Erosional Truncation	Chaotic	Mounded - Slump	Sand - shale (Mass Transport Deposit), lowstand System Tract, Sea Level Fall
11	Eocene 1 (Middle 1) - Eocene 2 (Middle 2)	11.a	Toplap - Onlap to Downlap,	sigmoid - oblique	Wedge - Mounded	Sand - shale rock, Highstand System tract, Sea level Rise still	Toplap - Onlap to Downlap,	Sigmoid - Oblique	Wedge - Mounded	Sand - shale rock, Highstand System tract, Sea level Rise still
12	Eocene 0 (Early) - Eocene 1 (Middle 1)	12.a	Onlap - Downlap	Sub Parallel - Lenticular	Fan Complex Simple	Submarine Fan Channel, Lowstand System Tract, Sea level Fall.	Onlap - Downlap	Sub Parallel - Lenticular	Fan Complex Simple	Submarine Fan Channel, Lowstand System Tract, Sea level Fall.
13	Pliocene - Eocene 0 (Early)	13.a	Onlap - downlap	Sigmoid - Oblique	Basin Fill	Submarine Fan complex, Lowstand System Tract, Sea level Fall.	Onlap - downlap	Sub parallel - Lenticular	Fan Complex Simple	Submarine Fan Channel, Lowstand System Tract, Sea level Fall.
14	Cretaceous - Pliocene	14.a	Onlap - downlap	Sigmoid - Oblique	Basin Fill	Shallow marine Fan complex, Lowstand System Tract, Sea level Fall.	Onlap - downlap	Sigmoid - Oblique	Basin Fill	Shallow marine Fan complex, Lowstand System Tract, Sea level Fall.

Figure 4.15: Summary of Seismic Stratigraphy Analysis from Miocene to Cretaceous.

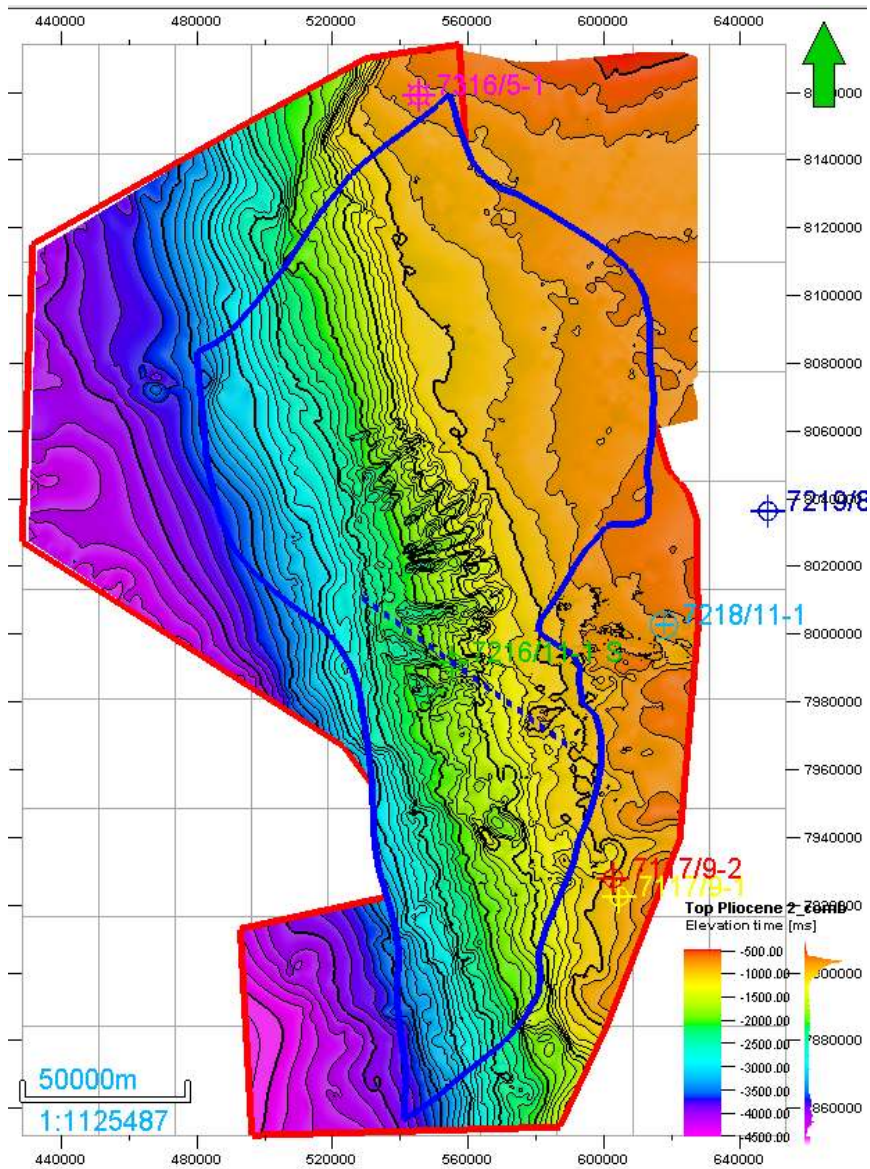
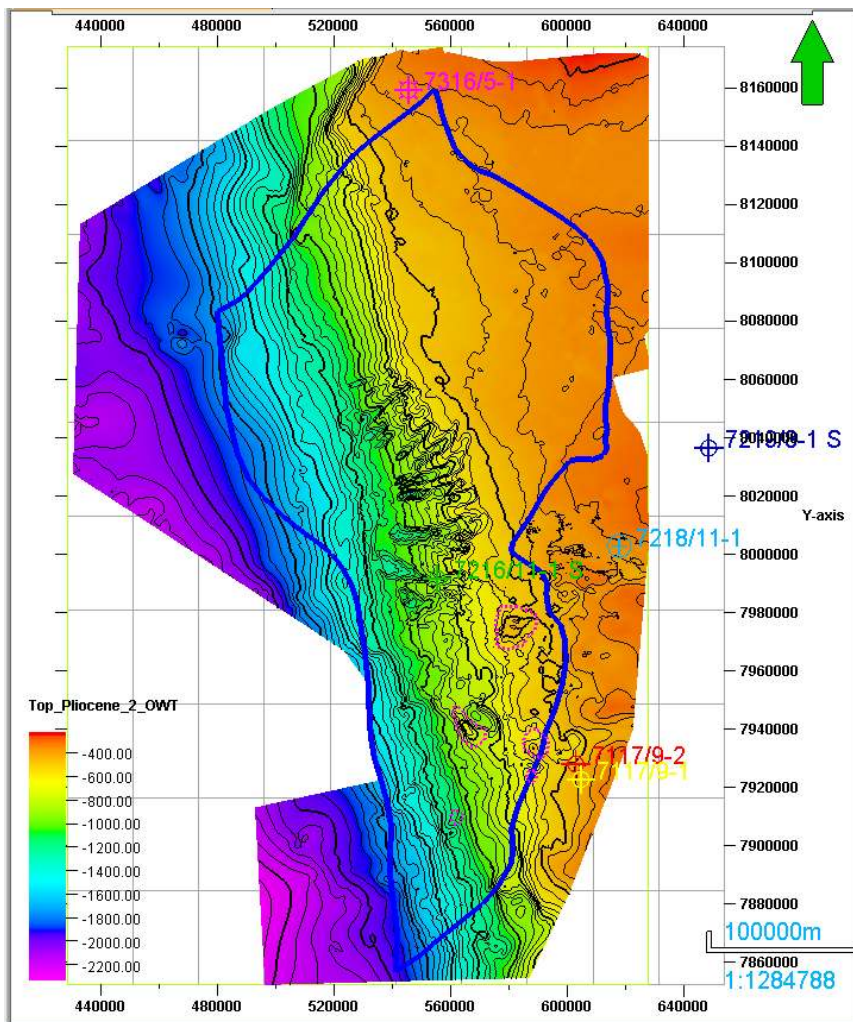
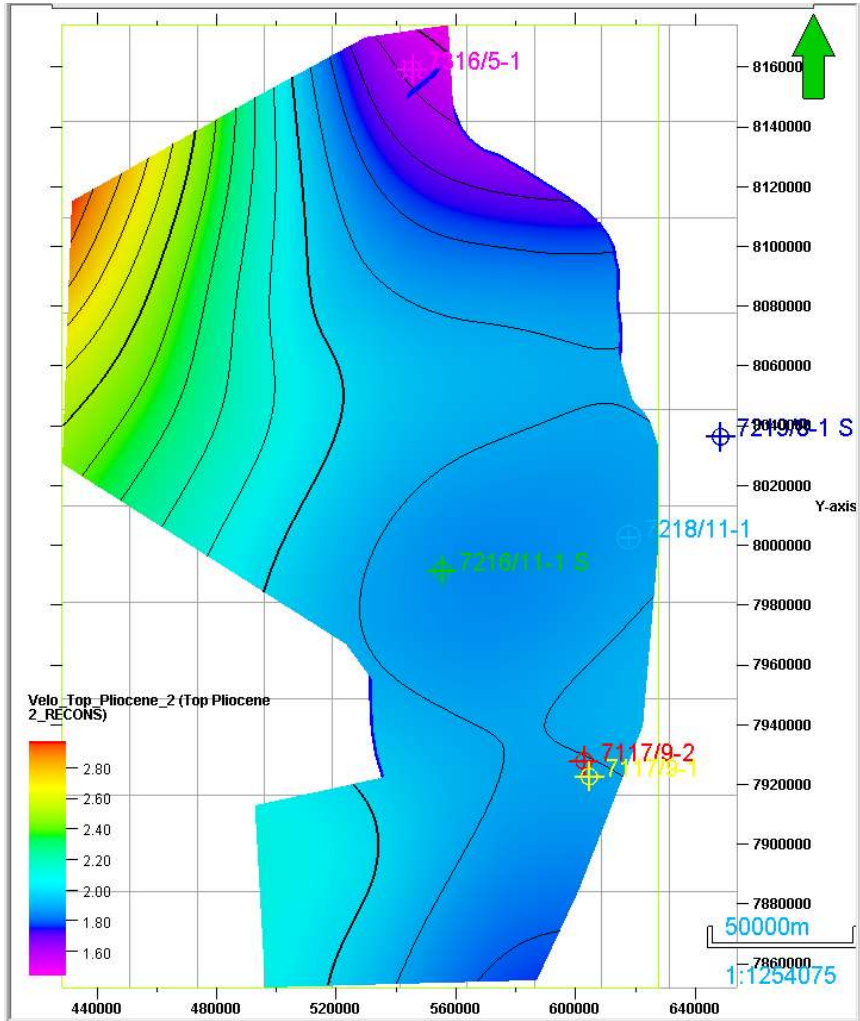


Figure 4.16: Time Maps of Top Pliocene 2.



**Figure 4.17:** One Way Time (OWT) Maps of Top Pliocene 2, derived from half values of time surface map Pliocene 2.



**Figure 4.18:** Interval Velocity Maps of Top Pliocene 2, derived from checkshots of wellbore data.



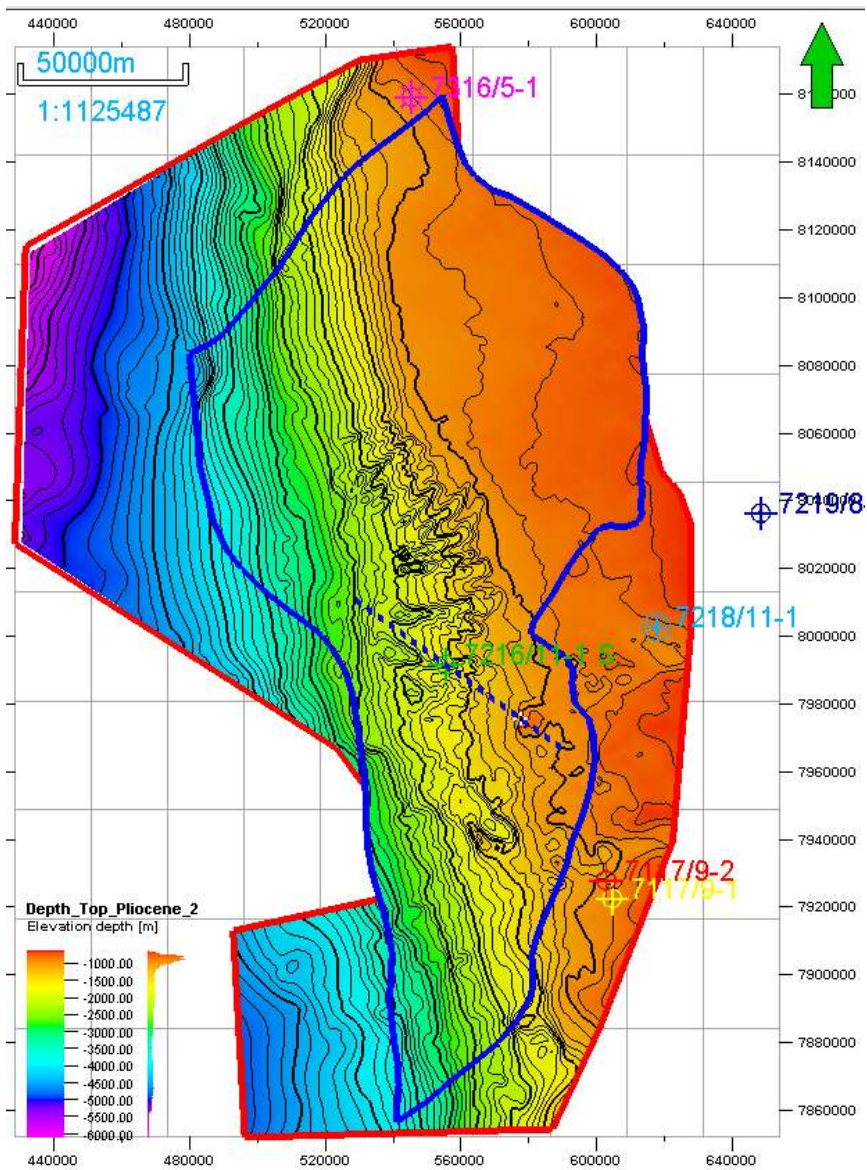


Figure 4.19: Depth Map of Top Pliocene 2, derived from OWT map multiplied by Interval velocity map.



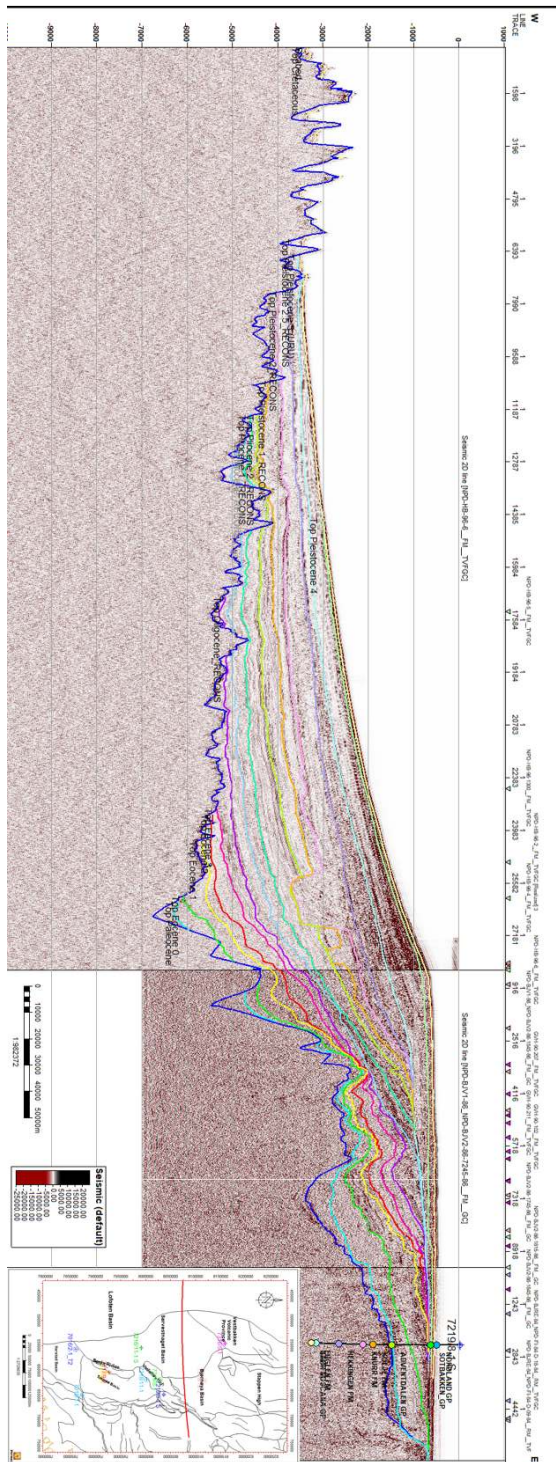
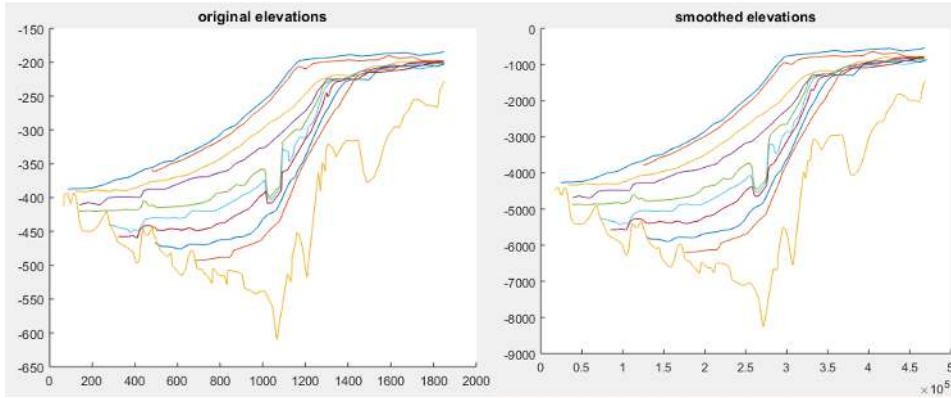
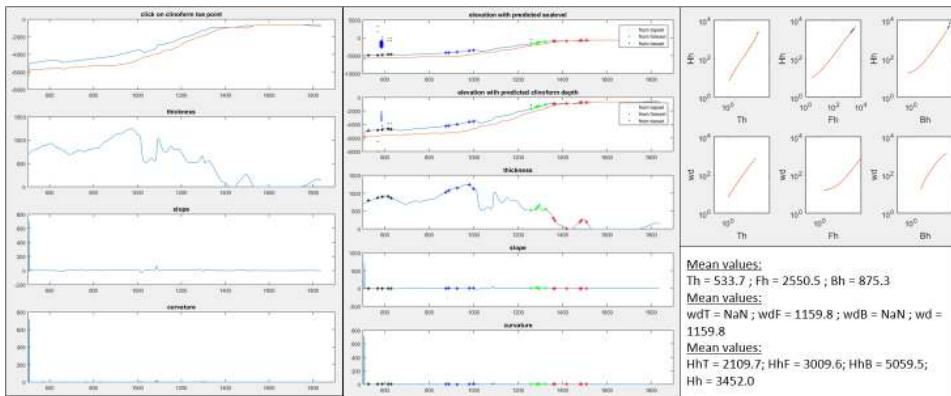


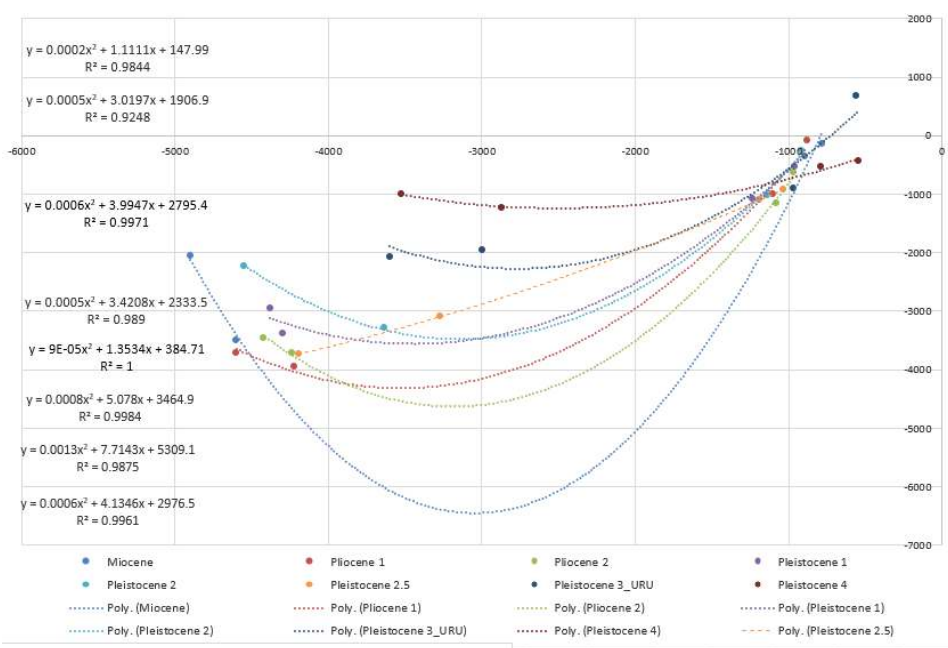
Figure 4.20: Regional Seismic Line with trend from West to East, including interpretation of clinofold of all ages.



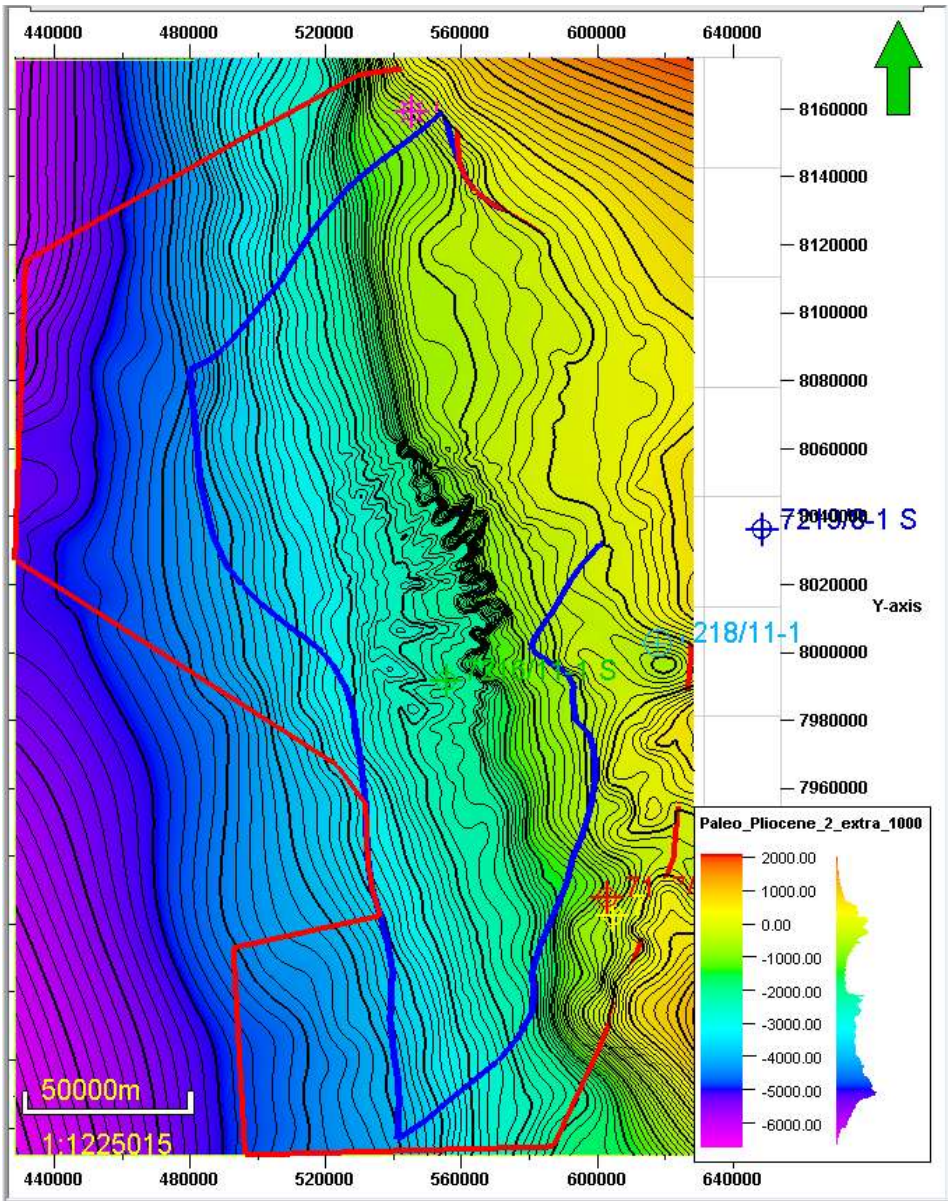
**Figure 4.21:** Results of Digitising 2D seismic section, as part of analysis preparation.



**Figure 4.22:** Results of Clinoform analysis calculation with equations based on Patruno et al. (2015) at Top Pliocene 2.

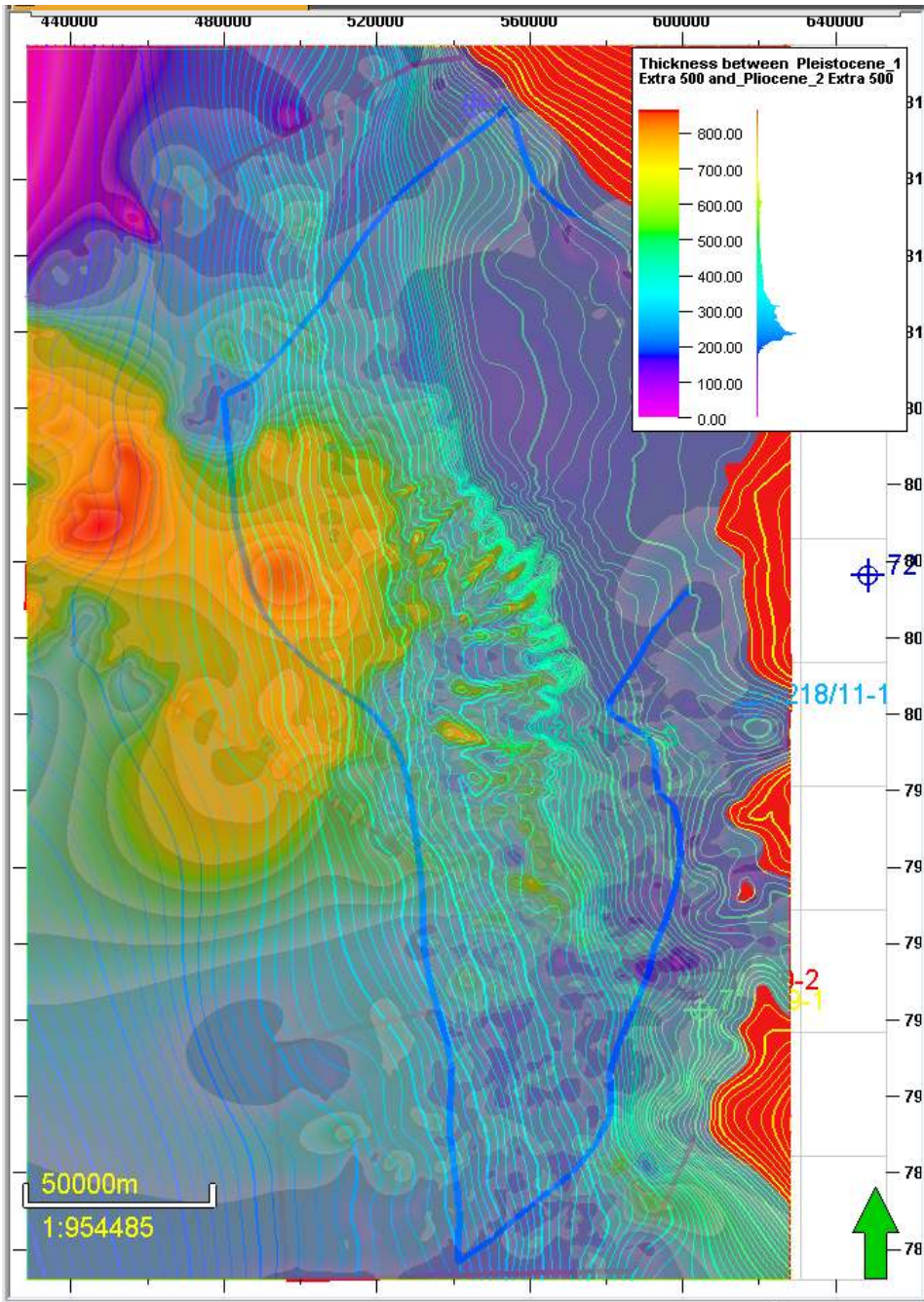


**Figure 4.23:** Cross-plot between Present Clinoform (x) and Paleo Clinoform (y) taken from Present and Paleo Depth from Clinoform analysis in table 4.3.

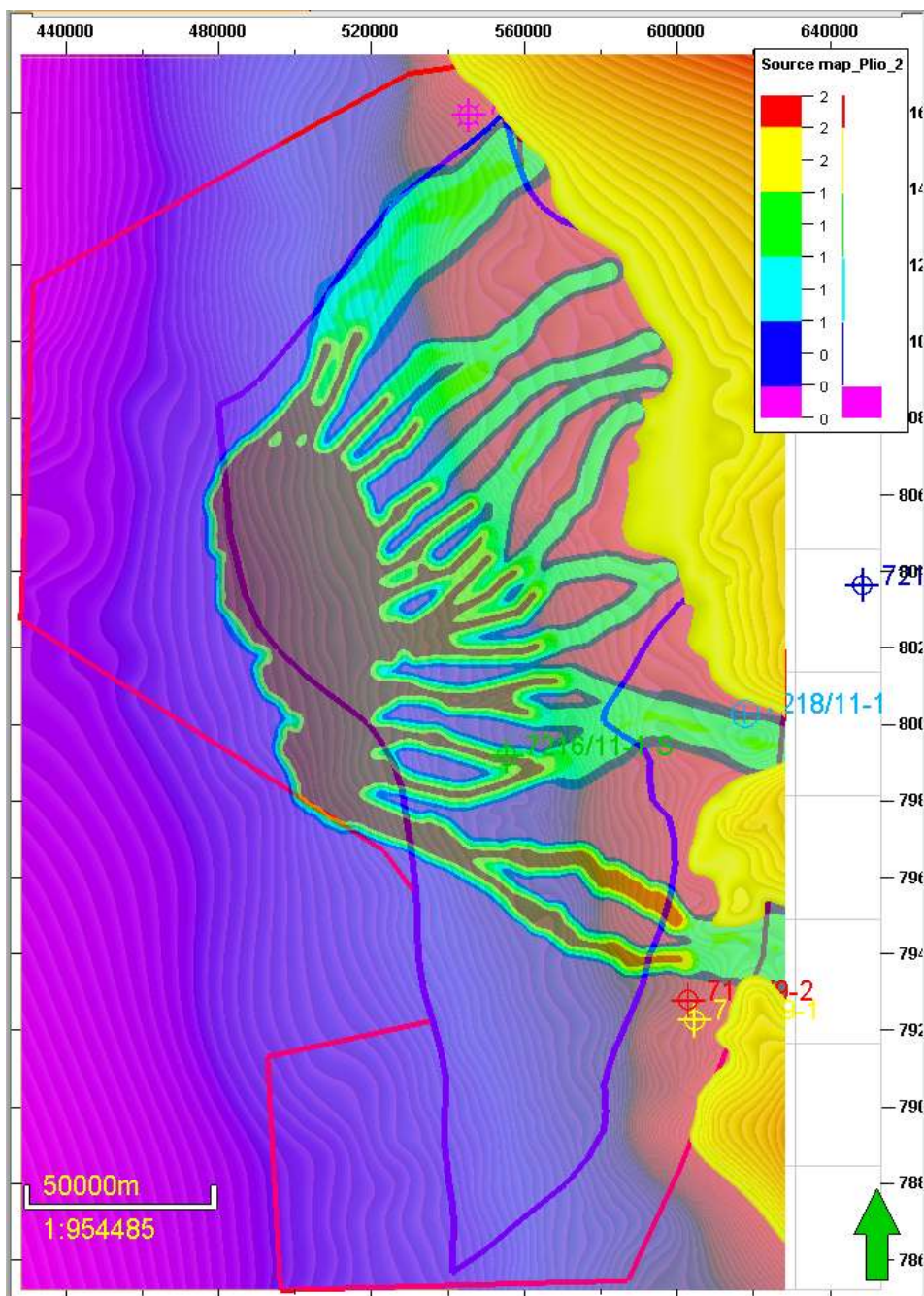


**Figure 4.24:** Paleobathymetry Map of Top Pliocene 2. derived from regression function of figure 4.23 Note : Map has been extrapolated for simulation in GPM.

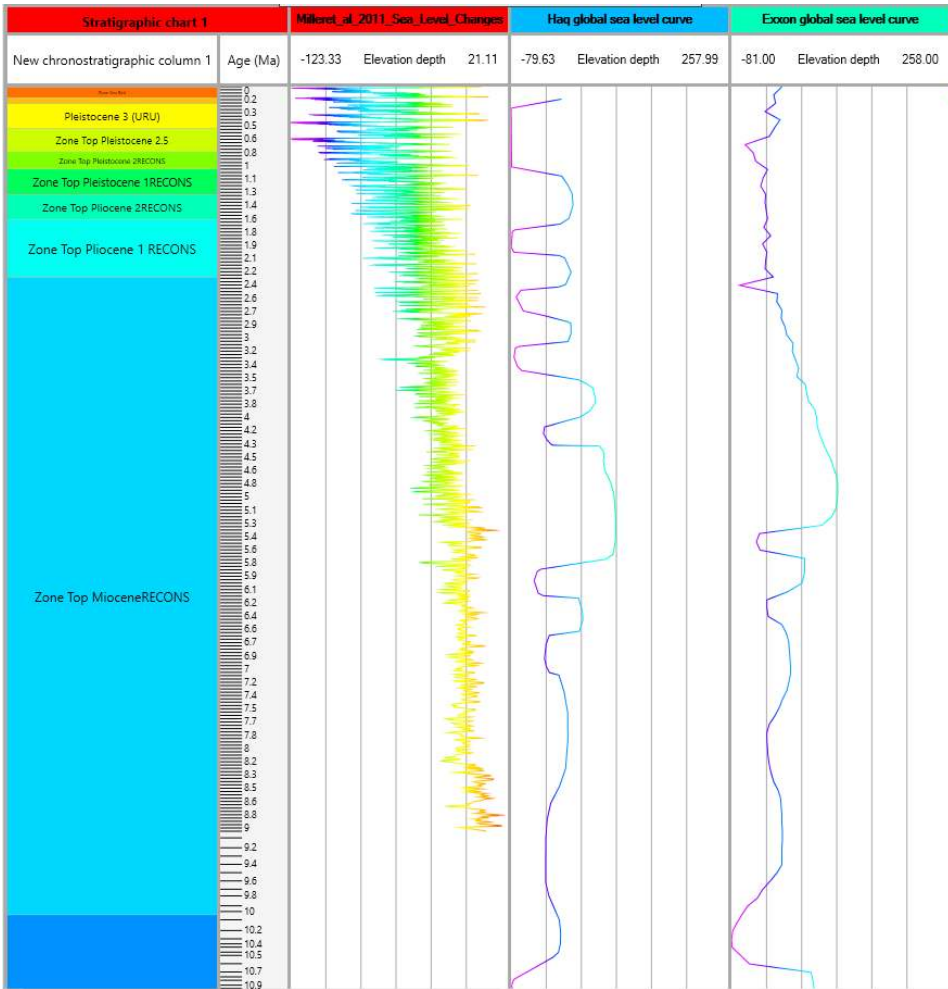




**Figure 4.25:** Thickness Map of Top Pliocene 2 to Top Pleistocene 1, overlying to Paleobathymetri Map of Top Pliocene 2.



**Figure 4.26:** Source Position Map of Top Pliocene 2, the value of 1 means location of steady flow, and value 2 means location of unsteady flow.



**Figure 4.27:** Comparison among sea level change, by Miller, Haq and Exxon. As it is shown in the Miller et al. (2005), Sea Level Change only covers from Miocene to Present, but offers more detailed sea level change.

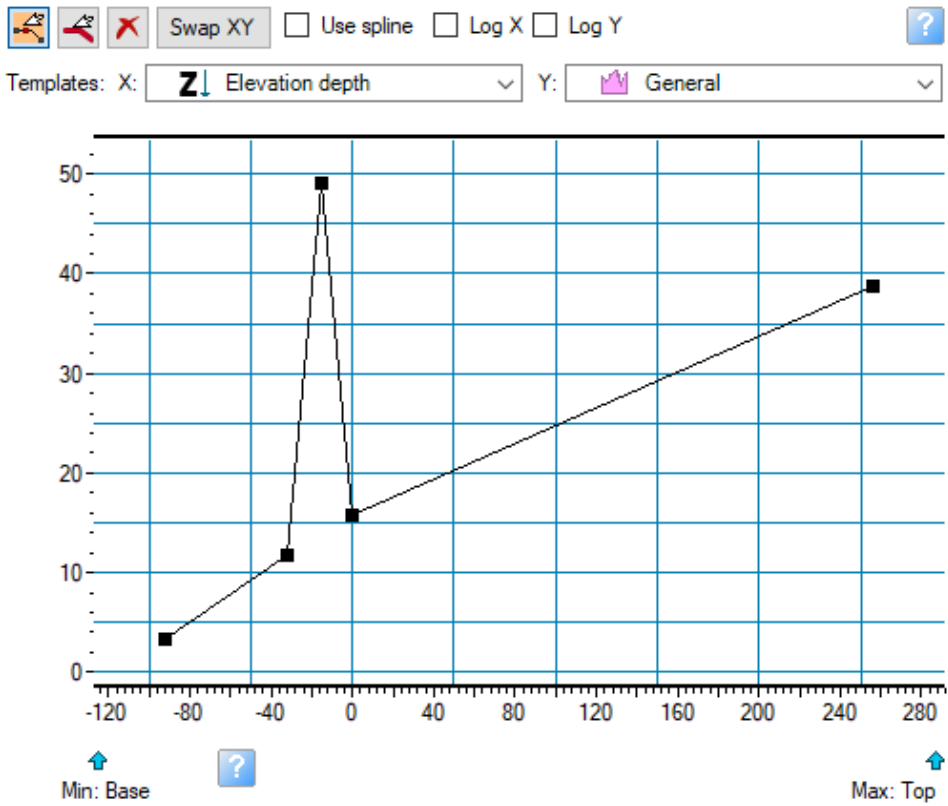
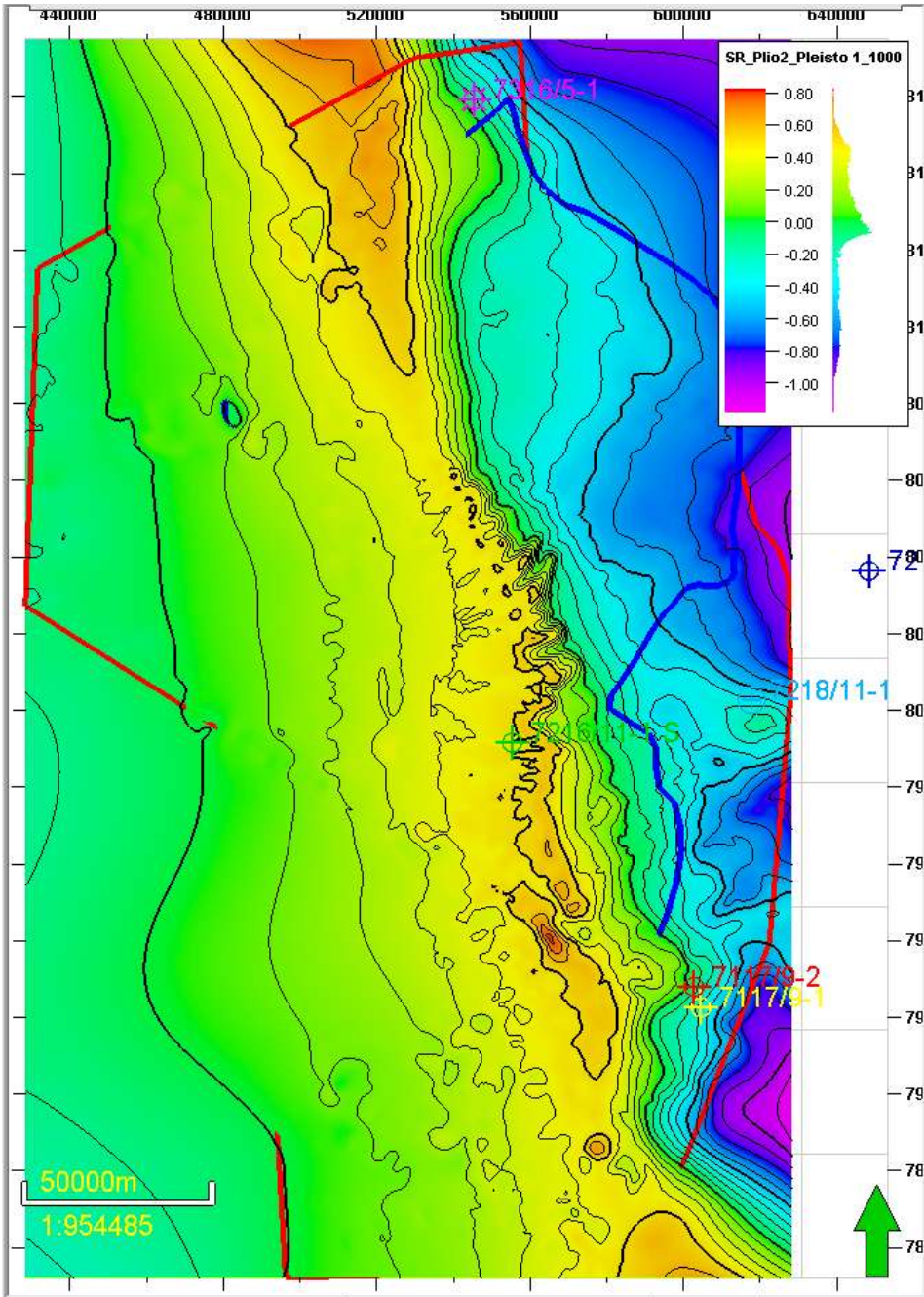
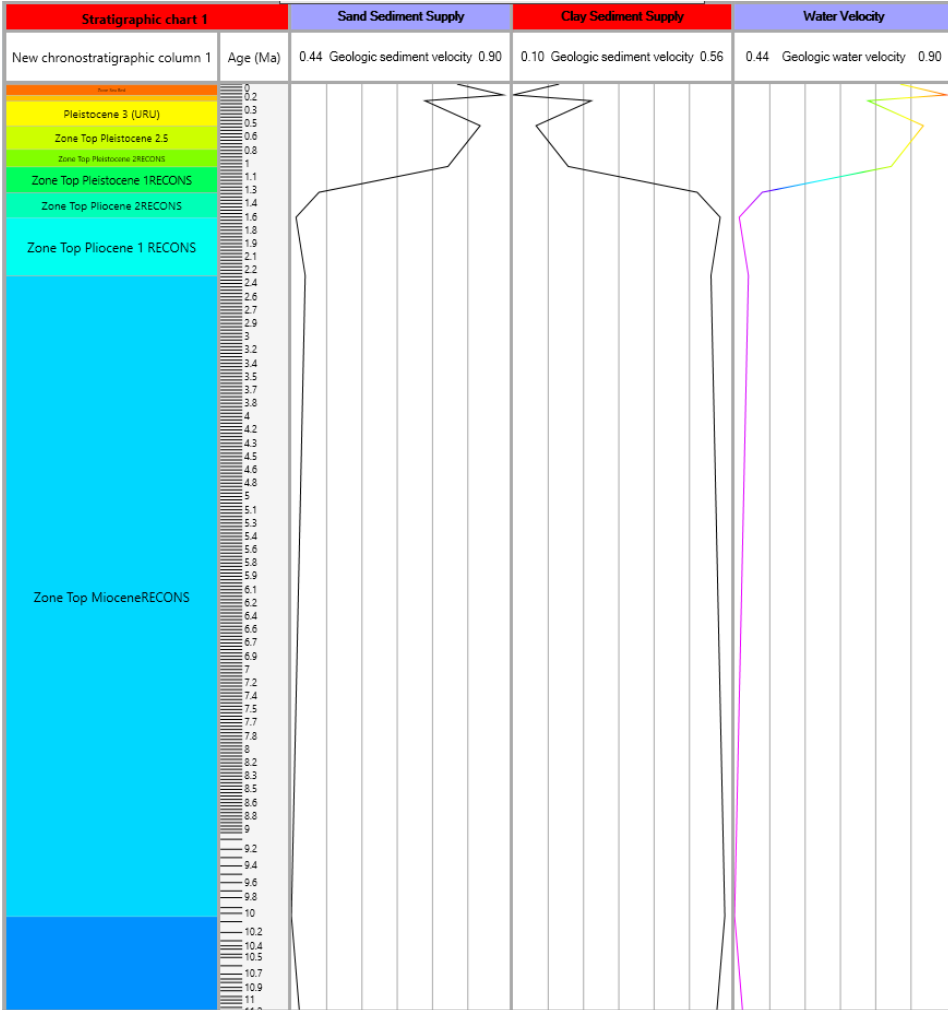


Figure 4.28: Diffusion equation from Lejri et al. (2017).

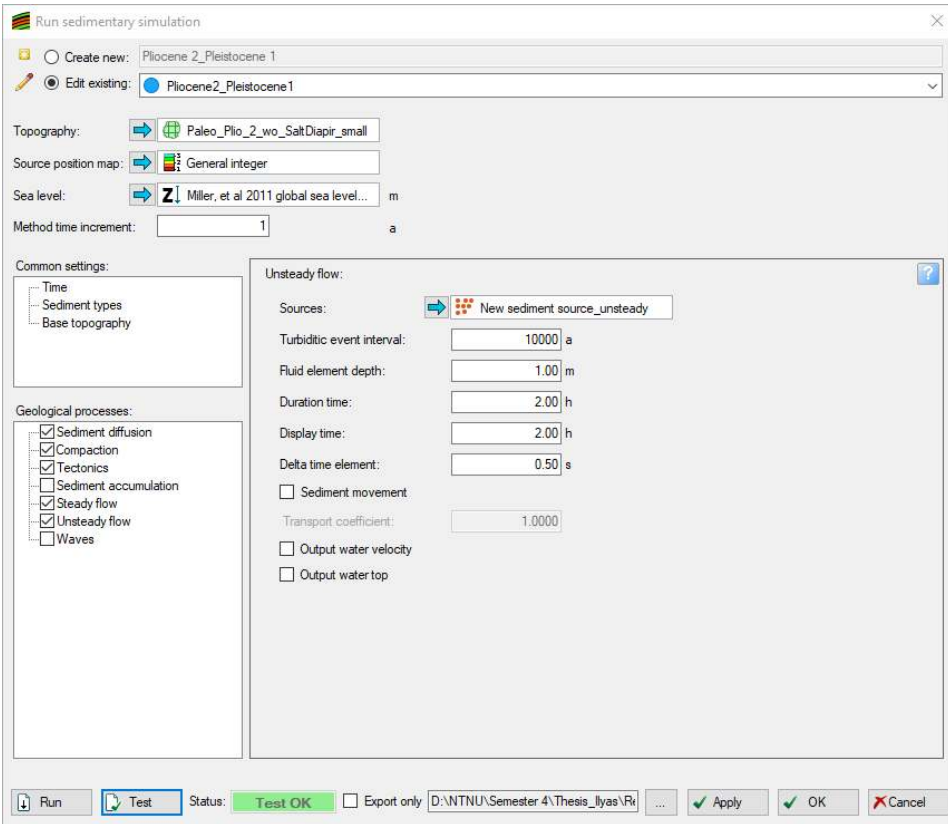




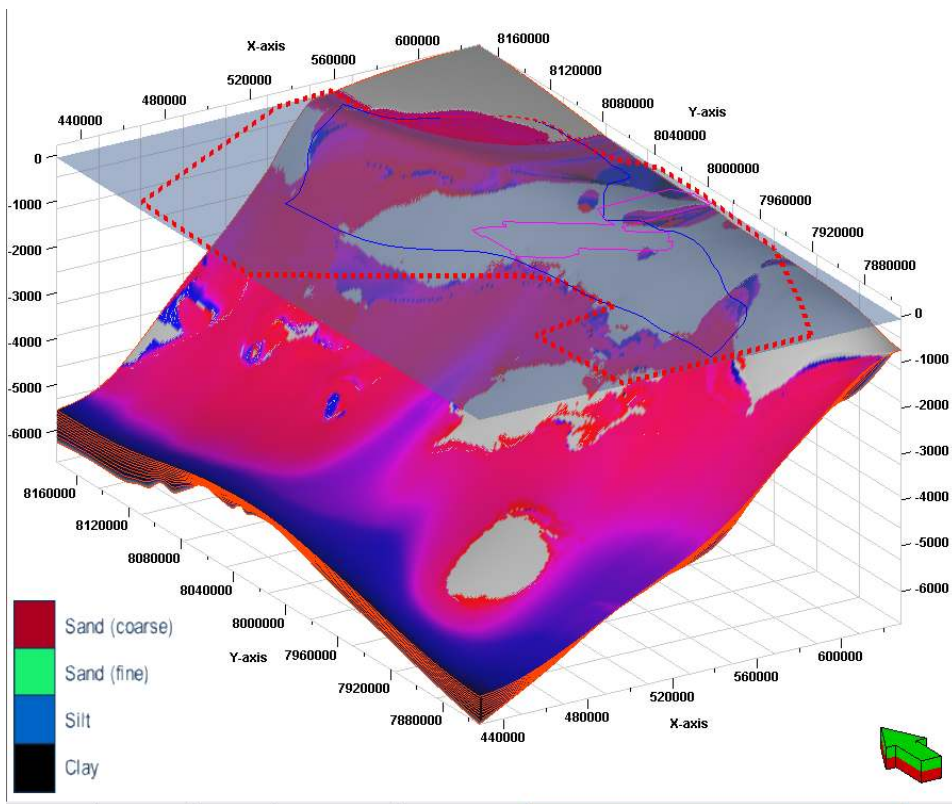
**Figure 4.29:** Subsidence/Uplift Rate Map from 13 Ma to 0 Ma, of Pliocene 2, Positive value means Uplift phase, and Negative value means Subsidence phase.



**Figure 4.30:** Sediment source and water supply chart.



**Figure 4.31:** An Example of Dialog Box Setting in Geological Process Modelling (GPM), in Pliocene 2 to Pleistocene 1.



**Figure 4.32:** Results of GPM Simulation at 0.99 Ma, Sediment package/clinothem of Pliocene 2 to Pleistocene 1.



## Discussion

### **5.1 Controlling Factors of Deep-Marine System, in Sørvestnaget Basin.**

#### **5.1.1 Allogenic Factors**

Allogenic factor is defined as global scale factor that influenced basin-scale sedimentary system. Allogenic processes operate at a basin-wide or global scale, such as sea-level change, basin-wide tectonics, and regional climatic change (Yang et al. (1998)). In this study, Basin scale factor was defined from Sea Level Change, and tectonic movement such as, uplift and subsidence, while climatic change was not considered as main influence factor, considering Sørvestsnaget Basin is relatively has same climate, which is still in glacial weather until now.(Faleide et al. (1984);Faleide et al. (1996))

#### **Sea level Change**

Sea level change in this study using model from Miller et al. (2005) as one of main input in simulator, but in several trials, the model from Haq, and Exxon Sea level change had applied as well. The result of simulation model using Miller et al. (2005), yield more precise and relatively thinner sediment packages (clinothem) than other sea level change model (Haq et al, and Exxon). Sea level change also yields different type of clinoform geometry, Low sea level will generate oblique type with sand-rich prone sediment package(clinothem)(Fig. 5.1), while high sea level will generate sigmoidal type with mud-rich prone sediment package (clinothem) (Fig. 5.2).

#### **Tectonic Movement**

Tectonic movement in this study only conducted in subsidence and uplift of phase, since the sediment packages(clinothems) of Miocene to Pleistocene are not relatively deformed. Tectonic movement in simulator is represented in subsidence/uplift rate map and vertical

---

movement of surface in function (function set as 1, since each age has its tectonic movement maps respectively.). These subsidence/uplift maps restore the paleobathymetry map to present depth map, also simple loading is applied as complementary calculation, or as substitution if the tectonic movement is unknown. The result of simulation with and without tectonic movement activation in simulator, yield significant difference in geometry and thickness of sediment packages(clinothems). This most likely has relationship with rate of erosion and sediment supply from high elevation (landward), therefore the more uplift occurred the more sediment will be eroded and transported into depocenter (basinward).(Fig.4.29)

### **5.1.2 Autogenic Factors**

Autogenic factor is defined as internal factor that influenced local process of sedimentary system. Autogenic processes operate locally, such as those intrinsic to specific depositional or geomorphic environments (Yang et al. (1998)). In this study, autogenic factor represented in diffusion equation, sediment type and flow type. Diffusion equation influences the sediment movement with relationship of elevation of sediment source and sea level elevation.

#### **Diffusion Equation**

In this study, diffusion equation using a equation from Lejri et al. (2017), which has tested in the similar environment and condition, but with different diffusion coefficient from 1, 50, 100, and 200. Diffusion coefficient directly influences the volume of sedimentation, therefore the higher diffusion coefficient, the more sediment would transport to the basin. However the coefficient can not be too higher, since it will cause an error and instability of simulation process.

#### **Sediment Type**

Sediment type in this study consists of four type; sand (coarse), sand (fine), silt, and clay. Each of sediment type has default setting from GPM itself, typically only grain diameter, grain density, compacted porosity and compacted permeability that is changed to data core. Fig.5.3

#### **Flow type**

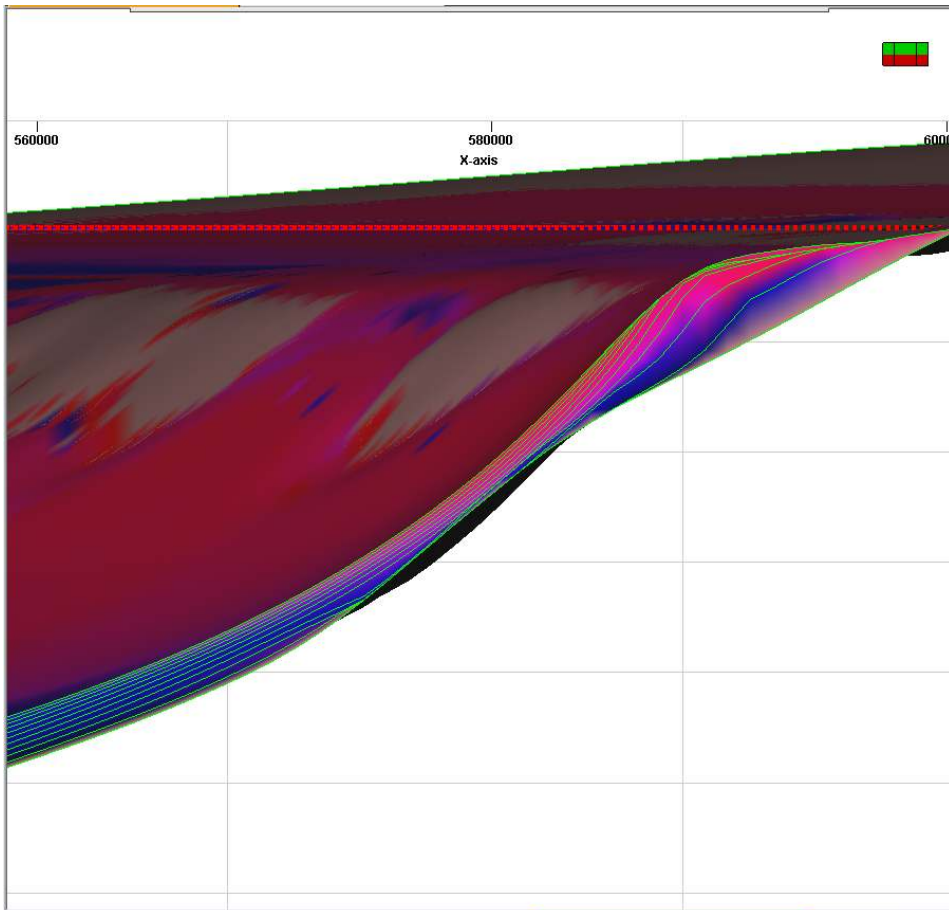
Flow type used in this study were steady and unsteady flow, both of them only being changed in part of duration of time interval, which depends on intensity or number of cycles of the flows in certain time. Fig.5.4

---

## 5.2 Geological Process Modelling Results for Hydrocarbon Exploration.

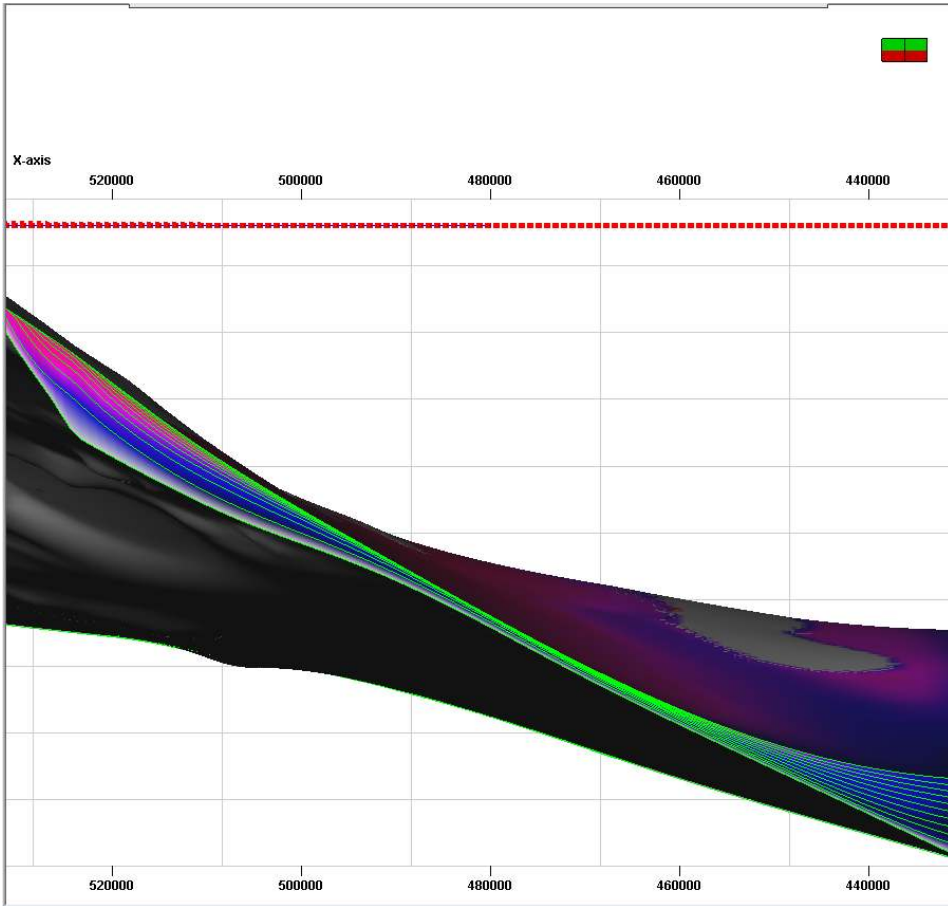
The results of Geological Process Modelling simulation from previous chapter can be used directly for geo-cellular model into Facies model and Porosity Model. However this model has not been validated and combined yet with well log data. Therefore, before using it in Geo-cellular model, the GPM results need to be adjusted with well logs interpretation and populated the data throughout all cells in model.

After all the well logs value has been adjusted, then well log analysis results, such as Lithology (derived from Petrophysical Analysis), Volume shale, Net to Gross, and Porosity Effective can be generated into different models that can be used for Hydrocarbon exploration. These multi model can be superimposed to defines geological potential map based on, porosity map, and net sand distribution.(Fig.5.5)

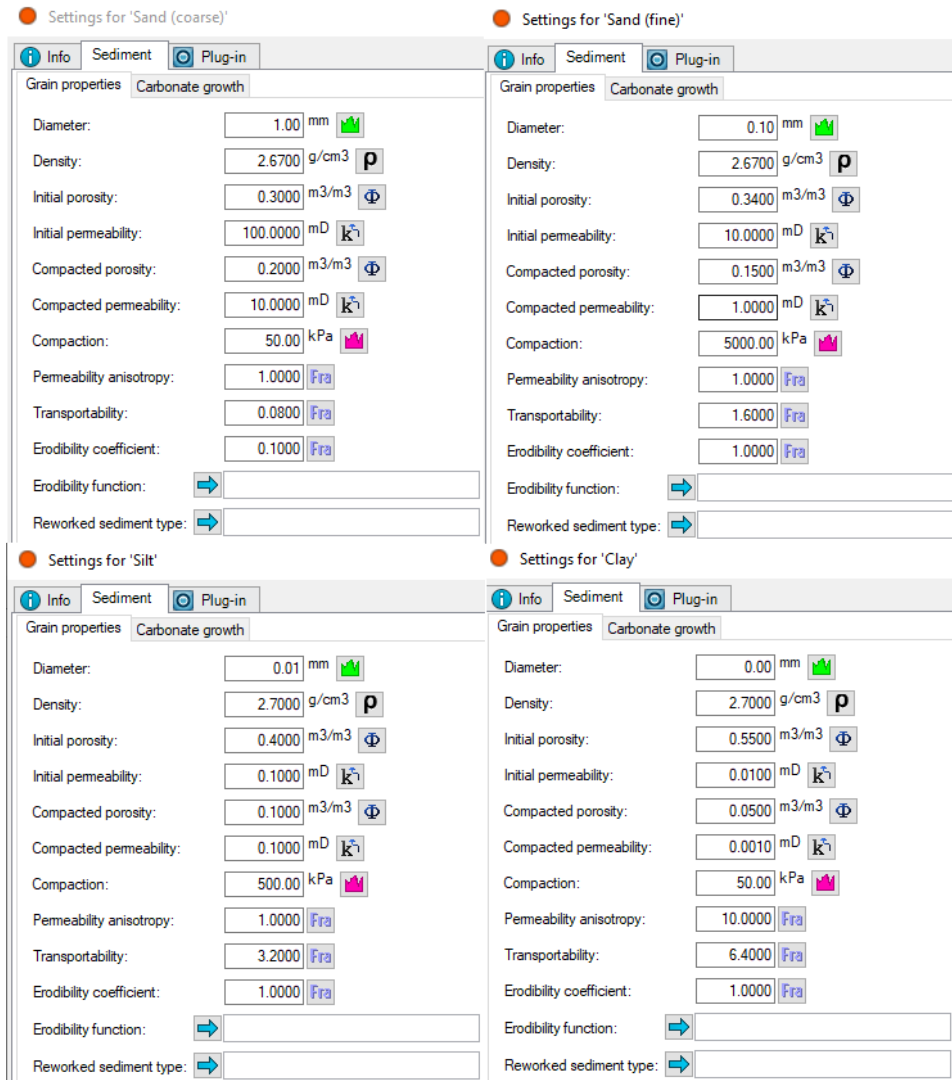


**Figure 5.1:** An example of Oblique Type of Clinoform in Pleistocene 3 (URU) to Pleistocene 4, viewed from South and exaggerated 10 times.

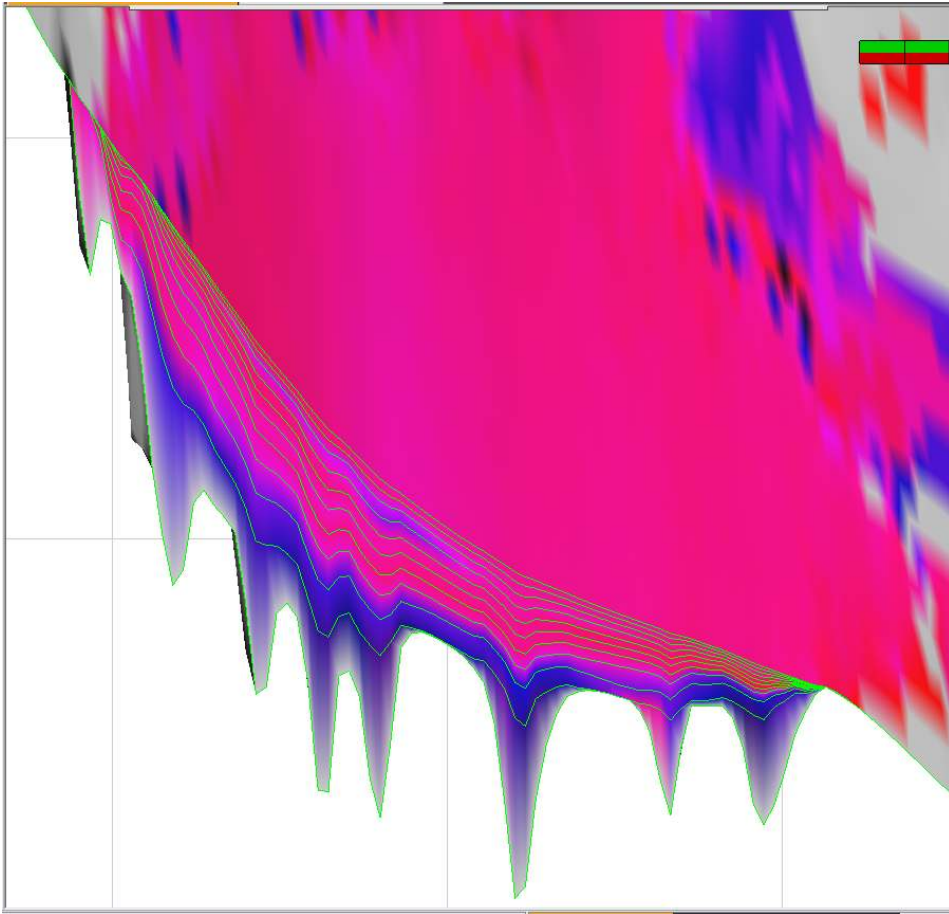




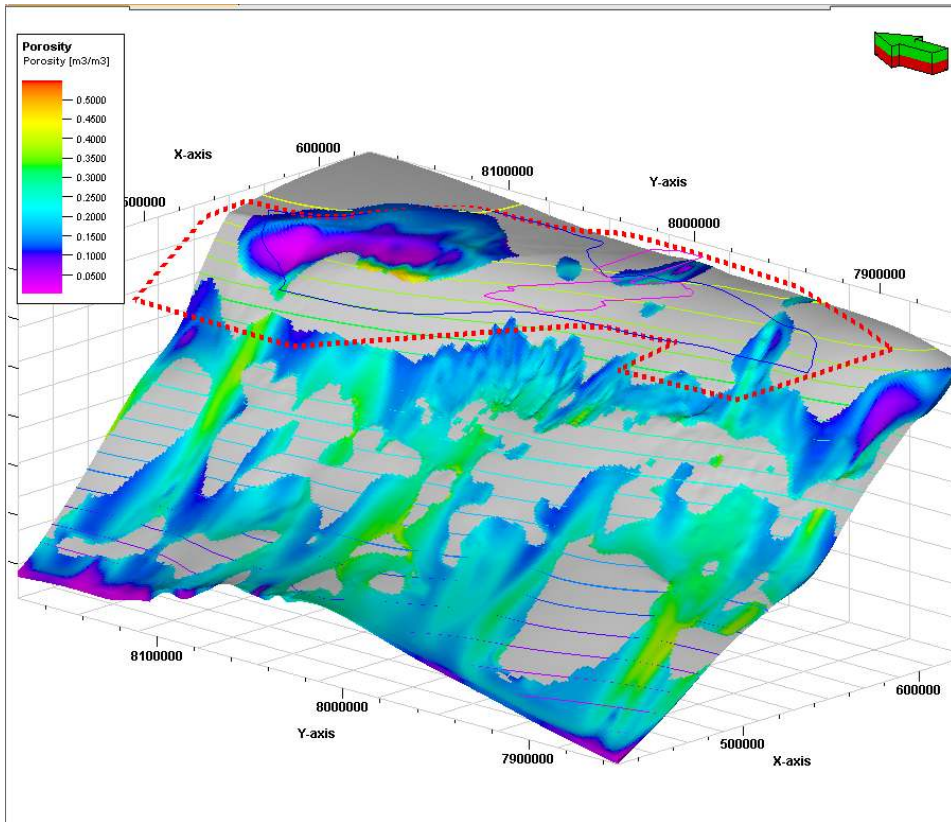
**Figure 5.2:** An example of Sigmoidal Type of Clinoform in Pleistocene 2 to Pleistocene 2.5, viewed from South and exaggerated 10 times.



**Figure 5.3:** Dialog box setting for sediments type properties, from upper left to bottom right: sand (coarse), sand (fine), silt, and clay.



**Figure 5.4:** An example of Unsteady Flow Type Deposit in Pliocene 2 to Pleistocene 1, viewed from west , section is perpendicular to incision valley, and exaggerated 100 times.



**Figure 5.5:** An example of Porosity Model in sediment package (clinothem) of Pliocene 2 to Pleistocene 1, viewed from Southwest and exaggerated 20 times.

---

---

## Conclusion

1. Well Log Analysis in the well 7216/11-1S, showed the calculation of petrophysical properties in Cenozoic Deep-Marine Deposits from Cretaceous to Pleistocene 1. From this calculation it was found, that interval Paleocene has the best porosity values ranged from 0.24 to 0.37, interval Eocene 3 porosity has value ranged from 0.32 to 0.15, interval Oligocene ranged from 0.06 to 0.12, and interval Miocene to Pleistocene 1 have porosity value ranged from 0.15 to 0.19. From that calculation it can be inferred that the interval of Paleocene, Eocene 3, and Pliocene 2 are the most promising as potential reservoir, in perspective of petrophysical values.
2. Based on sequence stratigraphy in well logs data and clinoform geometry from clinoform analysis, Sørvestsnaget Basin are divided into, 10 sediment packages corresponding to each age top surfaces from Eocene 3 to Pleistocene 4. In general, From Eocene 3 to Pleistocene 1 is at phase of Highstand System Track (HST) to Lowstand - Falling Stage System Tract (LST - FSST), with descending trajectory indicating the condition was in relative falling sea level. Meanwhile from Pleistocene 1 - Pleistocene 4 (to Seabed) is at phase of Transgressive System Tract (TST) with sometimes intermittent with Highstand System Track (HST), indicating the condition was in relative rising low level. This system tract directly influenced the dominant facies of sediment package, whether sand-rich prone, or mud-rich prone clinothem.
3. Paleobathymetry reconstruction from Clinoform Analysis has generated tectonic evolution from Miocene to Seabed. These Paleobathymetry used in Geological Process Modelling, can be new approach as tectonostratigraphy reconstruction of Sørvestsnaget Basin. This study confirming the beginning of salt diapirs which is approximately from Eocene to Oligocene until Pleistocene 3 (URU). Furthermore the phase of uplift and subsidence can be inferred from Subsidence rate maps that suggest Pleistocene 4 was the most deformed as subsidence, while Pliocene 1 was the most uplifted age.
4. Geological Process Modelling (GPM) results is new approach to map and model de-

---

posits of Sørvestsnaget Basin, based on physical properties and condition of Paleobasement (Paleobathymetri). This study found that Diffusion equation has considerably influenced the process and volume of sediment, suggesting to set the diffusion coefficient ranged from 100 to 200 for maximum deposition. Meanwhile for sediment source location, based on sediment thickness map and source position map, this study suggests that trend of depositional mostly came from Northeast location, most likely Stappen High, and Southeast location from areas between Veslemøy High and Senja Ridge.

5. The results from GPM can be used directly or indirectly for defining facies model, porosity and unconformities for interval reservoirs. These models still need to be validated and calibrated with well log analysis to confirm values of every cell in GPM model does not contradict with each other. Lastly, This study obviously needs further research especially in water velocity, and sedimentation rate specifically in Sørvestsnaget Basin, due to limited source of data and method that can be conducted at present time. The author believe that in the future, Stratigraphic Forward Modelling could be more reliable as tool for geological modelling rather than conventional modelling which still has high uncertainty.



# Bibliography

- Akbar, Y., 2018. Basement high - related cretaceous submarine fans growth in southwestern barents sea. Master Degree Thesis, NTNU Open, 1–99.
- Anindita, I., 2018. Tectonostratigraphy of cenozoic era in sørvestsnaget basin, southwest barents sea. Specialization Project 3rd Semester, NTNU Open, 1–40.
- Breivik, A. J., Faleide, J. I., Gudlaugsson, S. T., 1998. Southwestern barents sea margin: late mesozoic sedimentary basins and crustal extension. *Tectonophysics* 293, 21–44.
- Butt, F., Elverhøia, A., Solheim, A., Forsberg, C., 2000. Deciphering late cenozoic development of the western svalbard margin from odp site 986 results. *Marine Geology* 169, 373–390.
- Faleide, J., Gudlaugsson, S. T., Jacquart, G., 1984. Evolution of the western barents sea. *Marine and Petroleum Geology* 1 (27), 123–150.
- Faleide, J., Solheim, A., Fiedler, A., Hjelstuen, B., E.S., A., Vanneste, K., 1996. Late cenozoic evolution of the western barents sea-svalbard continental margin. *Global and Planetary Change* 12, 53–74.
- Henriksen, E., Ryseth, A. E., Larssen, G. B., Heide, T., Rønning, K., Sollid, K., Stoupakova, A. V., 2011. Tectonostratigraphy of the greater barents sea: implications for petroleum systems. *Arctic Petroleum Geology* 35 (10), 163–195.
- Knies, J., Matthiessen, J., Vogt, C., Laberg, J., Hjelstuen, B., M., S., Larsen, E., Andreassen, K., Eidvin, T., Vorren, T., 2009. The plio-pleistocene glaciation of the barents sea-svalbard region: a new model based on revised chronostratigraphy. *Quaternary Science Reviews* 28, 812–829.
- Kristensen, T., Rotevatn, A., Marvik, M., Henstra, G., R.L., G., R., R., 2018. Structural evolution of sheared margin basins: the role of strain partitioning sørvestsnaget basin, norwegian barents sea. *Basin Research* 30, 279–301.

- 
- Larsen, E., Andreassen, K., Nilssen, L. C., and, S. R., 2003. The prospectivity of the barents sea: ice ages, erosion and tilting of trap. *Marine and Petroleum Geology* 310, 129–143.
- Lejri, M., Madhoo, H., Claussmann, B., Truelove, L., Tveiten, J., Tetzlaff, D., Salomonson, P., 10 2017. Understanding the controls on clastic sedimentation using forward stratigraphic modeling and seismic sequence stratigraphy. In: *Proc. AAPG-SEG International Conference and Exhibition, London, United Kingdom*.
- Marheni, L., Omosanya, K., Johansen, S. E., Felix, M., Abrahamson, P., 10 2015. Sedimentation process and stratigraphic evolution of tertiary deep-water sediments in sørvestsnaget basin, southwestern barents sea,. In: *Proc. AAPG 3P Arctic Petroleum Potential Conference and Exhibition, Stavanger, Norway*.
- Miller, K. G., Kominz, M. A., V.Browning, J., D.Wright, J., S.Mountain, G., E.Katz, M., Sugarman, P. J., Cramer, B. S., Christie-Blick, N., Pekar, S. F., 2005. The phanerozoic record of global sea-level change. *SCIENCE* 310 (5752), 1293–1298.
- Mitchum Jr, R., Vail, P., Sangree, J., 1977. Seismic stratigraphy and global changes of sea level, part 6: Stratigraphic interpretation of seismic reflection patterns in depositional sequences. *AAPG Memoir* 26 (6), 123–150.
- Mjelde, R., Breivik, A., J. Elstad, H., Ryseth, A. E., Skilbrei, J. R., Opsal, J. G., Shimamura, H., Murai, Y., Nishimura, Y., 2014. Geological development of the sørvestsnaget basin, southwestern barents sea, from ocean bottom seismic, surface seismic and potential field data. *Norwegian Journal of Geology* 82 (19), 183–202.
- Omosanya, K., Harishidayat, D., Marheni, L., Johansen, S., Felix, M., Abrahamson, P., 2016. Recurrent mass-wasting in the sørvestsnaget basin southwestern barents sea: A test of multiple hypotheses. *Marine Geology* 376, 175 – 193.  
URL <http://www.sciencedirect.com/science/article/pii/S0025322716300214>
- Patruno, S., Hampson, G. J., Jackson, C. A., 2015. Quantitative characterisation of deltaic and subaqueous clinofolds. *Earth Science Review* 142, 79–119.
- Perez-Garcia, C., Safronova, P., Mienert, J., Berndt, C., Andreassen, K., 2013. Extensional rise and fall of a salt diapir in the sørvestsnaget basin, sw barents sea. *Marine and Petroleum Geology* 310, 129–143.
- Ravesteyn, J., 2013. Advanced reservoir characterisation for geological sequestration of co<sub>2</sub>: Surat basin demonstration project. Not Published, 1–55.
- Rider, M., 2002. *The Geological Interpretation of Well Logs*. Rider- French Consulting Ltd. Press.
- Ryseth, A., Augustson, J., Charnock, M., Haugerud, O., Knutsen, S.-M., Midbøe, P., Opsal, J., Sundsbø, G., 2003. Cenozoic stratigraphy and evolution of the sørvestsnaget basin, southwestern barents sea. *Norwegian Journal of Geology* 83 (10), 107–129.

- 
- Schlumberger, 2017. Petrel Geophysic. Training and Exercise Guide. NEXT, a Company of Schlumberger, Paris, France, 16th Edition.
- Tetzlaff, D., Tveiten, J., Salomonsen, P., Christ, A.-B., Athmer, W., G. Borgos, H., Sonneland, L., Martinez, C., Raggio, F., 11 2014. Geologic process modelling.
- Vorren, T. O., Richardsen, G., Knutsen, S.-M., Henriksen, E., 1991. Cenozoic erosion and sedimentation in the western barents sea. *Marine and Petroleum Geology* 8, 317–340.
- Worsley, D., 2008. The post-caledonian development of svalbardand the western barents sea. *Polar Research* 27, 298–317.
- Yang, W., Kominz, M. A., Major, R. P., 1998. Distinguishing the roles of auto-genic versus allogenic processes in cyclic sedimentation, cisco group (virgilian and wolfcampian),north-central texas. *Geological Survey of America Bulletin* 110 (10), 1333–1353.

